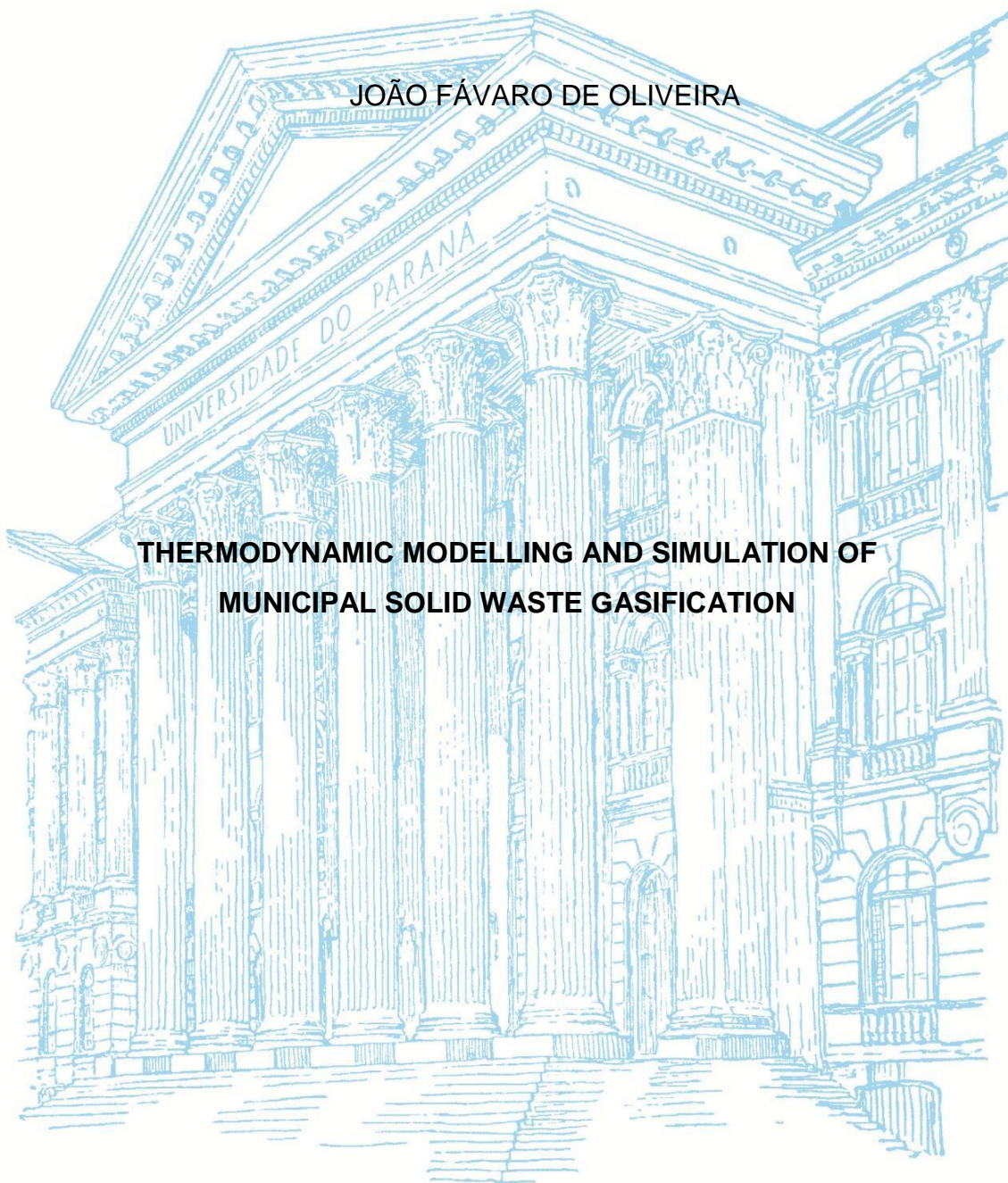


**FEDERAL UNIVERSITY OF PARANÁ**

**JOÃO FÁVARO DE OLIVEIRA**

**THERMODYNAMIC MODELLING AND SIMULATION OF  
MUNICIPAL SOLID WASTE GASIFICATION**



**CURITIBA**

**2016**

JOÃO FÁVARO DE OLIVEIRA

THERMODYNAMIC MODELLING AND SIMULATION OF MUNICIPAL SOLID WASTE  
GASIFICATION

Dissertation submitted in partial fulfillment of the requirements for the degree of Master of Science, in the field of: Chemical Engineering, Chemical Engineering Graduate Program (PPGEQ). Technology Sector, Federal University of Paraná.

Advisor: Prof. Dr. Marcos Lúcio Corazza  
Co-Advisor: Prof. Dr. Fernando A. P. Voll

**CURITIBA**

**2016**

---

O48t

Oliveira, João Fávoro de  
Thermodynamic modelling and simulation of municipal solid waste  
gasification/ João Fávoro de Oliveira. – Curitiba, 2016.  
107 f. : il. color. ; 30 cm.

Dissertação - Universidade Federal do Paraná, Setor de Tecnologia,  
Programa de Pós-Graduação em Engenharia Química, 2016.

Orientador: Marcos Lúcio Corazza – Co-orientador: Fernando A. P. Voll.  
Bibliografia: p. 101-105.

1. Resíduos - Gaseificação. 2. Energia elétrica - Produção. 3. Gases de  
combustão. I. Universidade Federal do Paraná. II. Corazza, Marcos Lúcio. III.  
Voll, Fernando A. P. . IV. Título.

CDD: 662.87

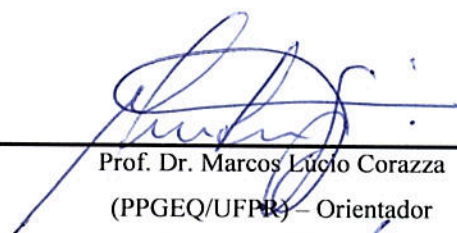
---



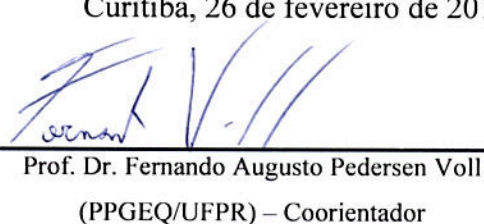
## ATA DE DEFESA DE DISSERTAÇÃO

Aos vinte e seis dias do mês de fevereiro de 2016, no Auditório Inferior do Prédio da Engenharia Química no Centro Politécnico – UFPR foi instalada pelo Dr. Marcos Lúcio Corazza, professor do Programa de Pós-Graduação em Engenharia Química, a Banca Examinadora para a octogésima quinta defesa de dissertação de mestrado na área de concentração: Desenvolvimento de Processos Químicos. Estiveram presentes no ato, professores, alunos e visitantes. A Banca Examinadora, atendendo à determinação do colegiado do Programa de Pós-Graduação em Engenharia Química, foi constituída pelos professores doutores: Marcos Lúcio Corazza (PPGEQ/UFPR), Fernando Augusto Pedersen Voll (PPGEQ/UFPR), Marcelo Kaminski Lenzi (PPGEQ/UFPR) e Marcio Schwaab (DEQ/UFRGS). Às 13h30min, a banca iniciou os trabalhos, convidando o candidato **João Fávaro de Oliveira** a fazer a apresentação da dissertação de mestrado intitulada “*Thermodynamic modelling and simulation of municipal solid waste gasification*”. Encerrada a apresentação, iniciou-se a fase de arguição pelos membros participantes. Tendo em vista a dissertação e a arguição, a banca decidiu pela APROVAÇÃO do candidato, (de acordo com a determinação dos artigos 68º e 69º da Resolução 65/09 – CEPE/UFPR de 30.10.2009).

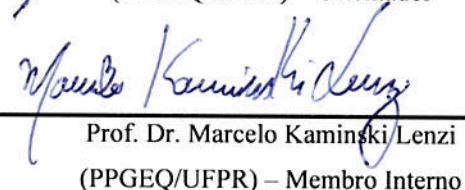
Curitiba, 26 de fevereiro de 2016.



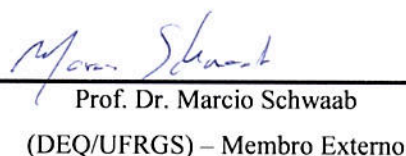
Prof. Dr. Marcos Lúcio Corazza  
(PPGEQ/UFPR) – Orientador



Prof. Dr. Fernando Augusto Pedersen Voll  
(PPGEQ/UFPR) – Coorientador



Prof. Dr. Marcelo Kaminski Lenzi  
(PPGEQ/UFPR) – Membro Interno



Prof. Dr. Marcio Schwaab  
(DEQ/UFRGS) – Membro Externo

## **ABSTRACT**

Handling, management and disposal of the growing Municipal Solid Waste Production (MSW) is not a simple task and it has been focus of intense research. World organizations, Federal, State and Municipal governments need technological solutions that allow them to correct handle the challenge of urban waste disposal. At the same time, demand for electricity in Brazil has risen in last years. As part of the solution, the process of electric generation from the municipal solid waste gasification can match the availability of raw material concentrated in one location with the proximity of a power plant to the demanded area. The gasification is a thermal process that transforms organic materials in synthesis gas, from which is possible to generate electricity. Thereby, it is required the prediction of the synthesis gas amounts that can be produced to make possible the correct and optimal design of a complete waste-to-energy process. In this context, this work is aimed to a theoretical study regarding the urban solid waste gasification process. An equilibrium model has been developed to predict the product gas of the gasification of the Curitiba City Municipal Solid Waste (MSW). A method to evaluate the ultimate analysis of MSW when there is lack of experimental information was proposed and used. Simulations of different gasification scenarios were carried out, including predictions at supercritical conditions. Model developed was validated against literature and used for evaluate and optimizing the gasification conditions. The optimum reaction set point may vary according to the fuel composition, amount of air injected into the system, moisture and pressure in the gasifier. A comparison between the stoichiometric and non-stoichiometric approaches was also evaluated. The stoichiometric approach can be equivalent to the non-stoichiometric, but does not easily allow the additions of substances to evaluate its formation. In a general way, from the theoretical results obtained in this

work it can be seen that the urban solid waste presents a potential technical feasibility to be used as a raw material for energy-production systems.

**Key words:** Gasification, Municipal Solid Waste, Equilibrium modelling, synthesis gas, syngas.

## RESUMO

O manejo, gerenciamento e a destinação final da crescente produção de resíduos sólidos urbanos (RSU) não é tarefa simples e vem sendo foco de intensa pesquisa. Organizações mundiais, governos federal, estaduais e municipais demandam soluções tecnológicas que possam os permitir lidar com o desafio da correta destinação dos resíduos urbanos. Ao mesmo tempo, a demanda por eletricidade no Brasil tem crescido nos últimos anos. Como parte da solução, o processo de geração de energia elétrica a partir de resíduos sólidos urbanos pode compatibilizar a disponibilidade de matéria-prima concentrada em um único local com a proximidade da usina com a carga. A gaseificação é um processo térmico que transforma materiais orgânicos em gás de síntese, do qual é possível gerar energia elétrica. Assim, é necessário se prever a quantidade de gás de síntese que pode ser produzida para que seja possível e otimizado o dimensionamento de um processo completo do tipo resíduo em energia. Neste contexto, este trabalho visa ao estudo teórico do processo de gaseificação do resíduo sólido urbano. Um modelo de equilíbrio foi desenvolvido para prever a quantidade de gás da gaseificação da cidade de Curitiba. Um método para avaliar a análise elementar do RSU, na ausência de informações experimentais, foi proposto e utilizado. Simulações de diferentes cenários para gaseificação foram calculados, incluindo condições supercríticas. O modelo desenvolvido foi validado com dados da literatura e utilizado para otimizar as condições de gaseificação. A condição ótima de reação pode variar de acordo com a composição do combustível, quantidade de ar injetada no sistema, umidade e pressão do gaseificador. Foi feita uma comparação entre as abordagens estequiométrica e não-estequiométrica. A abordagem estequiométrica pode ser equivalente a não-estequiométrica, porém não permite facilmente a adição de maior quantidade de substâncias para avaliação. De maneira geral, dos resultados teóricos obtidos neste trabalho, os resíduos sólidos urbanos tem viabilidade técnica de serem usados como matéria-prima para produção de energia elétrica.

**Palavras-chave:** Gaseificação, Resíduos Sólidos Urbanos, Modelagem de Equilíbrio, gás de síntese, syngas.

## **ACKNOWLEDGMENTS**

To God.

To my family, for supporting me in my decisions.

To my Advisor and Co-Advisor that were always available and made efforts to help me to develop this work.

To the Federal University of Paraná and the Chemical Engineering Graduate Program for giving me the opportunity to study and to further develop myself.

To Companhia Paranaense de Energia- COPEL for allowing me to participate in the Master Program and in the development of this work.



## TABLE OF CONTENTS

<b>ABSTRACT</b> .....	3
<b>RESUMO</b> .....	5
<b>ACKNOWLEDGMENTS</b> .....	6
<b>FIGURES LIST</b> .....	9
<b>TABLES LIST</b> .....	12
<b>1. CHAPTER I: INTRODUCTION</b> .....	14
1.1 WASTE AS ENERGY SOURCE .....	18
1.2 EFFICIENCY COMPARISON AMONG THERMAL TREATMENT TECHNOLOGIES.....	19
1.3 OBJECTIVES.....	20
<b>2. CHAPTER II: BIBLIOGRAPHIC REVIEW</b> .....	21
2.1 GASIFICATION.....	21
2.1.1 GASIFICATIONS AGENT .....	23
2.1.2 THE GASIFICATION PROCESS .....	25
2.1.3 DRYING.....	26
2.1.4 PYROLISIS.....	27
2.2 TYPES OF GASIFIERS .....	28
2.2.1 FIXED OR MOVING BED REACTORS .....	30
2.2.2 UPDRAFT GASIFIERS.....	31
2.2.3 DOWNDRAFT GASIFIERS .....	32
2.2.4 CROSSDRAFT GASIFIERS .....	33
2.2.5 FLUIZIZED BED GASIFERS .....	34
2.2.5.1 BUBBLING FLUIDIZED BED.....	35

2.2.5.2	CIRCULATING FLUIDIZED BED .....	36
2.2.6	ENTRAINED-FLOW GASIFIERS.....	37
2.2.7	PLASMA GASIFIER.....	38
2.3	GASIFICATION THERMODYNAMIC MODELLING.....	39
2.4	BASES TO PRESENT FUEL COMPOSITION.....	52
2.4.1	AS RECEIVED BASIS .....	53
2.4.2	AIR-DRY BASIS.....	54
2.4.3	TOTAL DRY-BASIS.....	54
2.4.4	DRY ASH-FREE BASIS.....	55
2.5	BIOMASS GASIFICATION IN SUPERCRITICAL WATER.....	55
<b>3.</b>	<b>CHAPTER III : MATERIALS AND METHODS .....</b>	<b>58</b>
3.1.	MUNICIPAL SOLID WASTE COMPOSITION .....	58
3.2.	MATHEMATICAL DEVELOPMENT OF STOICHIOMETRIC MODEL.....	63
3.3.	MATHEMATICAL DEVELOPMENT OF NON-STOICHIOMETRIC MODEL.....	65
3.4.	SIMULATIONS OF CURITIBA'S MUNICIPAL SOLID WASTE GASIFICATION .	69
<b>4.</b>	<b>CHAPTER IV: RESULTS AND DISCUSSION .....</b>	<b>75</b>
4.1.	VALIDATION OF THE STOICHIOMETRIC MODEL .....	75
4.2.	STOICHIOMETRIC MODEL FOR CURITIBA'S MSW GASIFICATION (SCENARIO 1).....	77
4.3.	VALIDATION OF THE NON-STOICHIOMETRIC MODEL .....	78
4.4.	NON-STOICHIOMETRIC VERSUS STOICHIOMETRIC APPROACHES.....	82
4.5.	OPTIMIZATION OF CURITIBA'S MSW GASIFICATION .....	85
<b>5.</b>	<b>CHAPTER V: CONCLUSIONS .....</b>	<b>99</b>
<b>6.</b>	<b>REFERENCES .....</b>	<b>101</b>
<b>7.</b>	<b>GLOSSARY .....</b>	<b>105</b>

## FIGURES LIST

Figure 1 - Waste disposal distribution in low-income and upper middle-income countries. Source: World Bank, 2012. ....	14
Figure 2 – Hierarchy in waste destination. Source: World Bank, 2012.....	15
Figure 3 - Final destination of MSW in Brazil (ton/day). Source: Adapted ABRELPE. ..	16
Figure 4 - Final destination of Paraná's MSW (ton/day). Source: ABRELPE. ....	17
Figure 5 - Possible applications for the synthesis gas and gasification. Source: Gasification Council, 2015.....	22
Figure 6 – Ternary diagram C-H-O of the gasification process. Source: Adapted from Basu (2010).....	24
Figure 7 – Potential paths for gasification. Source: Adapted from Basu (2010). ....	28
Figure 8 - Applicability range for the biomass gasifiers. Source: Adapted from Basu (2010).....	29
Figure 9 - Different types of gasifiers and their commercial suppliers. Source: Adapted from Basu (2010).....	30
Figure 10 - Schematic of an updraft gasifier.....	32
Figure 11 – Schematic of a downdraft gasifier. ....	33
Figure 12 – Schematic of a crossdraft gasifier. ....	34
Figure 13 - Schematic of a Winkler bubbling fluidized bed. Source: Basu (2010). ....	36
Figure 14 – Schematic of a CFB gasifier. Source: Basu (2010). ....	37
Figure 15 – Schematic of an Entrained –Flow gasifier. ....	38
Figure 16 – Schematic of a Plasma gasifier. Source: AlterNRG. ....	39
Figure 17 – Schematic for the Energy balance for the model developed by Barba et al. (2011).....	46

Figure 18 - Different basis to express the fuel composition (BASU, 2010). O - Oxygen, Mi - Inherent moisture, N - Nitrogen, Ms - superficial moisture, C – Carbon, S- Sulfur. ....	53
Figure 19 - Municipal Solid Waste Processing philosophy to generate electrical energy. Source: This work.....	70
Figure 20 - Algorithm used to generate the simulation data of the Curitiba's MSW gasification. ....	72
Figure 21 - Simulation of wood chips gasification at 1073.15K. ....	76
Figure 22 - Molar composition variation, in a dry basis, of the product gas of the Curitiba's MSW gasification.....	78
Figure 23 - Results for the supercritical water gasification of ethanol at 1073.15 K and 22.1 MPa. Solid Line: this work; Symbols: Byrd et al. (2007). ....	79
Figure 24 - Comparison between the experimental data from Antal et al. (2000) and the model prediction. ....	82
Figure 25 –Scenario 6. Results for stoichiometric model developed based on Zainal et al. (2001) versus results for non-stoichiometric model developed in this work. Bars represent: ■ Stoichiometric, ■ Non-stoichiometric, ■ Alauddin (1996), Experimental, ■ Zainal et al. (2001). Moisture (a) 0%, (b) 10%, (c) 20%, (d) 30% and (e) 40%. ....	83
Figure 26 – Comparison for the gasification of Curitiba's municipal solid waste. Results for stoichiometric model adapted from Zainal et al. (2001) versus results for non-stoichiometric model (Scenario 1) developed in this work. Bars represent: ■ Stoichiometric, ■ Non-stoichiometric. Moisture (a) 0%, (b) 10%, (c) 20%, (d) 30% and (e) 40%. ....	84
Figure 27 – Scenario 2. Product gas of Curitiba's MSW gasification. Amount of air varying from 0.1 to 1 mol of air per mol of MSW that enters the gasifier. MSW's moisture varying from 0% to 60%.Legend: —●— H <sub>2</sub> , —■— CO, —▲— CO <sub>2</sub> , —×— CH <sub>4</sub> , —●— O <sub>2</sub> , —◆— C, —■— H <sub>2</sub> S, —★— N <sub>2</sub> , —✱— LHV. Moisture (a) 0%, (b) 10%, (c) 20%, (d) 30%, (e) 40%, (f) 50% and (g) 60%. ....	86

Figure 28 - Scenario 2. Low Heating values of the product gas of Curitiba's MSW gasification. .... 87

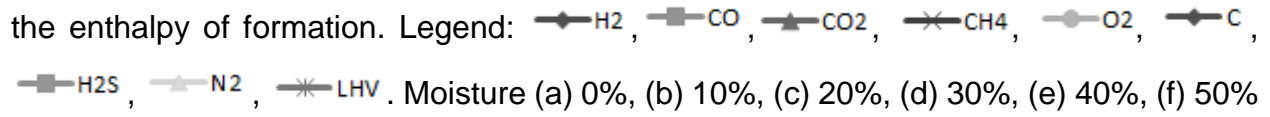
Figure 29 – Scenario 3. Product gas of Curitiba's MSW gasification. Amount of air varying from 0.1 to 1 mol of air per mol of MSW that enters the gasifier. MSW's moisture varying from 0% to 60%. Simulation carried out using the method proposed from Basu to evaluate the enthalpy of formation. Legend: . Moisture (a) 0%, (b) 10%, (c) 20%, (d) 30%, (e) 40%, (f) 50% and (g) 60%..... 90

Figure 30 - - Scenario 3. Low Heating values of the product gas of Curitiba's MSW gasification. Simulation carried out using the method proposed from Basu to evaluate the enthalpy of formation..... 91

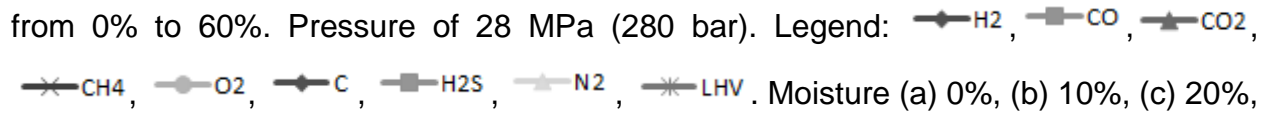
Figure 31 –Scenario 4. Product gas of Curitiba's MSW gasification. Amount of air varying from 0.1 to 1 mol of air per mol of MSW that enters the gasifier. MSW's moisture varying from 0% to 60%. Pressure of 28 MPa (280 bar). Legend: . Moisture (a) 0%, (b) 10%, (c) 20%, (d) 30%, (e) 40%, (f) 50% and (g) 60%. .... 93

Figure 32 - Scenario 4. Low Heating values of the product gas of Curitiba's MSW gasification. Pressure of 28 MPa (280 bar). .... 94

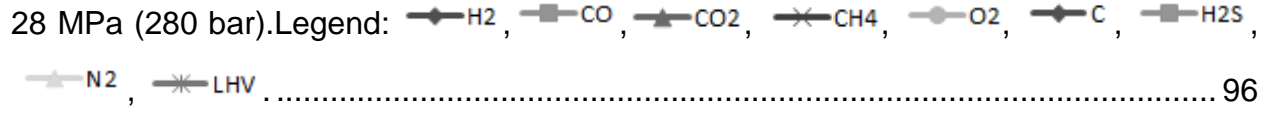
Figure 33 - Scenario 5. Product gas of Curitiba's MSW SCWG gasification. Temperatures of (a) 823.15K, (b) 923.15K, (c) 1073.15K, (d) 1173.15K and (e) 1273.15K. Pressure of 28 MPa (280 bar).Legend: . .... 96

Figure 34 - Scenario 5. Low heating value variation with MSW feed inlet variation. Temperatures of 823.15K, 923.15K, 1073.15K, 1173.15K and 1273.15K. Pressure of 28 MPa (280 bar). .... 97

## TABLES LIST

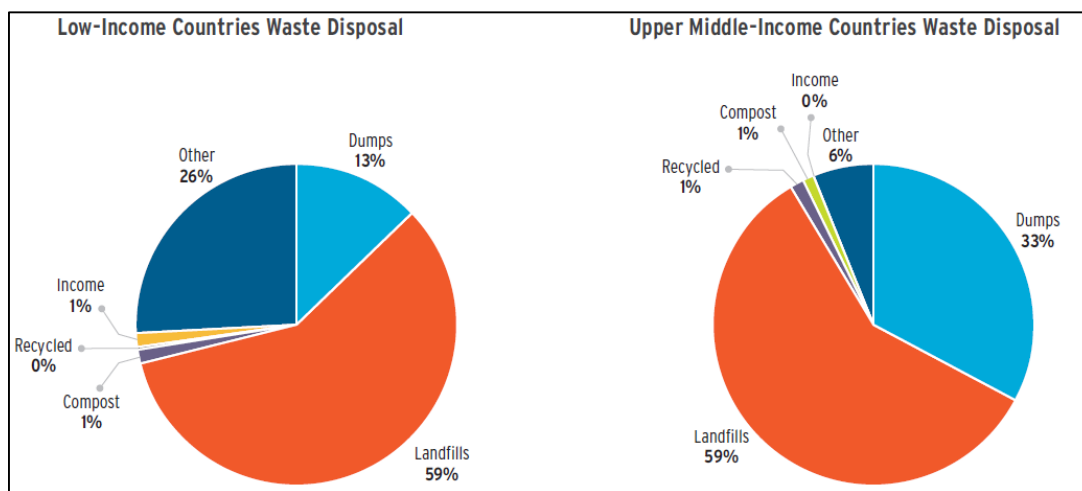
Table 1 -Collect and Generated MSW in Paraná State. Source: ABRELPE and IBGE. 17	
Table 2 –Comparison among the MSW thermal treatment technologies. Source: Wilson et al. (2013). .....	19
Table 3 – Waste-to-Energy Technologies and their corresponding Yields. Source: Young, G. C. (2010). .....	20
Table 4 - Reaction that can occur during the gasification process. Source: Adapted from Basu (2010).....	26
Table 5 – Gravimetric Composition with the ultimate analysis of São Paulo’s Municipal Solid Waste (BALCAZAR, 2011).....	59
Table 6 - Gravimetric composition of Curitiba's MSW (TAVARES, 2007). .....	60
Table 7 - Ultimate analysis estimation of Curitiba's MSW. Source: This work.....	61
Table 8 – Proposed scenarios for simulation. ....	71
Table 9 - Standard Enthalpy of formation and Standard Gibbs Free Energy (ideal gas state) of the components of the product gas and MSW.....	73
Table 10 – Ideal gas heat Capacities of pure compounds predicted as the product gas. ....	74
Table 11 - Comparison of results obtained in this work with the results presented by Zainal et al. (2001) and with the experimental results by Alaudin (1996). .....	76
Table 12 - Molar composition, in dry basis, of the gasification products of Curitiba's MSW at 1073.15 K, where m is the amount in kmol of air inject per kmol of MSW in the system. ....	77
Table 13 - Ultimate analysis from Corn-starch by Antal et al. (2000). .....	80
Table 14 - Results from the developed model. Gas composition in dry basis. ....	81
Table 15 - Low heating value variation with air inlet amount and moisture. ....	88

Table 16 - Scenario 3. Low heating value variation with air inlet amount and moisture. Simulation carried out using the method proposed from Basu to evaluate the enthalpy of formation. ....	91
Table 17 - Scenario 4. Low heating value variation with air inlet amount and moisture. Pressure of 28 MPa (280 bar). ....	94
Table 18 - Scenario 5. Low heating value variation with MSW feed inlet variation. Temperatures of 823.15K, 923.15K, 1073.15K, 1173.15K and 1273.15K. Pressure of 28 MPa (280 bar). ....	97
Table 19 – Optimum results for scenarios 2, 3 4 and 5. ....	98

## 1. CHAPTER I: INTRODUCTION

In 2012, the production of Municipal Solid Wastes was approximately 1.3 billion of tons per year, and this it is expected to grow to about 2.2 billion of tons per year by 2025. This means a significant rise on the waste generation rate per capita from 1.2 to 1.42 kg/person/day within a period of 15 years (WORLD BANK, 2012).

The generation rates of Municipal Solid Wastes (MSW) are under strong influence of the economic development, industrialization levels, consumption habits and local weather. In general, the higher the economic development and urbanization rates, the bigger are the amounts of waste produced. Income level and urbanization are highly related and as the income level and life quality standards grow, the consumption of goods and services increase and thus the waste generation increases. Bearing in mind that the residents living in urban areas can produce twice as much waste as those living in the rural areas (WORLD BANK, 2012). Figure 1 shows how the disposal of waste is distributed in low-income countries and upper middle-income countries.



**Figure 1 - Waste disposal distribution in low-income and upper middle-income countries. Source: World Bank, 2012.**



There is worldwide accepted hierarchy when waste management is concerned, as presented in Figure 2. Its first use appeared in Ontario's pollution probe in the 70's. Such hierarchy begun with the three Rs (Reduce, Reuse and Recycle), and usually is added another R for Recover. This classification takes in consideration financial aspects, environment, social and handling for the waste (WORLD BANK, 2012).

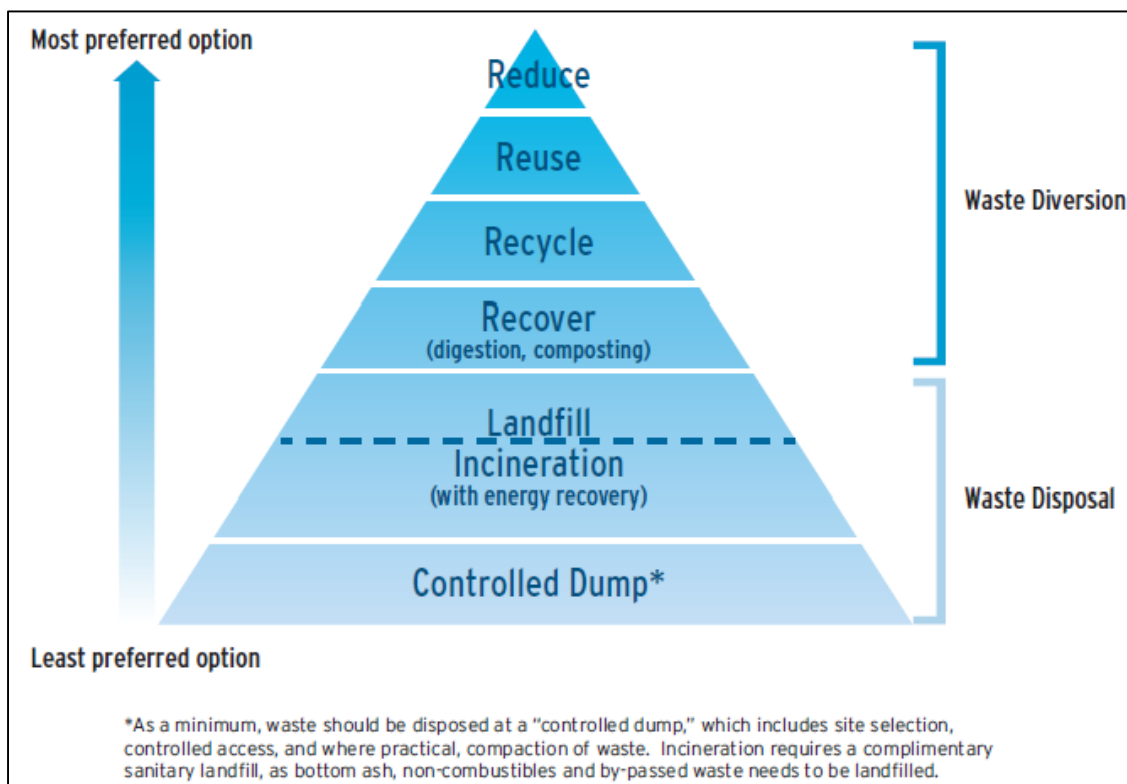


**Figure 2 – Hierarchy in waste destination. Source: World Bank, 2012.**

The disposal of municipal solid waste in Brazil is a challenge. The national plan for Solid Waste (PNRS), established by Federal law n°12.305/2010, introduced the concepts of avoidance, reduce, reuse, recycle and reuse of the solid wastes. In which the disposal in landfill will be the last option for final disposal. It also had established the total removal of the unsanitary landfills until August 2014. However with the Senate law project n°425/2014, the deadline to implement the law was modified and now it relates the deadline with the number of inhabitants within the municipality. The maximal deadline can reach until 2021. To meet such demand, the State of Paraná established the program

“PARANÁ SEM LIXÕES” (Parana without unsanitary landfills), throughout the law decree 8656 of July 31, 2013.

The compliance to meet the new law, however, is not a simple task. The report from the Environmental Paraná Institute (IAP), published in February 2013, shows that many municipalities (about 30%) are in irregular situation and still disposal their waste in unsanitary landfills.

The Brazilian Solid Waste Outlook from 2013, published by ABRELPE, Figure 3, quantified a total amount of 189,219 tons/day of municipal solid waste collected, of which 58.3% are disposed in landfills, 24.3% “controlled landfills” and 17.4% to unsanitary landfills. The Outlook also reveals that from the 5570 Brazilian municipalities, only 2226 are disposing their waste in landfill, 1775 in “controlled landfills” and 1569 to unsanitary landfills.

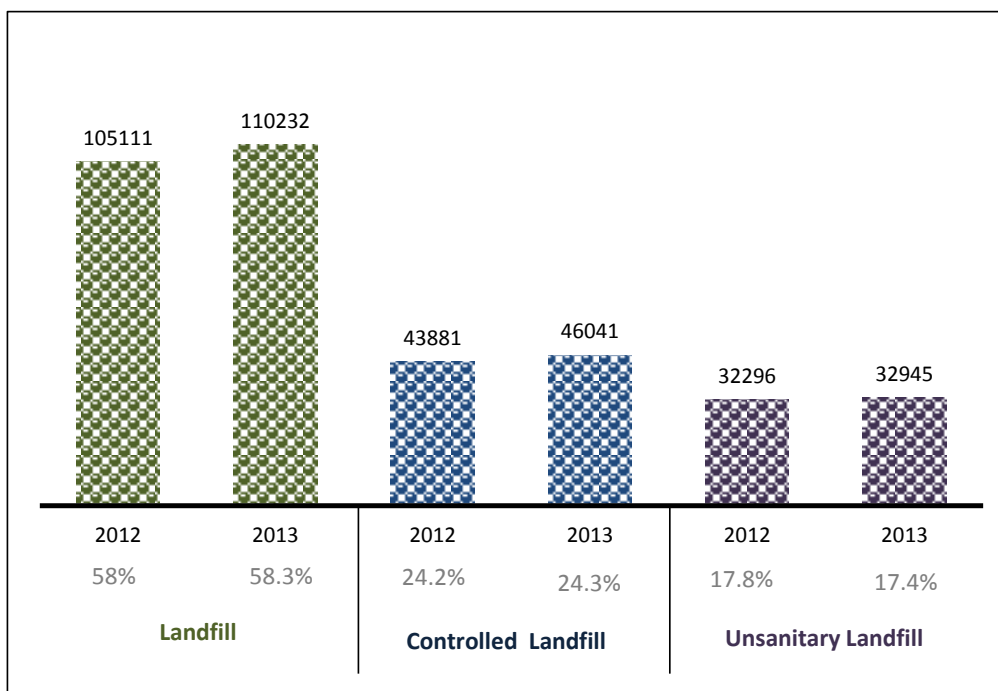


Figure 3 - Final destination of MSW in Brazil (ton/day). Source: Adapted ABRELPE.

ABRELPE estimated the index of MSW *per capita* generated for Brazil and its macro-regions, in which the Brazilian average, in 2013, is 1.041 kg/person/day. In south the average is 0.761 kg/person/day. The region with the greatest average *per capita* is Southeast, with 1.209 kg/person/day. For the collected MSW the Brazilian average is 0.941 kg/person/day, in which the south with 0.716 kg/person/day, being the also the southeast region with the bigger average with 1.173 kg/person/day.

In the state of Paraná, *per capita* average of collected MSW is slightly higher above the South Region with 0.739 kg/person/day, with a waste collected average of 8123 ton/day. Some of these numbers are shown in Table 1 and Figure 4.

**Table 1 -Collect and Generated MSW in Paraná State. Source: ABRELPE and IBGE.**

Total population		Collected MSW				Generated MSW (t/day)	
		kg/hab/day		t/day			
2012	2013	2012	2013	2012	2013	2012	2013
10,577,755	10,997,465	0.735	0.739	7,771	8,123	8,507	8,638

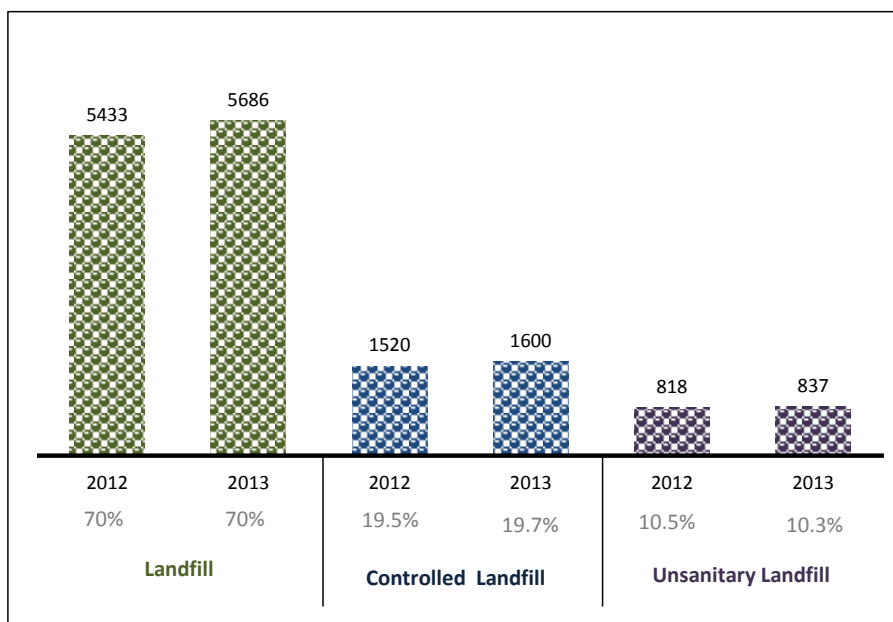


**Figure 4 - Final destination of Paraná's MSW (ton/day). Source: ABRELPE.**

## 1.1 WASTE AS ENERGY SOURCE

As the Brazilian society develops itself, the demand for goods and services also increases. This rise also causes the increase of energy consumption. Specifically for electricity, in 2014, the electricity consumption was 535.2 TWh, being projected for 2018 641.8 TWh and for 2023 a consumption of 780.4 TWh (PDE 2023, 2014).

To meet such increase in electricity demand, the Brazilian Research Company (EPE) has chosen to expand the Brazilian generation power capacity also with thermoelectric power plants between the years 2019 and 2023, amounting 7500 MW of installed capacity (PDE 2023, 2014).

The thermoelectric power plant shows itself more advantageous when near the demanded area. In addition, it becomes more cost effective when the fuel is near and concentrated in a single area, not being necessary to spend with transportation to bring the fuel to the power plant (ZAMBON ET AL., 2003; BRASIL, 2003).

Biomass fueled power plants encounter difficulties to operate mainly due to the cost of biomass and due to the fact that biomass is usually disperse in a large area and not concentrated in just one location (BARBA ET AL., 2011).

This obstacle can be overcome throughout the use of the Residue Derived Fuel (RDF), which originates from Municipal Solid Waste that is present in large amounts in areas where it is disposed. Yet, the heterogeneous composition of RDF restricts its use for other kind of industry (cement industry, steel, etc.) that always prefer raw material with low quality variability. Being, then, an opportunity to the energetic use of RDF throughout gasification (BARBA ET AL., 2011).

There are several technologies for the conversion of waste into energy. They are usually denominated Waste-to Energy or WTE technologies (WILSON ET AL., 2013).

Combustion and incineration is the thermal breakdown of waste through the supplying of excess air, producing flue gas (CO<sub>2</sub>, O<sub>2</sub>, N<sub>2</sub> and steam) and heat (ALTERNATIVE WASTE CONVERSION TECHNOLOGIES, ISWA, 2013).

Gasification can be defined as the thermal breakdown of the waste under a sub-stoichiometric atmosphere of oxygen and has as product the synthesis gas or syngas (ALTERNATIVE WASTE CONVERSION TECHNOLOGIES, ISWA, 2013).

Pyrolysis is the thermal breakdown of the waste in absence of air, and has as products coke, pyrolysis oil and synthesis gas (ALTERNATIVE WASTE CONVERSION TECHNOLOGIES, ISWA, 2013).

## 1.2 EFFICIENCY COMPARISON AMONG THERMAL TREATMENT TECHNOLOGIES

Among the various waste-to-energy technologies, the gasification is attractive that as being seen as a feasible option for high efficiency for electricity generation or to produce liquid fuels and chemicals (KANGAS ET AL., 2014).

A comparison made by Wilson et al. (2013), Table 2, shows that conventional gasification would have higher yield to the electricity generation at a smaller unitary cost than other technologies.

**Table 2 –Comparison among the MSW thermal treatment technologies. Source: Wilson et al. (2013).**

<b>Performance parameter</b>	<b>Incineration</b>	<b>Pyrolysis</b>	<b>Plasma Gasification</b>	<b>RDF Conventional Gasification</b>
<b>Capacity ton/day</b>	250	250	250	250
<b>Conversion efficiency (MWh/ton)</b>	0.5	0.3	0.4	0.9
<b>Construction Cost</b>	70	40	100	28
<b>Power generation capacity MWh/day</b>	160	180	108	224
<b>Unitary Cost/kWh installed</b>	435	222	1000	125
<b>Unitary Cost (US\$/nominal ton/day)</b>	500	160	960	112

Source: Adapted from Wilson et al. (2013)

Also, as already showed by Young, G. C. (2010), when compared, Table 3, the various thermal treatments for MSW, it can be observed also a higher yield for electricity generation with gasification.

**Table 3 – Waste-to-Energy Technologies and their corresponding Yields. Source: Young, G. C. (2010).**

<b>Technology</b>	<b>Net Energy to the Grid</b>
<b>Incineration</b>	544 kWh/ton MSW
<b>Pyrolysis</b>	571 kWh/ton MSW
<b>Pyrolysis/gasification</b>	685 kWh/ton MSW
<b>Conventional gasification</b>	685 kWh/ton MSW
<b>Arco-Plasma Gasification</b>	816 kWh/ton MSW

### 1.3 OBJECTIVES

The goal of this work is to develop a model to correct predict the gasification product gas. Also once the correct predictions are validated an optimization of the process conditions is required.

## 2. CHAPTER II: BIBLIOGRAPHIC REVIEW

### 2.1 GASIFICATION

Gasification is a chemical process that converts organic based materials such as biomass in gases that can be utilized as gaseous fuels or as raw-material to produce chemicals (BASU, 2010).

Gasification is an old process with the objective to obtain a gaseous fuel, which has better transport features, better combustion efficiency and that also can be utilized as raw-material to others processes (CENBIO, 2002).

Gasification and combustion are two thermochemical processes that are closely related. However, there is an important difference between them. Gasification compacts the energy in the chemical bounds in the molecules of the product gas, while combustion breaks the bounds to release the energy in the molecules. The gasification process adds hydrogen and removes carbon from the raw-material to produce gases with high content of hydrogen/carbon (H/C), while combustion oxides the hydrogen and carbon in water and carbon dioxide (BASU, 2010).

The gasification process converts biomass in synthesis gas or syngas. It is the production of this gas that makes the gasification so different from incineration. In gasification, the biomass is not a fuel but a raw-material for a thermochemical conversion process. Instead of producing only heat and electricity, the synthesis gas can be transformed in a highly valued commercial product, as showed in Figure 5, such as transportation fuels, chemicals, fertilizers and even for the replacement of natural gas (GASIFICATION COUNCIL, 2015).

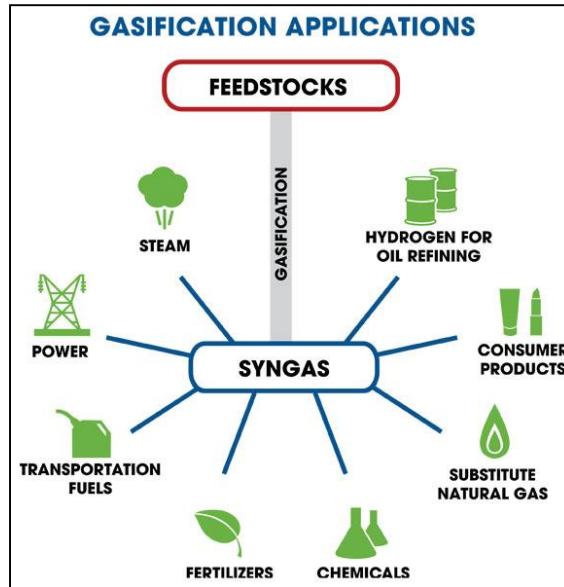


**Figure 5 - Possible applications for the synthesis gas and gasification. Source: Gasification Council, 2015.**

The biomass gasification process has various complex reactions, that are still not well known (CENBIO, 2002), but they occur at elevated temperatures in reduction conditions (KANGAS ET AL., 2014).

Pyrolysis is a thermal decomposition process that partially removes carbon from the raw-material, but does not add hydrogen. Gasification, in the other hand, requires a gasification agent such as steam, air or oxygen in order to rearrange the molecules from the raw-material, in such a way that is possible to convert it from its solid state to gases or liquids, within this process hydrogen is aggregate to the product (BASU, 2010).

Another step that can be added is the tar cracking, which transforms the molecules that compose the tar in gases such as CO, CO<sub>2</sub> and CH<sub>4</sub> (CENBIO, 2002).



### 2.1.1 GASIFICATIONS AGENT

Gasification requires an agent that can rearrange the molecular structure of the feedstock to convert it into useful gaseous fuels (BARUAH & BARUAH, 2014).

The correct use of the gasification agent is essential to the process. The gasification agents react with solid carbon and the heavy hydrocarbons to crack them in light gases, such as CO and H<sub>2</sub>. The most common gasification agents are (BASU, 2010):

- Oxygen
- Steam
- Air

Depending on the gasifying agent the gasifiers can also be classified differently (Baruah & Baruah, 2014).

Oxygen is popular a gasification agent, although is used first for the combustion step. It can be supplied pure or as air to the gasifier. The caloric value and composition of the produced gas are strong functions of the nature of the gasifier agent (BASU, 2010).

Figure 6 illustrates the conversion paths and the different products that can be formed:

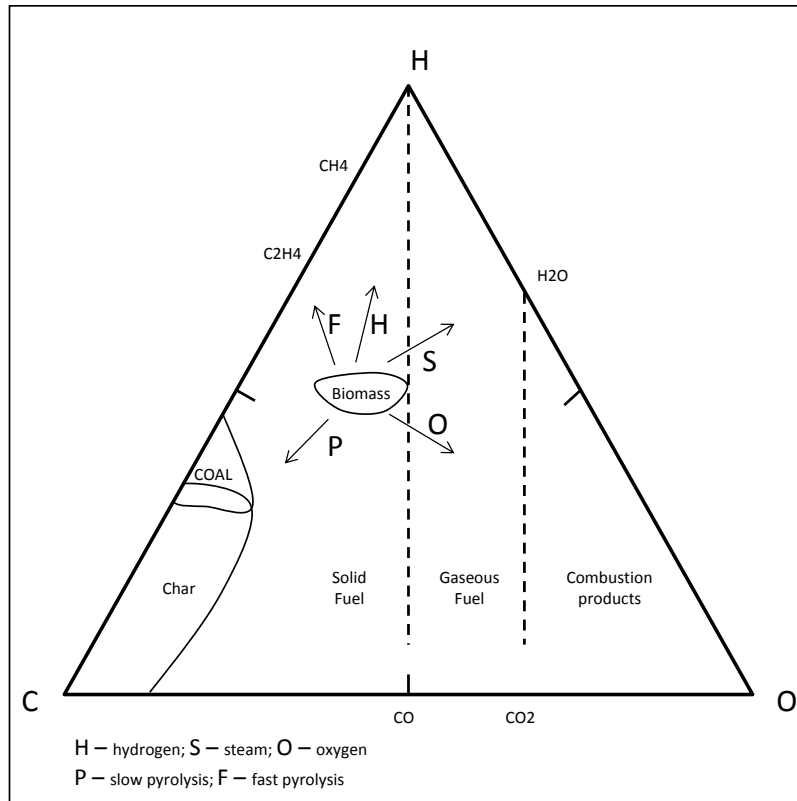


**Figure 6 – Ternary diagram C-H-O of the gasification process. Source: Adapted from Basu (2010).**

If oxygen is used as gasification agent, the path of conversion moves towards the oxygen apex. The product includes CO for low oxygen content and CO<sub>2</sub> for high contents. When the amount of oxygen exceeds the stoichiometric proportion the process is out of the gasification and becomes combustion. When further moving to the oxygen apex the products diminish the hydrogen content and increase the amount of carbon, CO and CO<sub>2</sub> (BASU, 2010).

When steam is used as gasifier agent, the reaction moves towards the hydrogen apex. The product, thus, will have a highly hydrogen content per Carbon unit (rate H/C). Some intermediary reaction products, such as CO and H<sub>2</sub>, also help to gasify the solid carbon (BASU, 2010).

The choice of the gasifying agent influences the caloric value of the gaseous products. If air is used instead of oxygen, the nitrogen will dilute the final product (BASU, 2010).

### 2.1.2 THE GASIFICATION PROCESS

The gasification of biomass usually involves the reactions that involves various phenomena such as drying, pyrolysis, oxidation and reduction (PATRA & SHETH, 2015).

According to Basu, 2010 a typical biomass gasification process usually includes the following steps:

- Pre-heating and Drying
- Thermal breakdown and pyrolysis
- Partial combustion of some gases and vapors and carbon
- Gasification of the decomposed products

Although these processes are modelled in series, there is no clear boundary among them and they often overlap (BASU, 2010)

First the biomass is heated then the thermal degradation or material pyrolysis begins. The pyrolysis products (usually gas, solid and liquid) react with each other and with the gasification agent to form the final gasification product. The gasifications reactions are mostly endothermic in nature (PATRA & SHETH, 2015). In most commercial gasifiers the thermal energy, required to drying, pyrolysis and endothermal reactions come from certain amounts that are been combusted. Table 4 shows a list with the most important reactions that can occur during the gasification process (BASU, 2010).

Table 4 - Reaction that can occur during the gasification process. Source: Adapted from Basu (2010).

Typical Gasification Reactions			
Reaction Type	Reaction	$\Delta H_r(\text{kJ/mol})$ at 25°C Source	
<b>Carbon Reactions</b>			
R1 (Boudouard)	$\text{C} + \text{CO}_2 \rightleftharpoons 2\text{CO}$	172	1
R2 (water-gas or steam)	$\text{C} + \text{H}_2\text{O} \rightleftharpoons \text{CO} + \text{H}_2$	131	2
R3 (hydrogasification)	$\text{C} + 2\text{H}_2 \rightleftharpoons \text{CH}_4$	-74.8	2
R4	$\text{C} + 0.5\text{O}_2 \rightarrow \text{CO}$	-111	1
<b>Oxidation reactions</b>			
R5	$\text{C} + \text{O}_2 \rightarrow \text{CO}_2$	-394	2
R6	$\text{CO} + 0.5\text{O}_2 \rightarrow \text{CO}_2$	-284	4
R7	$\text{CH}_4 + 2\text{O}_2 \rightleftharpoons \text{CO}_2 + 2\text{H}_2\text{O}$	-803	3
R8	$\text{H}_2 + 0.5\text{O}_2 \rightarrow \text{H}_2\text{O}$	-242	4
<b>Shift Reaction</b>			
R9	$\text{CO} + \text{H}_2\text{O} \rightleftharpoons \text{CO}_2 + \text{H}_2$	-41.2	4
<b>Methanation Reactions</b>			
R10	$2\text{CO} + 2\text{H}_2 \rightleftharpoons \text{CH}_4 + \text{CO}_2$	-247	4
R11	$\text{CO} + 3\text{H}_2 \rightleftharpoons \text{CH}_4 + \text{H}_2\text{O}$	-206	4
R14	$\text{CO}_2 + 4\text{H}_2 \rightleftharpoons \text{CH}_4 + 2\text{H}_2\text{O}$	-165	2
<b>Steam-Reforming Reactions</b>			
R12	$\text{CH}_4 + \text{H}_2\text{O} \rightleftharpoons \text{CO} + 3\text{H}_2$	206	3
R13	$\text{CH}_4 + 0.5\text{O}_2 \rightarrow \text{CO} + 2\text{H}_2$	-36	3
Sources:			
1 - Higman and van der Burgt, 2008, p.12.			
2 - Klass, 1998, p. 276.			
3 - Higman and van der Burgt, 2008, p. 3.			
4 - Knoef, 2005, p. 15.			

### 2.1.3 DRYING

In the drying stage moisture present in fuel evaporates releasing steam (BARUAH & BARUAH, 2014).

High moisture levels are big losses for the system, especially when regarding power generation. Each kilogram of moisture takes out of the system 2260 kJ of energy, used to vaporize the water. A certain amount of the pre-heating is required, then, for the

gasifier to be efficient. For the production of the fuel gas, with a good caloric value, it is recommended that the moisture of the biomass be between 10% and 20% (BASU, 2010).

The final drying occurs after the raw-material inlet in the gasifier, where it receives the gasifier internal heat streams (BASU, 2010).

#### 2.1.4 PYROLYSIS

The volatile component of the feedstock is vaporized as it is heated. These vapors will be further transformed into mainly hydrogen, carbon monoxide, carbon dioxide, methane, hydrocarbon gases, tar, and water vapour (BARUAH & BARUAH, 2014).

In pyrolysis there is no external agent added. At the slow pyrolysis more carbon is formed. At the fast pyrolysis more liquid hydrocarbons are formed. In pyrolysis, that precedes the gasification, there is the thermal breakdown of the long chain hydrocarbons that become smaller gaseous molecules (condensable or not) and Figure 7 shows the potential path ways for gasification preceded by the pyrolysis step (BASU, 2010).

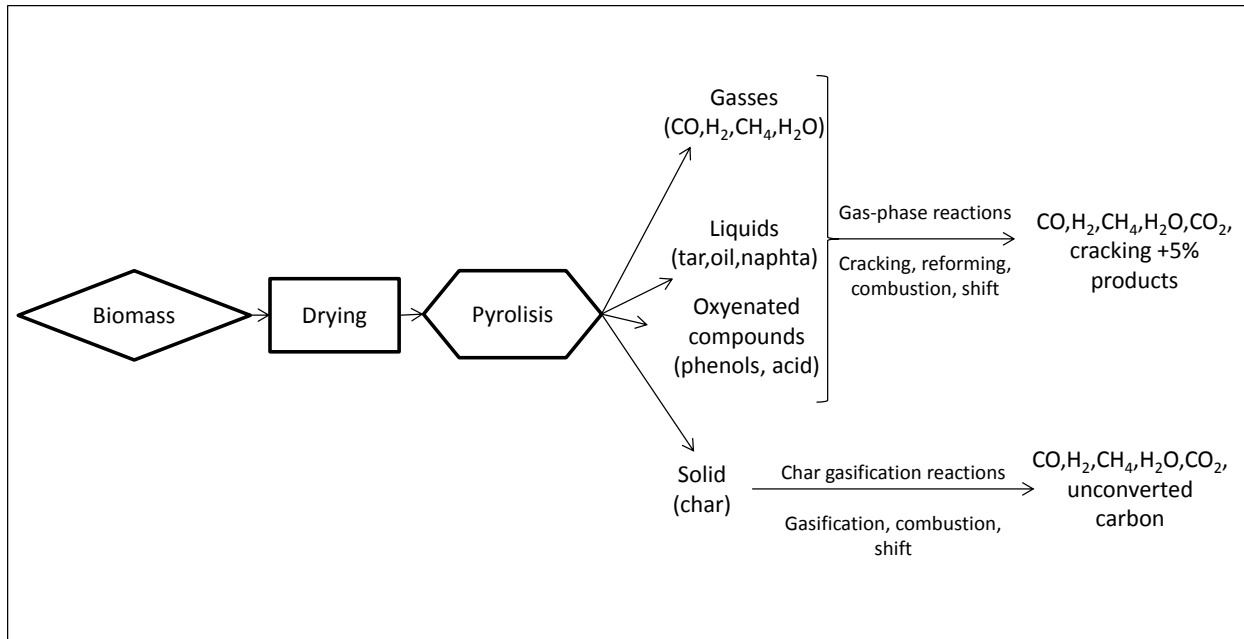


Figure 7 – Potential paths for gasification. Source: Adapted from Basu (2010).

## 2.2 TYPES OF GASIFIERS

The reactor where occur the gasification can be called gasifier (LOPES, 2014).

The gasifiers can be classified according various criteria (PUIG-ARNAVAT et al., 2010):

- By gasifying agent
- By heat source
- By the gasification pressure (atmospheric or pressurized)
- By the reactor design
  - Fixed Bed
  - Fluidized Bed (bubbling, circulating or twin-bed)
- Entrained flow
- Stage gasification (with physical separation of the zones pyrolysis, Oxidation and/or reduction).

The sequence of the gasification reactions is dependent of the gasifier. Depending on the design, the gasifier can promote more or less contact between the gas and solid

phases (BASU, 2010). Altering, thus, the yield of the gasification reactions and tar formation.

According to Basu, 2010, there are three main types of gasifiers:

- Fixed or moving bed
- Fluidized bed
- Entrained flow

Each one of these gasifier types are subdivided in more specific ones. Each gasifier has a specific range for application (Figure 8 and Figure 9). It is based on the thermal energy capacity that the equipment can deliver (BASU, 2010).

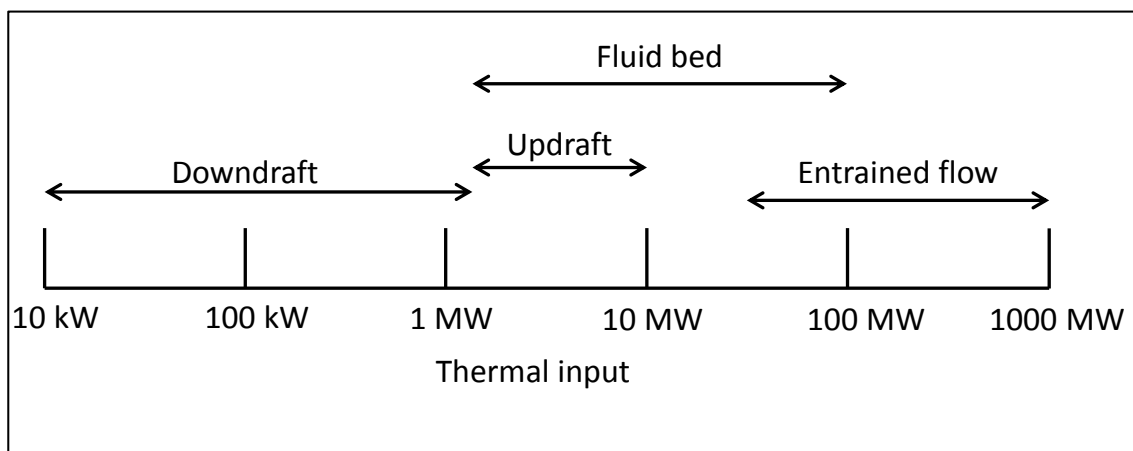


**Figure 8 - Applicability range for the biomass gasifiers. Source: Adapted from Basu (2010).**

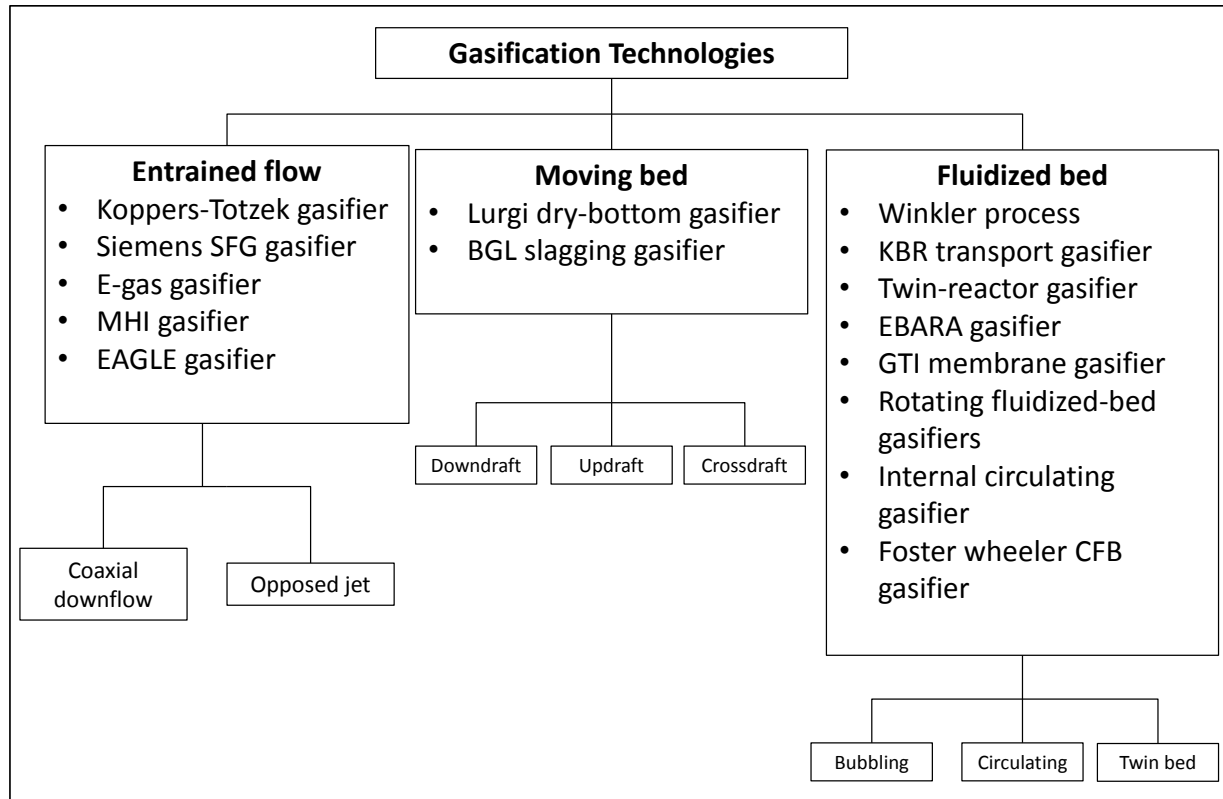


**Figure 9 - Different types of gasifiers and their commercial suppliers. Source: Adapted from Basu (2010).**

### 2.2.1 FIXED OR MOVING BED REACTORS

They are called fixed bed because the fuel is supported on a grate. They can also be called moving bed, because the fuel moves from the inlet in the top until below, As a Plug-flow for the solid phase. This type of gasifier can be assembled in small sizes and very cheap. Therefore a large number of small scale fixed/moving bed gasifiers are founded in the whole world. However the turbulence and the heat transfer inside the reactor is poor, thus it is difficult to obtain a uniform distribution for the fuel, temperature and gas composition inside the reactor. The fuel can form agglomerates inside the gasifier. There are three main types: (1) updraft, (2) downdraft and (3) crossdraft (BASU, 2010).



In fixed bed gasifiers the solid fuel is gasified in layers, in such a way that the different zones (drying, pyrolysis, reduction and oxidation) are distinguishable (LOPES, 2014).

### 2.2.2 UPDRAFT GASIFIERS

The updraft gasifiers have a simple and old design. The gasification agent (air, oxygen or steam) has an upward flow. At the same time, the fuel moves downward, thus creating a countercurrent flow and then comes out from the top. The gasification agent enters the gasifier throughout a grate or distributor, where it encounters a layer of hot ashes. The ash falls from the grate, in which is removed by a mechanism inside the reactor. It is important to notice that there are zones where the oxidation, gasification, pyrolysis and drying occur (BASU, 2010). Figure 10 show the schematics of a typical updraft gasifier.

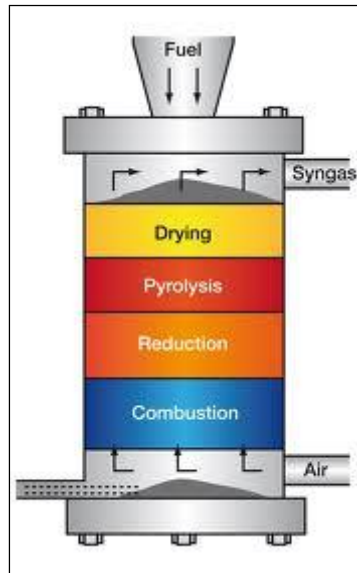


**Figure 10 - Schematic of an updraft gasifier.**

At the top of the gasifier, the fed biomass is dried and passes through the pyrolysis zone, where it is decomposed to volatiles, tar and char. This volatile-free biomass combine with the gas stream leaving the reduction zone located above the bottom, the combustion zone. In the combustion zone, the biomass gets oxidized and flue gases are generated (PATRA & SHETH, 2015).

The tar production is very high (30-150 g/Nm<sup>3</sup>), which makes this gasifier not adequate for production of high volatility. They are better used for fuel with high ash content (until 25%) and high moisture (BASU, 2010).

### 2.2.3 DOWNDRAFT GASIFIERS

In a downdraft gasifier, both biomass and air move the downward direction in the lower section of the gasifier unit (PATRA & SHETH, 2015).

In this reactor the gasification agent (oxygen, air and steam) and the fuel has a downward flow, or co-current. The product gas goes through a hot ash layer, where tar is cracked. For this reason, the downdraft gasifiers are the ones with less tar production (BASU, 2010). However the caloric value of the product gas is lower (LOPES, 2014). Figure 11 show the schematics of a typical downdraft gasifier.

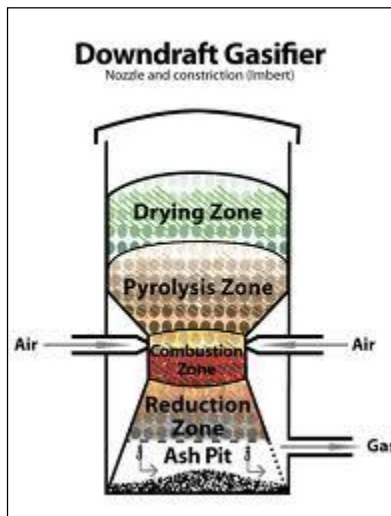


**Figure 11 – Schematic of a downdraft gasifier.**

Downdraft Gasifiers work well with internal combustion engines, because of its lower tar content in the product gas ( $0.015\text{-}3\text{g}/\text{Nm}^3$ ). Also they need less time to ignite (20-30 minutes) (BASU, 2010).

#### 2.2.4 CROSSDRAFT GASIFIERS

The crossdraft gasifier, Figure 12, works with a co-current flow, between the bed and the fuel. The Fuel is fed in the top, while the gasification agent (oxygen, air and steam)

enter from the side. The product gas comes out by the opposite side to the feed. Due to a configuration it is also called sidedraft (BASU, 2010).

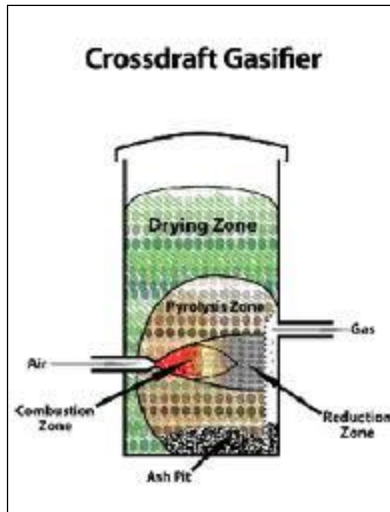


**Figure 12 – Schematic of a crossdraft gasifier.**

A hot combustion/gasification zone forms around the air entrance and pyrolysis and drying zones get formed in the vessel (PATRA & SHETH, 2015).

This type of gasifier is usually used in small scale units. One feature is that, due to its small reaction zone the reactor provides quick responses. The time to ignite of this gasifier is from 5 to 10 minutes. With this reactor is also possible the utilization of internal combustion engines, once the content of tar in the product gas stay in the range of 0.01 and 0.1 g/Nm<sup>3</sup>. They require also simpler systems for gas cleaning (BASU, 2010).

The gasifying feed rate in this reactor is greater than the other types, with that in its interior is created a combustion zone with high temperatures, with quick gas liberation (LOPES, 2014)

## 2.2.5 FLUIZIZED BED GASIFIERS

Fluidized bed gasifiers are known by their excellent turbulence and homogeneous temperature distribution (BASU, 2010). In this type of reactor there are no distinct reaction zones (LOPES, 2014). A fluidized bed is composed by granular solids, called bed materials, which are maintained in a semi-suspended (fluidized) state due to the flow of the gasifying agent. Its good gas-solid mixture and high thermal inertia make the gasifier almost insensible to the fuel quality. Besides, the thermal homogeneity reduces the risk of the fuel to agglomerate (BASU, 2010). The main objective of this gasifier type is the conversion of biomass in a product free from tar (LOPES, 2014). According to Milne et al (1998), the average of the tar content is 10 g/Nm<sup>3</sup>. There are two main types of fluidized bed: Bubbling and circulating (BASU, 2010). The basic difference between them is the bed velocity (LOPES, 2014; CENBIO, 2002).

#### 2.2.5.1 BUBBLING FLUIDIZED BED

Bubbling fluidized bed reactors, Figure 13, are especially recommended for medium sized units (<25MWth). The gasifier developed by Fritz Winkler in 1921 is, perhaps, the oldest commercial gasifier that has been largely used to the gasification of the coal. For biomass it is one of the most popular options (BASU, 2010).

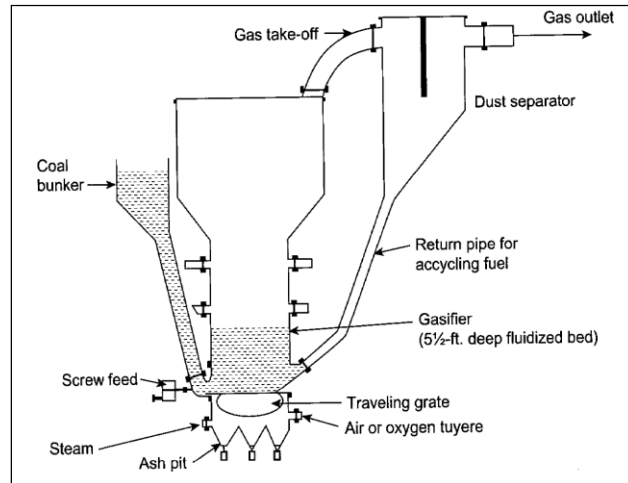


**Figure 13 - Schematic of a Winkler bubbling fluidized bed. Source: Basu (2010).**

Commonly used in a fluidized bed, the biomass has its size reduced to less than 10 mm and then fed to the reactor. This biomass is fluidized with steam and air/oxygen (BASU, 2010).

The fluidized bed gasifiers can operate in high or low temperature, in atmospheric pressure or pressurized. The high temperature Winkler gasifier (HTW) is an example of a reactor that operates in high temperature and pressurized. The gasification agent is fed into the reactor in different levels. The bed is maintained at 10 bar and 800°C to avoid ash fusion (BASU, 2010) by controlling the air/biomass ratio (Patra & Sheth, 2015). The region above the bed has a temperature of 1000°C to minimize the production of methane and other hydrocarbons. The HTW process produces a better quality gas when compared to the low temperature processes. Although originally developed for coal, it can be used for biomass and MSW (BASU, 2010). The tar content of the product gas is low (<1-3 g/Nm<sup>3</sup>) (PATRA & SHETH, 2015).

#### 2.2.5.2 CIRCULATING FLUIDIZED BED

The circulating fluidized-bed is based on the mechanism of continuous circulation of the bed material between the reaction vessel and a cyclone separator, where the ash is separated and the bed material and char return back to the reaction vessel (PATRA & SHETH, 2015). A Circulating Fluidized Bed (CFB), Figure 14, has a special appeal to biomass due to the long residence time that it can promote. It is especially when suitable for fuels with high volatility. A CFB has typically a riser, a cyclone and a solid recycling system. The riser works as the gasifiers. In the CFB the solids are dispersed all over the rise height, allowing a long residence time for the gas and the particulate matter. Depending on the fuel application, the riser can operate from 800 to 1000°C. Many manufactures have developed CFB gasifiers (BASU, 2010).

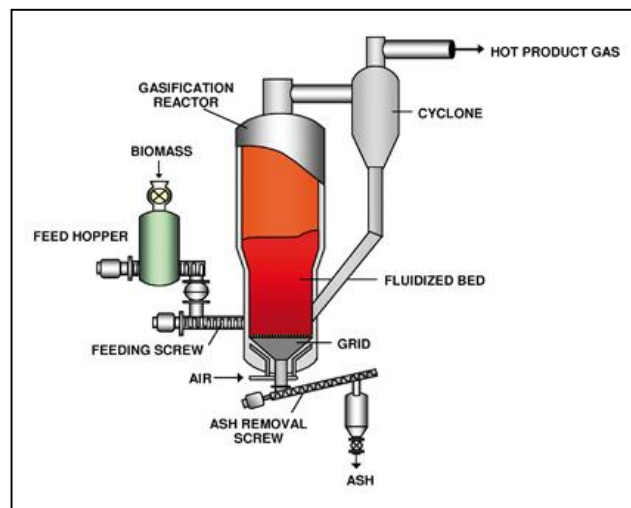


**Figure 14 – Schematic of a CFB gasifier. Source: Basu (2010).**

## 2.2.6 ENTRAINED-FLOW GASIFIERS

The entrained-flow gasifier, Figure 15, is most successful and largely used for large scale coal, oil coke and refinery waste gasification. It is especially suitable with various coal types, except the ones with low rank, which as lignite and biomass are not attractive due the high moisture content (BASU, 2010).

The compatibility with the entrained-flow for biomass gasification is questionable due to many reasons. They have low residence time (some of them only seconds), the fuel has to be very fine, which for fibrous biomass is difficult to achieve. For biomass with CaO, but without alkali the fusion point is high and thus there is need for more oxygen. The fusion ash-melting point of biomass with alkali is much higher than the coal's. Therefore, although it is good at destroying tar, the entrained-flow gasifier shows many problems with biomass and is not recommended (BASU, 2010).

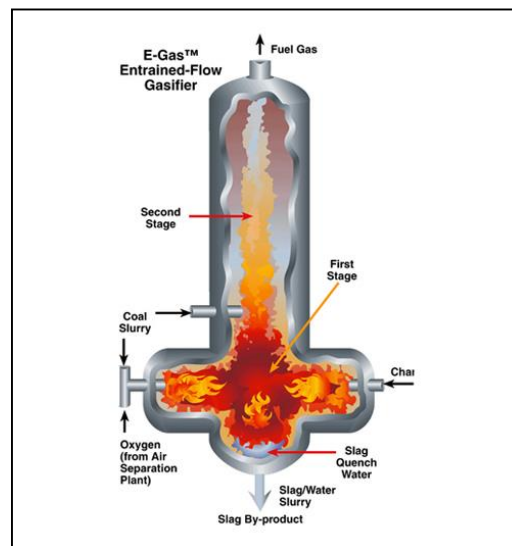


**Figure 15 – Schematic of an Entrained –Flow gasifier.**

## 2.2.7 PLASMA GASIFIER

Plasma gasification uses an external heat source to gasify the biomass, resulting very little combustion. Almost all of carbon is converted to fuel gas (MOUNTOURIS ET AL.,2006).

In plasma gasification, the plasma at high temperature helps the gasification of the biomass. This technology is suitable for municipal solid waste (MSW) and other wastes.



This process implicate in the disintegration of the carbon based materials in a poor oxygen environment. The heart of the process is the plasma torch, where an electric arc is created between two electrodes inside a vase. An inert gas is injected through this arc. Although the arc temperature is very high (~13,000°C), the gasifier temperature is much lower (2,700-4,500°C). This temperature is enough to crack the most complex hydrocarbons in synthesis gas (CO+H<sub>2</sub>). At the same time, all inorganic compounds (glass, metals, silicates, heavy metals) are melted in a volcanic-type lava, which, after cooling, becomes a basaltic slag. The synthesis gas comes out of the reactor with a high temperature (1,000-2,000°C). Due to the high temperatures all the dioxins and furans are destroyed. A clear advantage of this gasifier is its robustness and it is practically insensible to the raw-material fed. However, the plasma torch can present a high electricity consume (BASU, 2010).



**Figure 16 – Schematic of a Plasma gasifier. Source: AlterNRG.**

## 2.3 GASIFICATION THERMODYNAMIC MODELLING

To begin any industrial process modelling it is required to know all the main features and amounts involved so one can evolve to costs and economic feasibility studies of the business. Modelling the gasification reactions occurring inside a gasifier is not a trivial matter. There are many modelling proposals in the current literature.

Detailed models with mass transfer can include computational fluid dynamics (CFD) calculations, which can provide the basis for a gasifier design. However, CFD models are usually very complex to be suitable with spreadsheets of mass and energy balances during the design phase (KANGAS ET AL., 2014).

Puig-Arnavat et al. (2010) gathered various gasification models for biomass. They are classified in kinetic models, thermodynamic equilibrium models, Aspen plus models and neural network models.

The kinetic models are based on experiments and can vary greatly according to the mechanism adopted in its development. In addition, it has some parameters that limit their applicability to other kind of configuration from the previous studied. Therefore, thermodynamic equilibrium models, which are independent of the reactor design, can be more suitable to the process study and to evaluate the influence of the main fuel characteristics (PUIG-ARNAVAT ET AL., 2010) and the thermodynamic equilibrium is often used as guide to process modelling, even though is not reached in practice (KANGAS ET AL., 2014).

The thermodynamic equilibrium cannot be reached during the gasification process, however, thermodynamic equilibrium models had been used by many authors, as, for example, Bacon et al., Zainal et al., Li et al. and many others. These authors showed that a good agreement between experimental and simulated data can be reached (PUIG-ARNAVAT ET AL., 2010).

Equilibrium models are usually divided in two types: stoichiometric and non-stoichiometric. The stoichiometric modelling requires a clear identified reaction mechanism that incorporates all the reactions and species involved in the process. In the non-stoichiometric modelling there is no need to specify a particular mechanism. In this last type, only the ultimate analysis of the fuel is required. Although both stoichiometric and non-stoichiometric approaches minimize the Gibbs free energy, the non-stoichiometric modelling is made without the need of specifying the reactions involved in

the process, in the other hand the stoichiometric modelling is based on the chemical species present in greater amounts, which means, only the ones with low values of free energy of formation (PUIG-ARNAVAT ET AL., 2010).

The two types of equilibrium modeling are essentially equivalent. A stoichiometric model can also use free energy data to determine the equilibrium constants for the proposed chemical reactions (PUIG-ARNAVAT ET AL., 2010).

The thermodynamic equilibrium models are important because they can predict the limits of the gasification reaction (PUIG-ARNAVAT ET AL., 2010). However, they still have limitations and need to assume certain premises that not always are the reality in the process. Many authors are proposing modifications in the equilibrium models and they obtained good results, depending on the type of the adopted reactor (PUIG-ARNAVAT ET AL., 2010).

With the objective of simplifying the modelling process and avoid complications, some authors have developed models using Aspen Plus. This is a software oriented to the resolution of calculations and problems for process simulations. Aspen plus facilitates the process creation, once it is possible to integrate many sections in one single model. This simulator has big data bank, which contains many properties from the chemical species involved. When needed, it is possible to construct more complex subroutines, using FORTRAN (PUIG-ARNAVAT ET AL., 2010).

Despite largely used in the simulation of coal, the simulation with biomass is less intensive. These simulations involve the composition of modules available in the software to perform hydrodynamic calculations with Gibbs free energy minimization, been possible also the use of kinetic models (PUIG-ARNAVAT ET AL., 2010).

Models that do not impose any mechanisms nor equilibrium are already in literature. Artificial neural networks have been extensively used in the field of pattern recognition, sign processing, functions approximation and process simulations. Sometimes hybrid neural networks are synthesized to model processes (PUIG-ARNAVAT ET AL., 2010).

Addressing the modelling of the municipal solid waste gasification, Barba et al., 2011, developed a thermodynamic equilibrium model based on the minimization of the Gibbs free energy.

The chemical energy in the synthesis gas is a function of its chemical composition, thus this composition is what determine the quality of the fuel (BARBA ET AL., 2011).

Although the biomass gasification is a well-known technology, it still not reached a commercial scale, due to many technical difficulties that are not resolved, such as the production of tar, which can cause plugging and damage the working of the gas turbines or engines (BARBA ET AL., 2011).

Recent efforts to better modelling the gasification process include the use of equilibrium models to predict the composition of the product gas in commercial gasifiers, as well as the application of kinetic models to specific types of reactors. These methods are limited to a small number of reactions and species with clearly identified mechanism and require an extensive and complex study about the reaction mechanisms involved (BARBA ET AL., 2011).

Although a literature analysis has showed that equilibrium modelling failed to predict experimental data, especially for hydrogen and methane, these models show the limits of the reactions that guide the design of the process (BARBA ET AL., 2011).

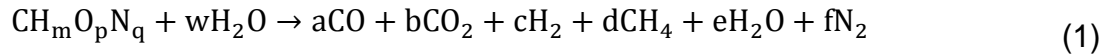
To the improvement of the equilibrium models, especially regarding methane, hydrogen and solid carbon content, many researchers modified their models by including corrective relations. In one side, this method improves the theoretical results, making them closer to the experimental ones, but, in the other hand it makes the models become unpredictable, making them not suitable to the modelling of industrial processes. Yet, another approximation have been studied that is to use temperatures lower than the real ones to apply the model (BARBA ET AL., 2011).

The model developed by Barba et al., (2011), is denominated Gibbs Free Energy Gradient Method Model (GMM), that claims to overcome the semi-qualitative point of view, typical from the equilibrium models to a quantitative point of view.

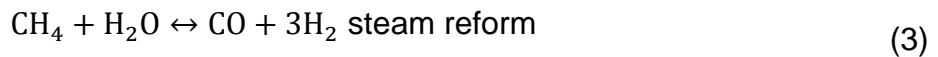
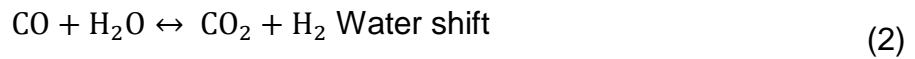
Barba's Model claim to be able to provide reliable results that match experimental data (BARBA ET AL., 2011).

Typical premises of an equilibrium model are: All reactions are at equilibrium; Carbon is completely gasified and is not present in among the reaction products; the reaction products are CO, CO<sub>2</sub>, H<sub>2</sub>O, CH<sub>4</sub>, N<sub>2</sub>, all in gaseous phase, with exception of solid ashes. The presence of tar is not considered (BARBA ET AL., 2011).

The following reaction is usually considered:



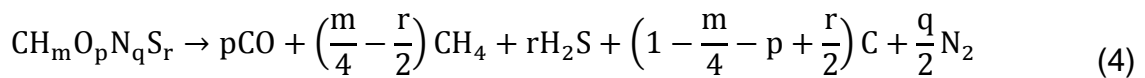
Where  $\text{CH}_m\text{O}_p\text{N}_q$  is the brute formula of RDF, taken from the ultimate analysis and ash-free. To the mass balance the elements C, H, N and O are considered and also the following relations:



For the reactions above, the Arrhenius equations are used to express the dependence of the kinetic constants with temperature (BARBA ET AL., 2011).

Barba et al. (2011) modifies the premises adopted above, by removing them, with exception of tar absence that remains. Barba et al. (2011) also modifies the formula of the RDF, by including sulfur.

As a first step, the decomposition in high temperature adopted by Barba et al. (2011), follows the relation:



Secondly, the produced gas modifies its composition according with the equilibrium relations with the equations adopted above (BARBA ET AL., 2011).

Barba et al. (2011) inserts yet two new parameters  $\delta$  and  $\gamma$ . These parameters are related with the effect of two reactions in which there is the participation of solid carbon in the real gasification process, air and steam. For  $\delta$ , the Boudouard reaction, in which the CO from the decomposition of the RDF produces solid carbon, was considered:



For  $\gamma$ , Barba et al. (2011) considered the reaction of carbon reform, in which solid carbon increases the yield of the product gas:

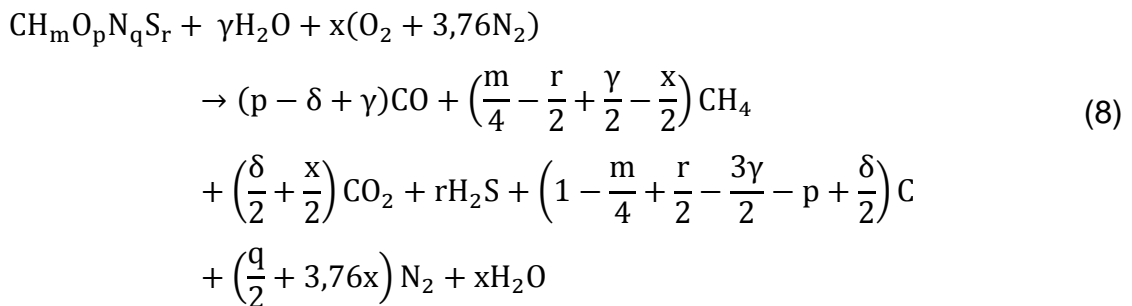


The effect of both parameters adopted by Barba et al. (2011) is that  $\delta$  increases the number of moles to the solid carbon, while  $\gamma$  diminishes that amount, due to the reform reaction.

A last equation is added to the Barba's model, the methane combustion reaction:



Considering that not all methane is consumed by oxygen, which is the one limiting the reaction, once it is admitted in sub stoichiometric conditions in the reactor, the final reaction becomes:



To evaluate the mass balance Barba et al. (2011) adopted the following expression, in which the water shift reaction is  $\alpha$ , and steam reform is  $\beta$  (in equation 9 and 10):

$$n_i(\alpha, \beta) = f(n_i^0) \quad (9)$$

Where  $i$ , are the chemical species CO, CO<sub>2</sub>, H<sub>2</sub>O, H<sub>2</sub>, CH<sub>4</sub>, N<sub>2</sub> e H<sub>2</sub>S, and  $n_i^0$  initial number of moles in the system.

To take into account the evolution of the system until it reaches the equilibrium, the state function for Gibbs free energy was considered, in which pressure and temperature are constants (BARBA ET AL., 2011).

$$G(\alpha, \beta)|_{T,P} = \sum_i n_i(\alpha, \beta) \cdot \mu_i(\alpha, \beta, T) \quad (10)$$

Where the chemical potential can be obtained by the following relation:

$$\mu_i = \mu_i^0(T) + RT \ln P_i \quad (11)$$

Where  $\mu_i^0(T)$  represents the standard chemical potential of the component  $i$ , that can be evaluated, considering  $T_0=298K$ , with the following expression:

$$\mu_i^0(T) = \mu_i^0(T_0) \frac{T}{T_0} - T \int_{T_0}^T \frac{h_i(T)}{T^2} dT \quad (12)$$

Where  $h_i$  is the standard molecular enthalpy of the species  $i$ .

Barba's approach uses the thermodynamic principle of equilibrium and states that the system always evolve from the initial conditions to an equilibrium condition, by reducing its energetic content, in which reaches a minimum value where all reactions simultaneously in equilibrium.

From the infinity routes between the initial conditions ( $\alpha = \beta = 0$ ) and the equilibrium point ( $\alpha = \alpha_{eq}$  e  $\beta = \beta_{eq}$ ) the system chooses the path that offers the maximum gradient  $\text{grad}[G(\alpha, \beta)]$ . The experimental knowledge from the residence times shows that this route does not stop in the reactor real conditions (BARBA ET AL., 2011).

From the mathematical point of view, Barba et al. (2011) derived the following functions:

$$G'_\alpha = \left( \frac{\partial G(\alpha, \beta)}{\partial \alpha} \right)_{\beta=\text{cost}}, G'_\beta = \left( \frac{\partial G(\alpha, \beta)}{\partial \beta} \right)_{\alpha=\text{cost}} \quad (13)$$

In the surface defined by  $\alpha$  and  $\beta$  axes, the direction of the gradient vector is given point by point by the ratio between the two derivatives. These two progress parameters were used to find the minimum value of the G function (BARBA ET AL., 2011).

The computational strategy used is based on the conjugated gradient method, which solves the system of equations by a pre-implemented software in MathCAD, called “minimize” (BARBA ET AL., 2011).

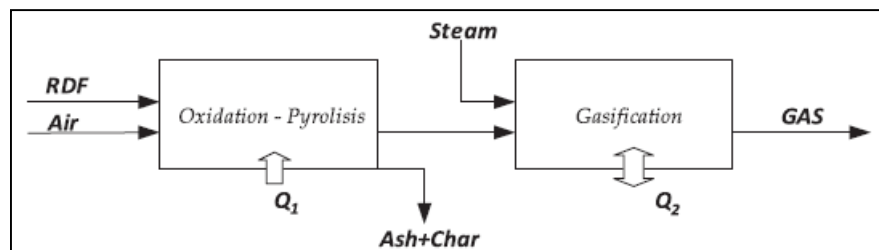


Figure 17 – Schematic for the Energy balance for the model developed by Barba et al. (2011).

The energy balance, Figure 17, was considered, by Barba et al. (2011), according to the following:

$$\left( \sum H \right)_{\text{IN}} + Q_1 \pm Q_2 = \left( \sum H \right)_{\text{OUT}} \quad (14)$$

Where:

$$\left( \sum H \right)_{\text{IN}} = H_{\text{air}} + H_{\text{RDF}} + H_{\text{steam}} \quad (15)$$



$$(\sum H)_{OUT} = H_{gas} + H_{Ash+Char} \quad (16)$$

$$H_{RDF} = H_{RDF}^0 + \int_{298,15}^{T_i} C_{p,RDF} dT \quad (17)$$

$$H_{RDF}^0 = LHV_{RDF} + \sum_{i=prod-comb} v_i H_i^0 \quad (18)$$

The results obtained by Barba's model were validated with literature data, in which a fluidized bed gasifier using pinewood, as raw-material and air and steam as gasification agent. Another experiment uses sawdust as fuel in a fluidized bed, using air as gasifying agent.

The model showed good agreement with experimental results, however it over estimated, although in a small amount, the gas production, once it does not take into account the tar production (BARBA ET AL., 2011).

Barba et al. (2011) also recommend that the model is more suitable with gasifiers that have not a big tar production, such as the fluidized bed.

The objective of Kangas et al. (2014) was to develop a gasification model that can provide a simultaneous solution for what the author denominated super-equilibrium reactions of hydrocarbons, ammonium and tar as well as its enthalpy relations in the gasification process.

Kangas et al. (2014) proposes a solution based on the Constrained Free Energy method (CFE), in which to the equilibrium calculations are imposed new non-materials restrictions (or virtual) to the solution of local and partial restrictions, instead of the global thermodynamic equilibrium.

As well as the conventional minimization of Gibbs free energy model, that applies the restrictions of mass balance to the system as necessary conditions to solve the system with the Lagrange method. Analogously other restriction called "non-materials" are also imposed as, for example, the extend of the reaction (which is a physical restriction, but without material content) (KANGAS ET AL., 2014).

Kangas et al. (2014) stated that the CFE method is been applied with good results in literature. The CFE methodology is used to describe the super-equilibrium occurring in the gasification process. Light hydrocarbons, ammonium, tar and coke tend to be decomposed when high temperature is considered in thermodynamic calculations and, thus, additional restrictions are needed to model the presence of those elements in the super-equilibrium conditions.

The thermodynamic equilibrium is evaluated throughout the Gibbs free energy minimization for an isothermal and closed system, applying the Lagrange method. The minimal is obtained when the partial derivatives are zero (KANGAS ET AL., 2014).

$$L = G - \pi\psi = \sum_{k=1}^k n_k \mu_k - \sum_{k=1}^k \pi_l \left( \sum_{k=1}^k v_{kl} n_k - b_l \right) \quad (19)$$

$$\left( \frac{\partial L}{\partial n_k} \right)_{n_{n \neq k}} = \mu_k - \sum_{l=1}^L \pi_l v_{kl} = 0 \quad (20)$$

$$\left( \frac{\partial L}{\partial \pi_l} \right)_{\pi_{n \neq l}} = \sum_{k=1}^K v_{kl} n_k - b_l = 0 \quad (21)$$

To perform the calculations, Kangas et al. (2014) uses two types of solvers called SolFasMix and ChemSheet.

The stoichiometric matrix with the additional and virtual components is composed as:

$$N = \begin{bmatrix} v_{1,1} & \dots & v_{1,L} & v_{1,L+X} \\ \dots & \dots & \dots & \dots \\ v_{K,1} & \dots & v_{K,L} & \dots \\ v_{K+X,1} & \dots & \dots & v_{K+X,L+X} \end{bmatrix} \quad (22)$$

Where X is the number of non-material restrictions. The additional virtual components (columns L+1 to L+X) represent the amount of the substance of a particular component in a particular phase, and it can be used alone to impose the formation of any component when performing local equilibrium calculations (KANGAS ET AL., 2014).

When the chemical system is extended with the addition of virtual variables (lines K+1 to K+X), that are related with their respective virtual components, it is possible to

impose a restriction to the formation of consume of many components (KANGAS ET AL., 2014).

Kanga's equilibrium and super-equilibrium reactions are written:

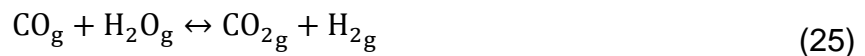
$$\sum_k a_k \mu_k = 0 \text{ (equilibrium reactions)} \quad (23)$$

$$\sum_k a_k \mu_k = \sum_{l=1}^{L+X} v_{kl} \pi_l \neq 0 \text{ (all restriction for the super-equilibrium reactions)} \quad (24)$$

Where  $a_k$  is the stoichiometric coefficient of a species  $k$  in a given reaction.

The thermodynamic system proposed by Kangas et al., 2014 is composed by 14 substances in the gaseous phase ( $\text{CO}$ ,  $\text{H}_2$ ,  $\text{O}_2$ ,  $\text{N}_2$ ,  $\text{H}_2\text{O}$ ,  $\text{CH}_4$ ,  $\text{C}_2\text{H}_2$ ,  $\text{C}_2\text{H}_4$ ,  $\text{C}_2\text{H}_6$ ,  $\text{C}_3\text{H}_8$ ,  $\text{C}_6\text{H}_6$ ,  $\text{C}_{10}\text{H}_8$ ,  $\text{NH}_3$ ,  $\text{O}_2$ ), liquid water ( $\text{H}_2\text{O}$ ) and two solid phases for the coke and ash ( $\text{C}$  e  $\text{SiO}_2$ ). It is also introduced an additional phase for biomass, which is composed by 4 elements ( $\text{C}$ ,  $\text{H}$ ,  $\text{O}$  e  $\text{N}$ ).

To describe the super-equilibrium reaction of coke, tar, ammonium and light hydrocarbons in the gasification, Kangas et al. (2014) uses the expressions obtained by Hannula and Kurkela. For the so called local equilibrium the water shift reaction is adopted.



Kangas's model has considered five different gasification scenarios. Three using wood chips, where the fuel properties are similar, but the gasification parameters such as temperature, oxygen/fuel ratio and steam/fuel ratio were varied. Another scenario Kangas et al. used forest waste and another one with wood chips. Kangas et al. (2014) validated two literature case studies in the literature, in which one with a fluidized bed gasifier (with air and steam injection) and another circulating fluidized bed with air injection.

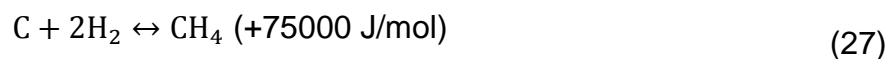
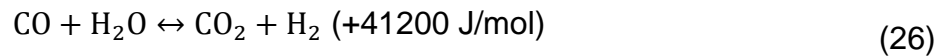
It was demonstrated that the super-equilibrium of coke, tar, ammonium and light hydrocarbon in the biomass gasification and the main products ( $\text{CO}$ ,  $\text{CO}_2$ ,  $\text{H}_2$ ,  $\text{H}_2\text{O}$  e  $\text{CH}_4$ ) can be predicted by the CFE method. The model's precision increases when the number

of restrictions also increases. However, it is not desired a system with many restrictions. By defining the restrictions to coke, tar, ammonium, carbon and CH<sub>4</sub> is possible to model the system with the same precision that when all the light hydrocarbons are considered. However, the modelling of tar was not satisfactory (KANGAS ET AL., 2014).

Kangas et al. (2014) recommends that the results obtained by the developed model may not be the same depending on the type of gasifier been analyzed. To overcome that it is recommended the use of kinetic models that can be added to the model, as well as to define other restrictions.

Babu and Sheth (2006) developed a stoichiometric equilibrium model and studied the effects of an enriched oxygen atmosphere in the product gas composition, caloric value and reaction temperature. They also studied the effect of pre-heated air injection into the system, as well as the effect of saturated steam fed with air.

The model assumes that all reactions are in thermodynamic equilibrium, that all pyrolysis product burns and achieves equilibrium in the reduction zone before leaving the gasifier. It also assumes a downdraft gasifier. The reactions are considered as follows (BABU AND SHETH, 2006):



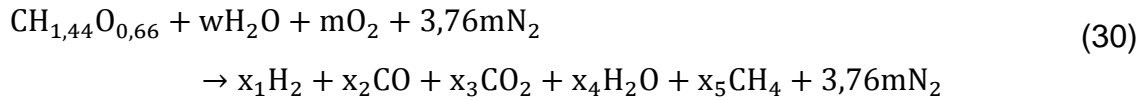
Where the equilibrium constant for the methane generation (K<sub>1</sub>) is:

$$K_1 = \frac{p_{\text{CH}_4}}{p_{\text{H}_2}^2} \quad (28)$$

And the equilibrium constant for the shift reaction (K<sub>2</sub>) is:

$$K_2 = \frac{p_{\text{CO}_2} p_{\text{H}_2}}{p_{\text{CO}} p_{\text{H}_2\text{O}}} \quad (29)$$

Babu and Sheth (2006) adopted a typical formula for biomass, and the following global gasification reaction:



The mass balance:

$$\text{Carbon: } 1 = x_2 + x_3 + x_5 \quad (31)$$

$$\text{Hydrogen: } 2w + 1,44 = 2x_1 + 2x_4 + 4x_5 \quad (32)$$

$$\text{Oxygen: } w + 0,66 + 2m = x_2 + 2x_3 + x_4 \quad (33)$$

For the energy balance the system was considered adiabatic.

$$\begin{aligned} H_{\text{fwood}}^0 + w(H_{\text{fH}_2\text{O}(l)}^0 + H_{\text{vap}}) + mH_{\text{fO}_2}^0 + 3,76mH_{\text{fN}_2}^0 \\ + \Delta T'(mC_{\text{pO}_2} + 3,76mC_{\text{pN}_2}) \\ = x_1H_{\text{fH}_2}^0 + x_2H_{\text{fCO}}^0 + x_3H_{\text{fCO}_2}^0 + x_4H_{\text{fH}_2\text{O}(\text{vap})}^0 + x_5H_{\text{fCH}_4}^0 \\ + \Delta T(x_1C_{\text{pH}_2} + x_2C_{\text{pCO}} + x_3C_{\text{pCO}_2} + x_4C_{\text{pH}_2\text{O}(\text{vap})} + x_5C_{\text{pCH}_4} \\ + 3,76mC_{\text{pN}_2}) \end{aligned} \quad (34)$$

Where  $\Delta T = T_2 - T_1$ , e  $\Delta T' = T'_2 - T_1$

$T_1$ = inlet temperature

$T_2$ =temperature in the reduction zone

$T'_2$ =air inlet temperature

When steam is added to the system the energy balance becomes:

$$\begin{aligned}
H_{fwood}^0 + w(H_{fH_2O(l)}^0 + H_{vap}) + mH_{fO_2}^0 + 3,76mH_{fN_2}^0 + s(H_{fH_2O(g)}^0) \\
+ \Delta T''C_{pH_2O(vap)} + \Delta T'(mC_{pO_2} + 3,76mC_{pN_2}) \\
= x_1H_{fH_2}^0 + x_2H_{fCO}^0 + x_3H_{fCO_2}^0 + x_4H_{fH_2O(vap)}^0 + x_5H_{fCH_4}^0 \\
+ \Delta T(x_1C_{pH_2} + x_2C_{pCO} + x_3C_{pCO_2} + x_4C_{pH_2O(vap)} + x_5C_{pCH_4} \\
+ 3,76mC_{pN_2})
\end{aligned} \tag{35}$$

And in the mass balance,  $w$  is replaced by  $w+s$ .

From the equations mentioned above (energy and mass balance, equilibrium relations), Babu and Sheth (2006) could compare the predicted values with experimental one, made by Jayah et al., which were showed to be in good agreement.

Babu and Sheth (2006) also simulated the effect of the oxygen enrichment in the air inlet in the gasifier. They verified that the more oxygen enters the systems better the quality of the produced syngas, but with less methane production. It was also demonstrated that the oxygen enrichment increases the reaction temperature.

The effect of the pre-heating of air in the gasifier inlet was also quantified by Babu and Sheth. They showed that there is a linear relation between the inlet air temperature and the reaction temperature, the higher the inlet air temperature the higher the reaction temperature.

The steam injection was also evaluated. It was demonstrated that the increase of the steam/biomass ratio increases the production of hydrogen, but diminishes the caloric value of the product gas. And also as the steam/biomass ratios increases the temperature required for gasification is lower (BABU AND SHETH, 2006).

## 2.4 BASES TO PRESENT FUEL COMPOSITION

The fuel composition it is usually expressed in different basis according to the situation. According to Basu (2010), the most common are:

As received

Air dry

Total dry

Dry and ash-free

A comparison among those basis is illustrated in the Figure 18.

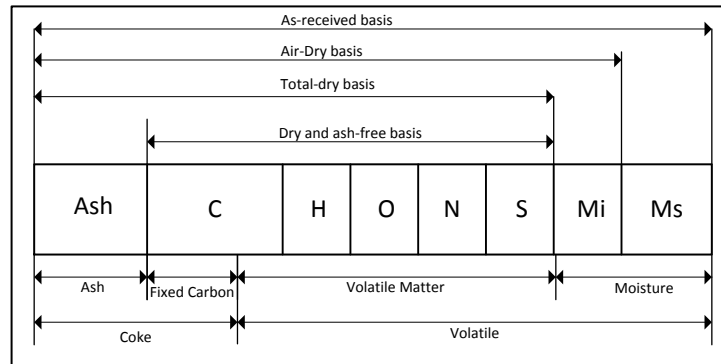


**Figure 18 - Different basis to express the fuel composition (BASU, 2010). O - Oxygen, Mi - Inherent moisture, N - Nitrogen, Ms - superficial moisture, C – Carbon, S- Sulfur.**

#### 2.4.1 AS RECEIVED BASIS

With as-received basis, the ultimate and proximate analysis can be written according to the following (BASU, 2010):

$$\text{Ultimate: } C + H + O + N + S + \text{Ash} + M = 100\% \quad (36)$$

$$\text{Proximate: } \text{VM} + \text{FC} + M + \text{Ash} = 100\% \quad (37)$$

Where VM, FC, M and Ash represents the weight percentages of volatile matter, fixed carbon, moisture and ash provided by the ultimate analysis. And C, H, O, N, S, Ash and M are the weight percentages of Carbon, Hydrogen, Oxygen, Nitrogen, sulfur, ash and Moisture provided by the Proximate analysis. The moisture and ash contents are the same for both analysis and the as-received base can be converted in other bases.

### 2.4.2 AIR-DRY BASIS

When the fuel is dried by air and its superficial moisture is removed while its inherent moisture remains the same. Then, to express in an air-dry basis, the amount is divided by the total mass taking the superficial moisture. For example, the percentage of Carbon in air-dried basis it's calculated according to the following (BASU, 2010):

$$C_{ad} = \frac{100C}{100 - M_a} \% \quad (38)$$

Where,  $M_a$  it is the mass of the superficial moisture removed from 100 kg of wet fuel after it is been dried by air. Other fuel components can be expressed in a similar way (BASU, 2010).

### 2.4.3 TOTAL DRY-BASIS

The fuel composition in an air-dry basis it is easy to measure, however to express the fuel in a base free of moisture one must take out the superficial and inherent moistures. For Carbon in a total air-dry basis (BASU, 2010):

$$C_{td} = \frac{100C}{100 - M} \% \quad (39)$$

Where  $M$  is the total fuel moisture (superficial +inherent):  $M=M_a+M_i$



#### 2.4.4 DRY ASH-FREE BASIS

Ash is another component that is many times suppressed with moisture. The fuel composition then becomes dry ash-free (DAF). Following the examples mentioned above, the percentage of carbon on a dry ash-free basis,  $C_{daf}$ , becomes (BASU, 2010):

$$C_{daf} = \frac{100C}{100 - M - Ash} \% \quad (40)$$

Where (100-M-Ash) is the mass of biomass without moisture and ash. The percentage of all fuel components in any base accounts 100 (BASU, 2010). For example:

$$C_{daf} + H_{daf} + O_{daf} + N_{daf} + S_{daf} = 100\% \quad (41)$$

#### 2.5 BIOMASS GASIFICATION IN SUPERCRITICAL WATER

In order to better gasify any biomass the gasification in supercritical water can be an interesting alternative.

Biomass usually contains more moisture than fossil fuels as, for example, coal. Typical thermal gasification with air, oxygen or subcritical steam show good results when applied to dry biomass. However, it becomes more inefficient when for high moisture content, because the moisture have to be taken out of the process during the gasification (BASU, 2010).

Water becomes a supercritical fluid above its critical point, which is 374.29°C and 22.089 MPa. When heated and pressurized above those conditions, it enters in a transition state between a liquid and gas. Unlike the subcritical conditions, there isn't a vaporization energy that needs to be exchanged to change its state (BASU, 2010).

Above critical pressure, there is no saturation temperature that separates the liquid and vapor. However, there is a temperature called pseudo-critical that corresponds to each pressure above which the transition from the liquid condition to the vapor condition. Such condition it is characterized by a sharp rise in the specific heat of the fluid (BASU, 2010).

According to Basu (2010), in supercritical conditions the water presents several important properties to gasification:

- a) It is a good solvent around its critical point
- b) Subcritical water is polar, while supercritical water is non polar and it can be used as solvent of organic compounds.
- c) Its high density when compared to subcritical steam at the same temperature, helping reactions, for example, with cellulose to produce hydrogen.
- d) Near the critical point, water has more ionic products when in subcritical conditions. However, when supercritical, the water becomes a poor medium to solve acid and basis.
- e) The same situation of the previous item applies to highly ionizable salts, been easier to separate an organic product from salt.
- f) The supercritical water is highly miscible with other gases, facilitating homogenous reactions.
- g) Its transportation properties are excellent. While its density is higher than subcritical steam, it is lower than the liquid state. Also supercritical water has low viscosity and low surface tension which can highly increase its diffusivity.

All that makes supercritical water an ideal agent for hydrothermal biomass gasification, when biomass has a high level of moisture and would be dried before been gasified. Besides the above mentioned, supercritical water gasification has other benefits:

- a) Low production of tar, since its precursors are highly soluble in supercritical water and can be easily removed afterwards.
- b) High Thermal efficiency for biomass with high moisture levels.
- c) High yield in hydrogen production
- d) Hydrogen is produced already in high pressure, ready for use.
- e) CO<sub>2</sub> it is easily separated due its higher solubility with pressurized water.

- f) Char formation is low.
- g) Heteroatoms like sulfur and Nitrogen are easily removed with the aqueous effluents.

According with Basu (2010), there are three major routes for supercritical water gasification:

- Liquefaction: Formation of liquid fuel above critical pressure (22,1MPa) but near critical temperature (300-400°C)
- Gasification to CH<sub>4</sub>: Conversion in SCW in a low-temperature range (350-500°C) in the presence of a catalyst.
- Gasification to H<sub>2</sub>: Conversion in SCW with or without catalysts at higher (>600°C) temperatures.

Bearing in mind the above mentioned advantages of supercritical gasification, it is worth to evaluate and to simulate the gasification in supercritical conditions. It will be showed that the advantages mentioned above, can be achieved although the energy calculations has to be carefully carried out. Because in order to create the supercritical conditions energy must be injected into the system making it not so advantageous depending on the economic objectives of the process.

### 3. CHAPTER III : MATERIALS AND METHODS

#### 3.1. MUNICIPAL SOLID WASTE COMPOSITION

The composition of the municipal solid waste can vary greatly depending on the location, consumption habits, economic factors and even according to the season of the year. Such composition can be obtained throughout gravimetric analysis, ultimate or proximate analysis (CARVALHAES, 2013; BASU, 2010; LIU et al., 2008; MACHADO, 2015; BALCAZAR, 2011; ZAINAL, 2001; TAVARES, 2007). In order to compose the empirical formula of MSW, required to the modeling of gasification, it is necessary to obtain its ultimate analysis. However, the ultimate analysis of Curitiba's MSW, to the best of our knowledge, was not found reported in the current literature. The works of Balcazar (2011), Carvalhaes (2013) and Machado (2015) provide the ultimate analysis to the municipal solid wastes of some cities from in Brazil such as São Paulo, Distrito Federal and São José dos Campos. In the work of Balcazar (2011), it is possible to find the ultimate analysis of each one of the MSW's components in the gravimetric analysis. Such values are presented in Table 5.

**Table 5 – Gravimetric Composition with the ultimate analysis of São Paulo’s Municipal Solid Waste (BALCAZAR, 2011).**

Components	São Paulo Waste Contents (% wt)	Moisture (% wt)	Ashes (% wt)	Ultimate analysis (% wt dry)				
				C	H	N	S	O
Organic waste	49.50%	70.00%	5.00%	48.00%	6.40%	2.60%	0.40%	37.60%
Paper	12.00%	10.20%	6.00%	43.50%	6.00%	0.30%	0.20%	44.00%
Paperboard	6.80%	5.20%	5.00%	44.00%	5.90%	0.30%	0.20%	44.60%
Plastic	22.90%	0.20%	10.00%	60.00%	7.20%	0.00%	0.00%	22.80%
Fabrics	2.40%	10.00%	2.50%	55.00%	6.60%	4.60%	0.20%	31.20%
Rubber	0.30%	10.00%	10.00%	78.00%	10.00%	2.00%	0.00%	0.00%
Leather	0.30%	10.00%	10.00%	60.00%	8.00%	10.00%	0.40%	11.60%
Wood	1.30%	1.50%	1.50%	49.50%	6.00%	0.20%	0.10%	42.70%
Glass <sup>a</sup>	1.50%	2.00%	98.90%	0.50%	0.10%	0.10%	0.00%	0.40%
Ferrous metal <sup>a</sup>	1.90%	2.00%	90.50%	4.50%	0.60%	0.10%	0.00%	4.30%
Aluminum <sup>a</sup>	0.90%	2.00%	90.50%	4.50%	0.60%	0.10%	0.00%	4.30%
Others	0.20%	3.20%	68.00%	26.30%	3.00%	0.50%	0.20%	2.00%

a - The organic materials in these products are labels and coating

Adapted from: Balcazar (2011)

Tavares (2007) measured the gravimetric composition of Curitiba’s MSW. In his work it is obtained the gravimetric composition for all seasons of the year. Table 6 shows the average of the Curitiba’s MSW gravimetric composition:

**Table 6 - Gravimetric composition of Curitiba's MSW (TAVARES, 2007).**

<b>MSW CURITIBA</b>	<b>Average % 2005/2006</b>
<b>NON RECYCLABLE</b>	
ORGANIC WASTE	<b>47.90%</b>
WOOD	<b>1.00%</b>
FABRICS	<b>4.10%</b>
LEATHER	<b>0.40%</b>
PLASTICS (FILM)	<b>12.10%</b>
DISPOSABLE DIAPER	<b>4.30%</b>
TETRA PAK	<b>1.50%</b>
<b>RECYCLABLE</b>	
PAPER	<b>13.00%</b>
KRAFT PAPER	<b>3.00%</b>
PLASTIC	<b>5.50%</b>
GLASS	<b>4.70%</b>
RUBBER	<b>0.30%</b>
FERROUS METAL	<b>1.80%</b>
NON FERROUS METAL	<b>0.20%</b>
<b>REJECTED</b>	<b>0.20%</b>
<b>TOTAL</b>	<b>100.00%</b>

Based on the mentioned above, it was possible to use the ultimate analysis presented by Balcazar (2011) to estimate the ultimate analysis of Curitiba's MSW. The following assumptions were considered: only the non-recyclable wastes enters the gasifier; dippers and tetrapacks are not considered in the composition, due to the lack of information with respect to the ultimate analysis of those components; considering same moisture as found in the São Paulo's MSW; ultimate analysis was considered in dry basis. The estimated composition of MSW from Curitiba as obtained in this work is presented in Table 7, which contains the calculation of the composition using a basis of 100 kg of MSW.

Table 7 - Ultimate analysis estimation of Curitiba's MSW. Source: This work.

AVERAGE %wt	MSW Composition			C		H		N		S		O		Ash	
2005/2006	%wt	Moisture %wt	kg	%wt	kg	%wt	kg	%wt	kg	%wt	kg	%wt	kg	%wt	kg
ORGANIC WASTE	47.90%	70.00%	14.37	48.00%	6.90	6.40%	0.920	2.60%	0.374	0.40%	0.057	37.60%	5.403	5.00%	0.719
WOOD	1.00%	1.50%	0.99	49.50%	0.49	6.00%	0.059	0.20%	0.002	0.10%	0.001	42.70%	0.421	1.50%	0.015
FABRICS	4.10%	10.00%	3.69	55.00%	2.03	6.60%	0.244	4.60%	0.170	0.20%	0.007	31.20%	1.151	2.50%	0.092
LEATHER	0.40%	10.00%	0.36	60.00%	0.22	8.00%	0.029	10.00%	0.036	0.40%	0.001	11.60%	0.042	10.00%	0.036
PLASTICS (FILM)	12.10%	0.20%	12.08	60.00%	7.25	7.20%	0.869	0.00%	0.000	0.00%	0.000	22.80%	2.753	10.00%	1.208
SUM:	65.50%	BASIS:	100	SUM:	16.9	SUM:	2.121	SUM:	0.581	SUM:	0.067	SUM:	9.770	SUM:	2.069
MSW Ultimate analysis (estimated):				53.60%		6.74%		1.85%		0.21%		31.03%		6.57	

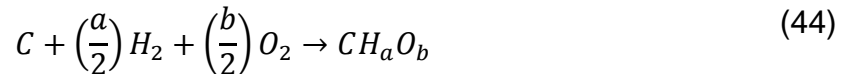
Normalizing to 1 kmol of carbon (in dry ash free basis) it is possible to obtain the empirical formula, thus:  $CH_{1.5079}O_{0.4342}N_{0.0295}S_{0.0015}$ .

And, the molecular mass can be calculated:

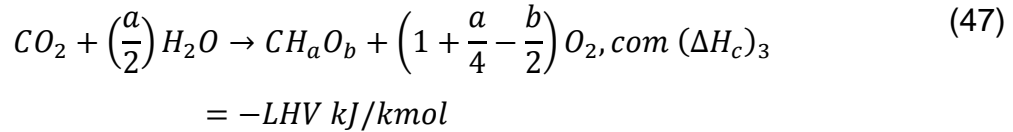
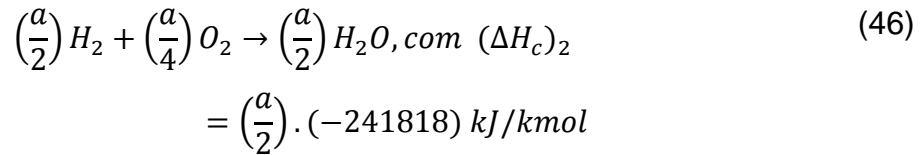
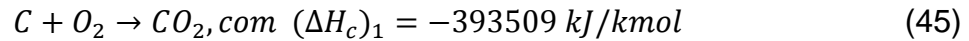
$$MM \left( \frac{kg}{kmol} \right) = 12(1) + 1(1.5079) + 16(0.4342) + 14(0.0295) + 32(0.015) \quad (42)$$

$$MM = 20.92 \frac{kg}{kmol} \quad (43)$$

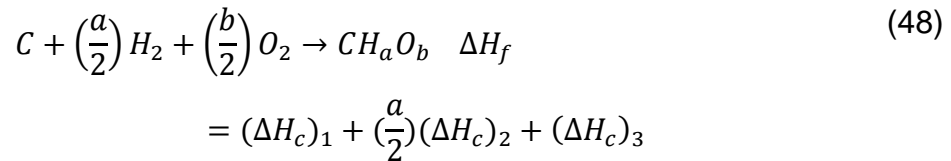
To estimate the enthalpy of formation of the municipal solid waste, the model proposed by Zainal et al. (2001) was considered and used in this study. The formation of the biomass with the empirical formula  $CH_aO_b$  can be written as:



Using the reactions:



Resulting in:



Although the above analysis does not compute elements such as nitrogen and sulfur, there is a good approximation, because the contribution of these elements it is small in relation to the carbon, hydrogen and oxygen.

To estimate the HHV it is possible to use the following relations:

A) Zainal et al. (2001)

$$\begin{aligned} HHV \left(\frac{J}{kg}\right) &= 0,2326(146,58C + 56,878H - 51,53O - 6,58A \quad (49) \\ &\quad + 29,45) \end{aligned}$$

Where C, H, O and A are the mass fractions of carbon, hydrogen, oxygen and ash of the dry biomass obtained in the ultimate analysis (ZAINAL ET AL., 2001).

B) Basu (2010)

$$\begin{aligned} HHV \left(\frac{kJ}{kg}\right) &= 349,1C + 1178,3H + 100,5S - 103,4O - 15,1N \quad (50) \\ &\quad - 21,1A \end{aligned}$$



Where C, H, S, O, N and A are the mass percentages of carbon, hydrogen, sulfur, oxygen, nitrogen and ash of the dry biomass obtained in the ultimate analysis.

In order to align the results and posterior analysis the method of Zainal et al. (2001) was adopted to the calculation of the higher heating value (HHV):

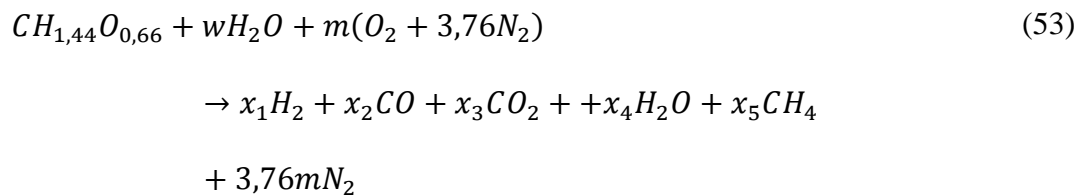
$$HHV = 454,025.67 \frac{kJ}{kmol} \quad (51)$$

Then:

$$\Delta H_f = -121,797.54 \frac{kJ}{kmol} \quad (52)$$

### 3.2. MATHEMATICAL DEVELOPMENT OF STOICHIOMETRIC MODEL

Zainal et al. (2001) developed a stoichiometric model to predict the product gas in gasification process. The model is composed for 6 unknown variables (m, x1, x2, x3, x4 e x5). For a solution to be possible it is necessary 6 equations. First, they adopted the hypothesis for the global gasification reaction as expressed in equation 53:



Where w is the amount of water present at the wood moisture, m is the amount of air fed to the system and x1, x2, x3, x4 e x5 the stoichiometric coefficients of the products of the reaction. It is worth to notice that Zainal et al. presented a “typical” empirical formula of wood.

The atomic mass balance generates three equations:

$$\text{Carbon: } 1 = x_1 + x_3 + x_5 \quad (54)$$

$$\text{Hydrogen: } 2w + 1,44 = 2x_1 + 2x_4 + 4x_5 \quad (55)$$

$$\text{Oxygen: } w + 0,66 + 2m = x_2 + x_3 + 2x_4 \quad (56)$$

Other equations come from the heat balance of the system. Assuming the gasification as an adiabatic process, Zainal et al. proposed the following equation:

$$\begin{aligned} h_{f\text{wood}}^0 + w \left( h_{f\text{H}_2\text{O}(l)}^0 + h_{vap}^{\text{H}_2\text{O}} \right) + mh_{f\text{O}_2}^0 + 3,76mh_{f\text{N}_2}^0 = x_1h_{f\text{H}_2}^0 + \\ x_2h_{f\text{CO}}^0 + x_3h_{f\text{CO}_2}^0 + x_4h_{f\text{H}_2\text{O}(v)}^0 + x_5h_{f\text{CH}_4}^0 + \Delta T(x_1C_{p\text{H}_2} + x_2C_{p\text{CO}} + \\ x_3C_{p\text{CO}_2} + x_4C_{p\text{H}_2\text{O}(v)} + 3,76mC_{p\text{N}_2}) \end{aligned} \quad (57)$$

By choosing two main reactions (Methanation and Shift), as representatives of the gasification process and using the relation between the Gibbs free energy and the equilibrium constant, as showed by Zainal et al. (2001) it is possible to come with an equation that relates the equilibrium constant, and thus the gas composition with the temperature. Giving to more equations to the system, making its solution possible.



To the reaction  $\text{C} + 2\text{H}_2 \rightarrow \text{CH}_4$ :

$$\ln K_1 = -\frac{21574,02}{T} - 0,476 \cdot \ln T - 0,000352 \cdot T + \frac{98000}{T^2} + 25,67 \quad (60)$$

$$K_1 = \frac{y_{\text{CO}}^2}{y_{\text{CO}_2}} \quad (61)$$

For the reaction  $\text{CO} + \text{H}_2\text{O} \rightarrow \text{CO}_2 + \text{H}_2$ :

$$\ln K_4 = +\frac{5870,53}{T} + 1,86 \cdot \ln T - 2,7 \cdot 10^{-4} \cdot T + \frac{58200}{T^2} - 18,007 \quad (62)$$

$$K_4 = \frac{y_{\text{CO}_2} y_{\text{H}_2}}{y_{\text{CO}} y_{\text{H}_2\text{O}}} \quad (63)$$

Bearing in mind that:

$$y_i = \frac{n_i}{\sum n_i} \quad (64)$$

### 3.3. MATHEMATICAL DEVELOPMENT OF NON-STOICHIOMETRIC MODEL

Voll et al. (2009) modeled the supercritical gasification of methanol, ethanol, glycerol, glucose and cellulose, using water as the gasification agent. These authors used a non-stoichiometric method by direct minimizing the Gibbs free energy which provides the number of moles for each species proposed as a reaction product. There were applied only two restrictions: The atomic mass balance and the non-negativity of the coefficients.

The Gibbs free energy can be written according to the following equation:

$$G = \sum_{i=1}^{NC} \sum_{j=1}^{NP} n_i^j \mu_i^j \quad (65)$$

Where  $n_i^j$  it is the number of mole of the component  $i$  at phase  $j$  and  $\mu_i^j$  the chemical potential of component  $i$  on the phase  $j$ . The equation can be written in terms of fugacities:

$$G = \sum_{i=1}^{NC} \sum_{j=1}^{NP} n_i^j (\mu_i^0 + RT \cdot \ln(\frac{\hat{f}_i^j}{f_i^0})) \quad (66)$$

Where  $\mu_i^0$  it's the chemical potential of the pure component I, at the reference state at Temperature T and 1 atm,  $f_i^0$  it is the fugacity of the pure component i at the reference state,  $\hat{f}_i^j$  it's the fugacity of the component i at the mixture at phase j, and R is the universal gas constant. Voll et al. 2009 considered a solid-gas system, where:

$$\hat{f}_i^g = \hat{\phi}_i \cdot y_i \cdot P \quad (67)$$

Where  $\hat{f}_i^g$  it is the fugacity of the component I at the mixture,  $y_i$  it is the molar fraction of the component i, and  $\hat{\phi}_i$  is the fugacity coefficient of the component i, all in the gaseous phase.

$$\hat{f}_C^s = f_C^{s,0} \quad (68)$$

Where  $\hat{f}_C^s$  is the fugacity of solid carbon, and  $f_C^{s,0}$  is the fugacity of pure solid carbon at the reference state.

Voll et al. (2009) have not considered the term  $RT \sum_{i=1}^n n_i^g \cdot \ln \hat{\phi}_i$  due to the following considerations: small influence of the pressure variation in the supercritical water gasification equilibrium, the variation of the term  $RT \sum_{i=1}^n n_i^g \cdot \ln y_i$  is much greater than of the term  $\sum_{i=1}^n n_i^g \cdot \ln \hat{\phi}_i$ . Voll et al 2009 calculated the fugacity coefficients according to the Peng-Robinson equation of state, and points out that they are far from the ideal conditions with  $\hat{\phi}_i \neq 1$  and the approximations work because the term is roughly constant during the minimization of G.

With the above consideration the equation finally becomes:

$$G = \sum_{i=1}^{NC} n_i^g [ \mu_i^{g,0} + RT(\ln P + \ln y_i) ] + n_C^s \cdot \mu_C^{s,0} \quad (69)$$

For the calculation of the chemical potential in the reference state for the pure component i,  $\mu_i^0$ , it is used the following relations:

$$\frac{\partial}{\partial T} \left( \frac{\bar{G}_i}{RT} \right) = - \frac{\bar{H}_i}{RT^2} \quad (70)$$

$$\left( \frac{\partial \bar{H}_i}{\partial T} \right)_p = Cp_i \quad (71)$$

$$Cp_i = Cp_a + Cp_b T + Cp_c T^2 + Cp_d T^3 \quad (72)$$

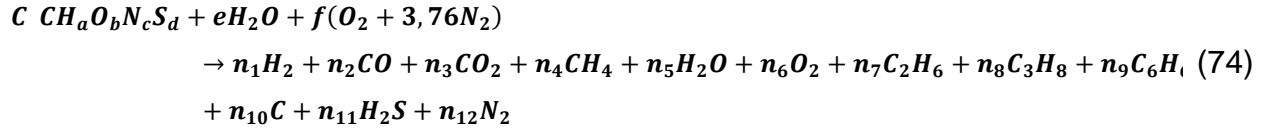
According to Rossi et al. (2009) it was found the following relation that corrects the temperature in the chemical potential  $\mu_i^0$  :

$$\begin{aligned} \mu_i^0(T) = & \left( \frac{T}{T_0} \right) \cdot \Delta G_{f_i}^0 + \left( 1 - \frac{T}{T_0} \right) \cdot \Delta H_{f_i}^0 \quad (73) \\ & - Cp_a \cdot \left( T \ln \left( \frac{T}{T_0} \right) - T + T_0 \right) - \frac{Cp_b}{2} \cdot (T - T_0)^2 \\ & - \frac{Cp_c}{6} \cdot (T^3 - 3T_0^2 \cdot T + 2T_0^3) - \frac{Cp_d}{12} \cdot (T^4 \\ & - 4T_0^3 \cdot T + 3T_0^4) \end{aligned}$$

The supercritical water gasification of the ethanol was then evaluated by Voll et al. (2009), at 1073.15 K and pressure 22.1 MPa, and compared to the results obtained by Byrd et al. (2007) As reagents it were proposed the ethanol ( $C_2H_5OH$ ) and water ( $H_2O$ ), and as products  $H_2$ ,  $CO$ ,  $CH_4$ ,  $C_2H_6$ ,  $C_3H_8$ ,  $C_2H_4$ ,  $C_3H_6$  and solid carbon (C). The number of moles found for  $C_2H_6OH$ ,  $C_2H_6$ ,  $C_3H_8$ ,  $C_2H_4$ ,  $C_3H_6$  and solid carbon was zero. The data bank utilized by Voll et al. (2009) was DIADEM.

The results in the model obtained by Voll et al (2009) were in good agreement with the experimental made by Byrd et al (2007).

For the simulation of Curitiba's MSW gasification the proposed global reaction is:



Where the parameters a, b, c and d are obtained from the ultimate analysis of the municipal solid waste, as calculate for Curitiba city in section 3.1. The coefficient e is the moisture present in the MSW, evaluated by equation 75.

$$e = \frac{24M}{18(1 - M)} \quad (75)$$

And, f is the amount of air, in moles, injected in the gasifier. The parameters n1 to n12 are the coefficients of the reaction products.

As the objective of the simulation is to further generate energy form the syngas, the process must be authothermic, where is not required any energy source to maintain the process. For the gasification process to be autothermic, the system must be adiabatic.

Thus:

$$\Delta H_{reaction} = 0 \quad (76)$$

$$\begin{aligned}
\sum H_{reagents} = 1. (h_{MSW}^0) + d. (h_{H_2O}^0 + \Delta h_{vap}^{H_2O}) + e. (h_{O_2}^0) \\
+ 3,76. (h_{N_2}^0)
\end{aligned} \quad (77)$$

$$\begin{aligned}
\sum H_{products} = n_1 h_{H_2} + n_2 h_{CO} + n_3 h_{CO_2} + n_4 h_{CH_4} + n_5 h_{H_2O} \\
+ n_6 h_{O_2} + n_7 h_{C_2H_6} + n_8 h_{C_3H_8} + n_9 h_{C_6H_6} + n_{10} h_C \\
+ n_{11} h_{H_2S} + n_{12} h_{N_2}
\end{aligned} \quad (78)$$

And the enthalpy of the products is evaluated according to the equation 79:

$$\int_{h_i^0}^{h_i} dh_i = \int_{T_{ref}}^T C_{p_i} dT \quad (79)$$

Where  $h_i^0$  is the standard enthalpy of the product  $i$ ,  $C_{p_i}$  is heat capacity of the component  $i$ ,  $T$  the temperature of the reaction and  $T_{ref}$  is the reference temperature equals to 298.15 K.

#### 3.4. SIMULATIONS OF CURITIBA'S MUNICIPAL SOLID WASTE GASIFICATION

The simulations are regarding to what happens inside the gasifier, until which a pre-processing step occurs generating the so-called Residue Derived Fuel (RDF), which enters into the gasifier free of recyclable material and other material not fit to enter the gasifier (Metal, glass, etc.). After the processing of the RDF the syngas generated follows to a gas cleaning system, that according to the quality of the gas and the final use may be needed or not. The syngas then follows to a power plant unit where is used as fuel, in an internal combustion engine or a boiler or a gas turbine. The electricity then is generated and goes to the grid. The process described above is shown in Figure 19.

It is important to notice that when this work refers to the municipal solid waste entering the gasifier it refers actually to the RDF. So the molecular formula of the MSW is actually the formula of the residue derived fuel after the pre-processing of the municipal solid waste.

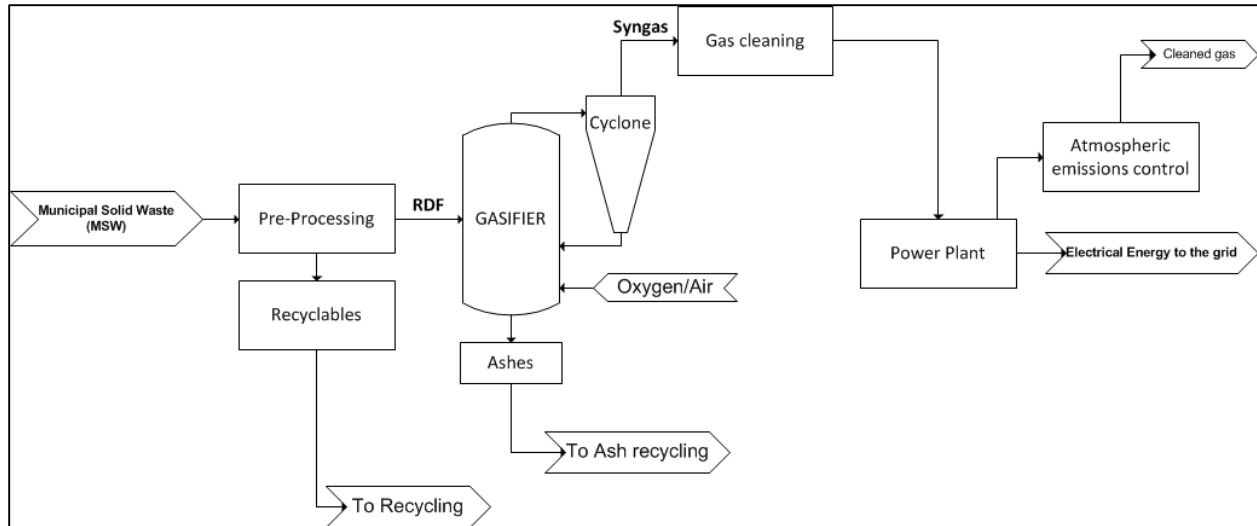


**Figure 19 - Municipal Solid Waste Processing philosophy to generate electrical energy. Source: This work.**

Initially, the models were validated comparing results obtained in this work with data presented in the literature, and then it was proposed five different scenarios for the simulation of the Curitiba's MSW gasification, showed in Table 8.

The first one is based on the stoichiometric model developed by Zainal et al. (2001), as showed in section 3.2. It was possible to develop a similar model to compare the results. The calculations were performed using the Solver tools (Microsoft Excel 2010) to solve the equation with the GRG nonlinear optimization method. Varying the same parameters  $m$ ,  $x_1$ ,  $x_2$ ,  $x_3$ ,  $x_4$  e  $x_5$  subjected to the following restrictions:  $x_1$ ,  $x_2$ ,  $x_3$ ,  $x_4$  e  $x_5$  should be greater or equal to zero and the amount of the atoms C, H and O that enter the system must be equal to the amount of atoms that leave the systems. The objective set in Solver was to make sure that the difference between the enthalpy of the products and the reagents is equal to zero.



**Table 8 – Proposed scenarios for simulation.**

Scenario	Biomass	Approach	Reactions Conditions	Gasifying agent	Proposed Products	Parameters analyzed
1	Curitiba's MSW	Stoichiometric	1 bar, adiabatic and $H^{\circ}f(\text{MSW})$ by Equation 49	$O_2$ , $N_2$ and $H_2O$	$H_2$ , $CO$ , $CO_2$ , $CH_4$ , $H_2O$ and $N_2$	Product gas composition behavior with biomass moisture and amount of air injected in the reactor, temperature of the reaction and low calorific value of the product gas.
2	Curitiba's MSW	Non-Stoichiometric	1 bar, adiabatic and $H^{\circ}f(\text{MSW})$ by Equation 49	$O_2$ , $N_2$ and $H_2O$	$H_2$ , $CO$ , $CO_2$ , $CH_4$ , $H_2O$ , $O_2$ , $C_2H_6$ , $C_3H_8$ , $C_6H_6$ , $C_{(solid)}$ , $H_2S$ and $N_2$	Product gas composition behavior with biomass moisture and amount of air injected in the reactor, temperature of the reaction and low calorific value of the product gas.
3	Curitiba's MSW	Non-Stoichiometric	1 bar, adiabatic and $H^{\circ}f(\text{MSW})$ Equation 50	$O_2$ , $N_2$ and $H_2O$	$H_2$ , $CO$ , $CO_2$ , $CH_4$ , $H_2O$ , $O_2$ , $C_2H_6$ , $C_3H_8$ , $C_6H_6$ , $C_{(solid)}$ , $H_2S$ and $N_2$	Product gas composition behavior with biomass moisture and amount of air injected in the reactor, temperature of the reaction and low calorific value of the product gas.
4	Curitiba's MSW	Non-Stoichiometric	280 bar, adiabatic and $H^{\circ}f(\text{MSW})$ Equation 49	$O_2$ , $N_2$ and $H_2O$	$H_2$ , $CO$ , $CO_2$ , $CH_4$ , $H_2O$ , $O_2$ , $C_2H_6$ , $C_3H_8$ , $C_6H_6$ , $C_{(solid)}$ , $H_2S$ and $N_2$	Product gas composition behavior with biomass moisture and amount of air injected in the reactor, temperature of the reaction and low calorific value of the product gas.
5	Curitiba's MSW	Non-Stoichiometric	280 bar and $H^{\circ}f(\text{MSW})$ Equation 49	$H_2O$	$H_2$ , $CO$ , $CO_2$ , $CH_4$ , $H_2O$ , $O_2$ , $C_2H_6$ , $C_3H_8$ , $C_6H_6$ , $C_{(solid)}$ , $H_2S$ and $N_2$	Product gas composition behavior with biomass feed concentration, temperature of the reaction and low calorific value of the product gas.
6	Wood Chips	Non-Stoichiometric	1 bar, adiabatic and $H^{\circ}f(\text{Wood})$ by Zainal et al. (2001)	$O_2$ , $N_2$ and $H_2O$	$H_2$ , $CO$ , $CO_2$ , $CH_4$ , $H_2O$ , $O_2$ , $C_2H_6$ , $C_3H_8$ , $C_6H_6$ , $C_{(solid)}$ , $H_2S$ and $N_2$	Product gas composition changes with biomass moisture and temperature of the reaction

Once found out the composition of the Curitiba's Municipal Solid Waste, Section 3.1, it is possible to generate its ultimate analysis. For scenarios 1, 2, 3, 4 and 6, the amount of air that can be fed to the gasifier and moisture are parameters varied to optimize the LHV. In scenario 5 the feed concentration of biomass was varied and the LHV optimized. Scenario 6 was proposed to compare with the validated stoichiometric based on the work of Zainal et al. (2001).

The flowchart in Figure 20 shows the algorithm used to generate the simulation data.

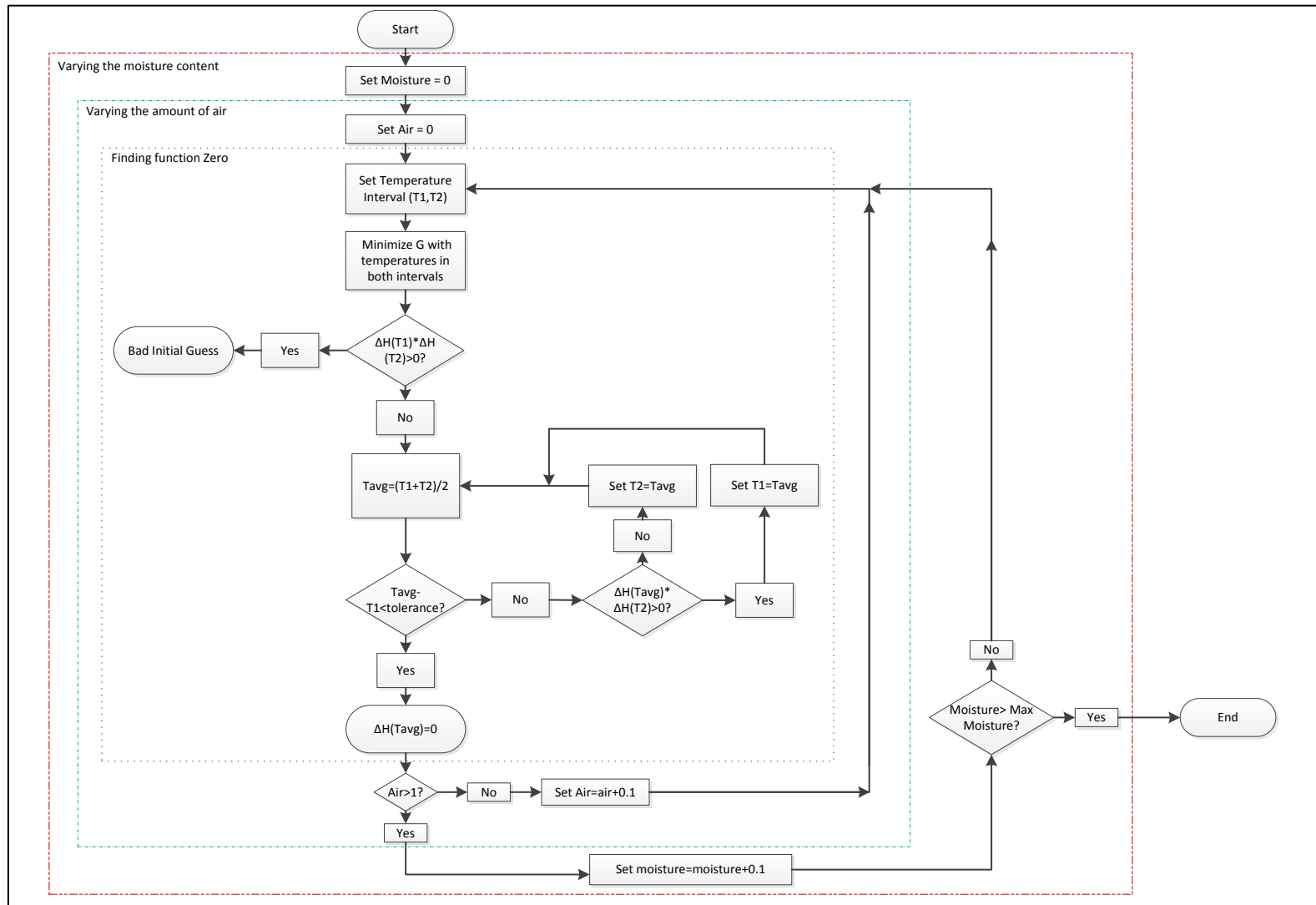


Figure 20 - Algorithm used to generate the simulation data of the Curitiba's MSW gasification.

Using the strategy showed in Figure 20, the simulation and optimization of the Curitiba's MSW gasification was carried out, varying the amount of air that enter the gasifier and also the MSW's moisture, according to the following criteria:

- Empirical formula for Curitiba MSW:  $CH_{1.5079}O_{0.4342}N_{0.0295}S_{0.0015}$
- Enthalpy of formation of Curitiba's MSW evaluated using the same method described by Zainal et. al. (2001) equation 49 (Scenarios 1, 2, 4 and 5). For scenario 3 the equation 50 was used.
- Substances predicted in the product gas (except for the MSW, that is assumed to be entire transformed during the gasification process), Standard Enthalpy of formation and Standard Gibbs Energy according to the following Table 9:

**Table 9 - Standard Enthalpy of formation and Standard Gibbs Free Energy (ideal gas state) of the components of the product gas and MSW.**

Component	H <sup>o</sup> f(kJ/kmol)	ΔG <sup>o</sup> f(kJ/kmol)	Source
CO <sub>2</sub>	- 393,509.00	- 394,359.00	Zainal et al. (2001)
CO	- 110,525.00	- 137,169.00	Zainal et al. (2001)
CH <sub>4</sub>	- 74,520.00	- 50,460.00	Zainal et al. (2001)
H <sub>2</sub> O liq	- 285,830.00	- 237,129.00	Zainal et al. (2001)
H <sub>2</sub> O vap	- 241,818.00	- 228,572.00	Zainal et al. (2001)
H <sub>2</sub>	-	-	Zainal et al. (2001)
O <sub>2</sub>	-	-	Zainal et al. (2001)
N <sub>2</sub>	-	-	Zainal et al. (2001)
C	-	-	Zainal et al. (2001)
MSW	-121,797.54 <sup>1</sup>	Not estimated	This work
C <sub>2</sub> H <sub>6</sub>	- 84,700.00	- 32,800.00	Prabir Basu (2010)
C <sub>3</sub> H <sub>8</sub>	- 103,800.00	- 23,500.00	Prabir Basu (2010)
C <sub>6</sub> H <sub>6</sub>	82,980.00	129,700.00	Prausnitz (1987)
H <sub>2</sub> S	- 20,600.00	- 33,600.00	Prabir Basu (2010)

<sup>1</sup>-For scenarios 1, 2, 4 and 5. In scenario 2 the value is -88,585.27 kJ/kmol. For scenario 6 -138,497 kJ/kmol.

- Pressure of 1 bar for scenarios 1, 2, 3 and 6, Pressure of 280 bar for scenarios 4 and 5,  $R = 8.314 \text{ kJ}/(\text{kmol}\cdot\text{K})$ , Reference temperature 298.15 K.
- Gibbs energy calculated according equations presented in Section 3.3.
- Calorific heat capacities calculated using equations according to Table 10.

**Table 10 – Ideal gas heat Capacities of pure compounds predicted as the product gas.**

Component	CpA	CpB	CpC	CpD	Range(K)	Source
H <sub>2</sub>	2.892E+01	-9.137E-04	2.921E-06	-5.719E-10	298-3098	NIST*
CO	2.583E+01	1.001E-02	-3.035E-06	3.184E-10	298-3098	NIST*
CO <sub>2</sub>	2.727E+01	4.233E-02	-1.818E-05	2.662E-09	298-3098	NIST*
CH <sub>4</sub>	1.090E+01	8.644E-02	-2.934E-05	3.526E-09	298-3098	NIST*
H <sub>2</sub> O	2.903E+01	1.298E-02	-1.426E-07	-4.110E-10	298-3098	NIST*
O <sub>2</sub>	2.580E+01	1.336E-02	-5.262E-06	7.933E-10	298-3098	NIST*
C <sub>2</sub> H <sub>6</sub>	1.412E+01	1.562E-01	-5.620E-05	7.111E-09	100-3000	NIST*
C <sub>3</sub> H <sub>8</sub>	1.433E+01	2.353E-01	-8.137E-05	6.074E-09	80-2854	ChemSep v6.99*
C <sub>6</sub> H <sub>6</sub>	1.795E+00	3.316E-01	-1.448E-04	2.150E-08	50-3000	NIST*
C	-3.333E+00	4.907E-02	-3.051E-05	6.577E-09	300-2000	DIADEM*
H <sub>2</sub> S	2.612E+01	2.653E-02	-7.695E-06	7.878E-10	298-3098	NIST*
N <sub>2</sub>	2.620E+01	8.320E-03	-1.975E-06	1.326E-10	298-3098	NIST*

\*Equation format used:  $Cp = CpA + CpB(T) + CpC(T)^2 + CpD(T)^3$  (J/mol-K)

- The main objective that was placed in Solver (Excel) was to minimize G; by changing the number of moles of H<sub>2</sub>, CO, CO<sub>2</sub>, CH<sub>4</sub>, H<sub>2</sub>O, O<sub>2</sub>, C<sub>2</sub>H<sub>6</sub>, C<sub>3</sub>H<sub>8</sub>, C<sub>6</sub>H<sub>6</sub> and C, whereas H<sub>2</sub>S and N<sub>2</sub> are known and come direct from mass balance. Following the restrictions that the mole number of products should be greater than

or equal to zero and the difference between the input and output of carbon, hydrogen and oxygen must be zero, bearing in mind that sulfur and nitrogen are already imposed as zero as a premise by applying the nonlinear GRG method.

#### **4. CHAPTER IV: RESULTS AND DISCUSSION**

First, in this chapter, it is shown the validation of both stoichiometric and non-stoichiometric models developed in this work, and then a comparison between the two methods is discussed. Afterwards the results of the simulation of the scenarios proposed in Chapter III are shown and discussed.

##### **4.1. VALIDATION OF THE STOICHIOMETRIC MODEL**

In order to validate the stoichiometric equilibrium model (presented in section 3.2), a simulation of wood chips gasification was performed and compared to results presented by Zainal et al. (2001). Figure 21 shows the obtained results is the present work.

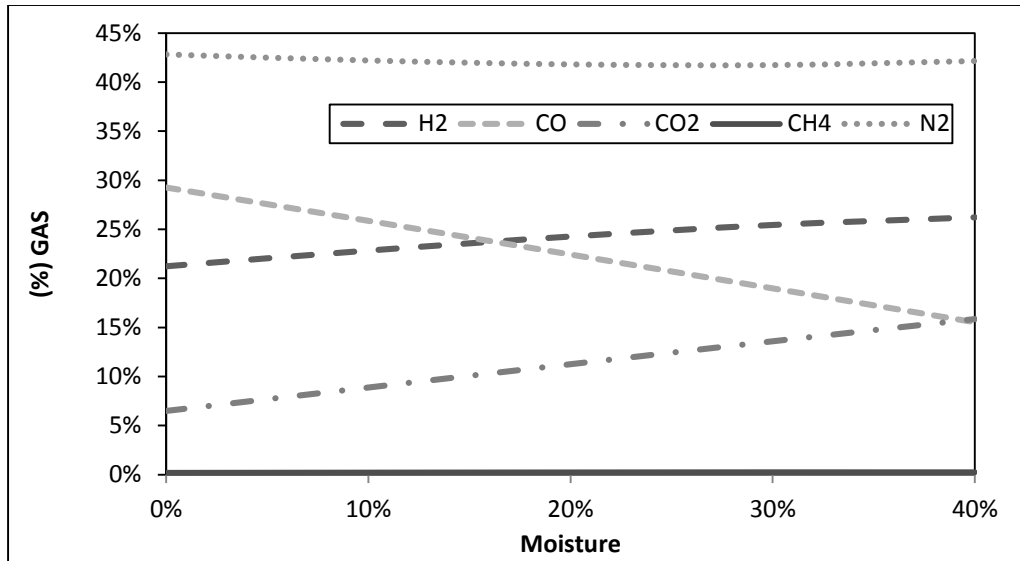


Figure 21 - Simulation of wood chips gasification at 1073.15K.

The results obtained are in visual agreement (graphical comparison) with results presented by Zainal et al. (2001). However, when Zainal et al. (2001) compare the numbers presented in the plotted results, one can notice that there are differences between the results written and in the graphical form. It is presented here, in Table 11, a numerical comparison of the model developed in this work with results presented by Zainal et al. (2001).

Table 11 - Comparison of results obtained in this work with the results presented by Zainal et al. (2001) and with the experimental results by Alaudin (1996).

Component	Reported by Zainal et al. (2001)			This work
	Experimental	Predicted	Graphical Interpretation <sup>(a)</sup>	
H <sub>2</sub>	15.23%	21.06%	24.26%	23.96%
CO	23.04%	19.61%	22.42%	21.69%
CH <sub>4</sub>	1.58%	0.64%	0.24%	1.46%
CO <sub>2</sub>	16.42%	12.01%	11.26%	11.66%
N <sub>2</sub>	42.31%	46.68%	41.81%	41.28%
O <sub>2</sub>	1.42%	0.00%	0.00%	0.00%

(a) Values read using *pega ponto* software

From results compared in Table 11, it can be observed that the values predicted by the model developed in this work are in good agreement with the results presented by Zainal et al. (2001). Therefore, the equations and approach implement in this work are reliable and can be used to further simulations and theoretical studies of biomass gasification.

#### 4.2. STOICHIOMETRIC MODEL FOR CURITIBA'S MSW GASIFICATION (SCENARIO 1)

To develop Scenario 1, as presented in Table 8, by using the stoichiometric approach for the modelling of the gasification of MSW already described in section 3.2 it was possible to simulate the product gas of the Curitiba's MSW gasification. Table 12 and Figure 22 show the results.

**Table 12 - Molar composition, in dry basis, of the gasification products of Curitiba's MSW at 1073.15 K, where m is the amount in kmol of air inject per kmol of MSW in the system.**

<b>m</b>	<b>Moisture</b>	<b>H<sub>2</sub></b>	<b>CO</b>	<b>CO<sub>2</sub></b>	<b>CH<sub>4</sub></b>	<b>N<sub>2</sub></b>
0.506	0%	16.14%	20.99%	7.64%	0.11%	55.12%
0.511	10%	17.33%	18.69%	9.34%	0.13%	54.52%
0.519	20%	18.41%	16.33%	11.05%	0.14%	54.08%
0.530	30%	19.30%	13.92%	12.77%	0.15%	53.87%
0.547	40%	19.91%	11.47%	14.46%	0.15%	54.02%

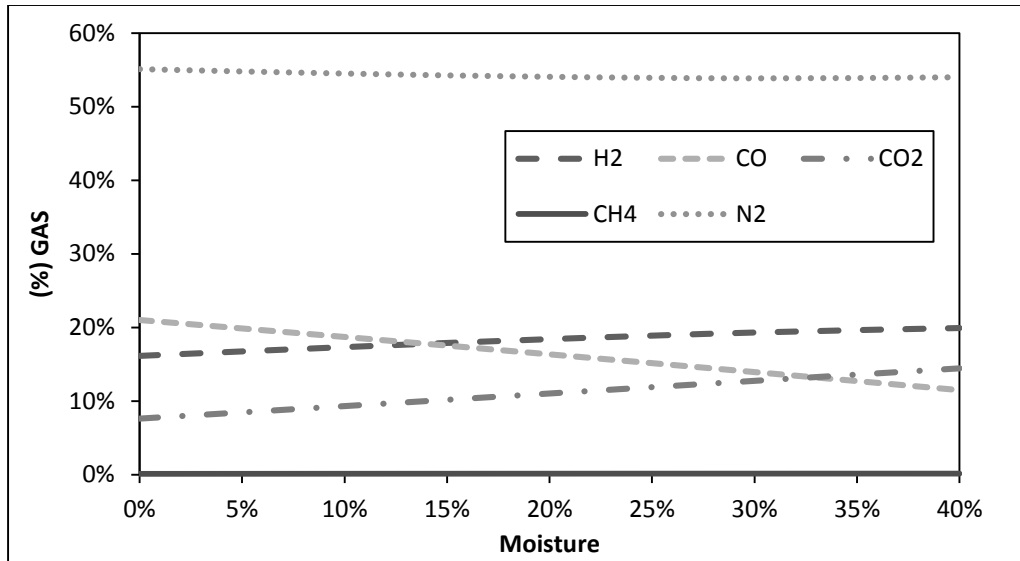


**Figure 22 - Molar composition variation, in a dry basis, of the product gas of the Curitiba's MSW gasification.**

From the results presented in Figure 22 it is possible to see that when only varying the moisture content of the MSW similar behavior to the wood is found. However, the content of the main gases (CO and H<sub>2</sub>) is lower. Implicating in a lower LHV of the product gas. This is due to lower carbon and hydrogen content in the MSW than in the wood.

#### 4.3. VALIDATION OF THE NON-STOICHIOMETRIC MODEL

Using the same methodology presented in section 3.3, it was possible to obtain the results presented in Figure 23, where they are compared to experimental results presented in the literature for the ethanol gasification.



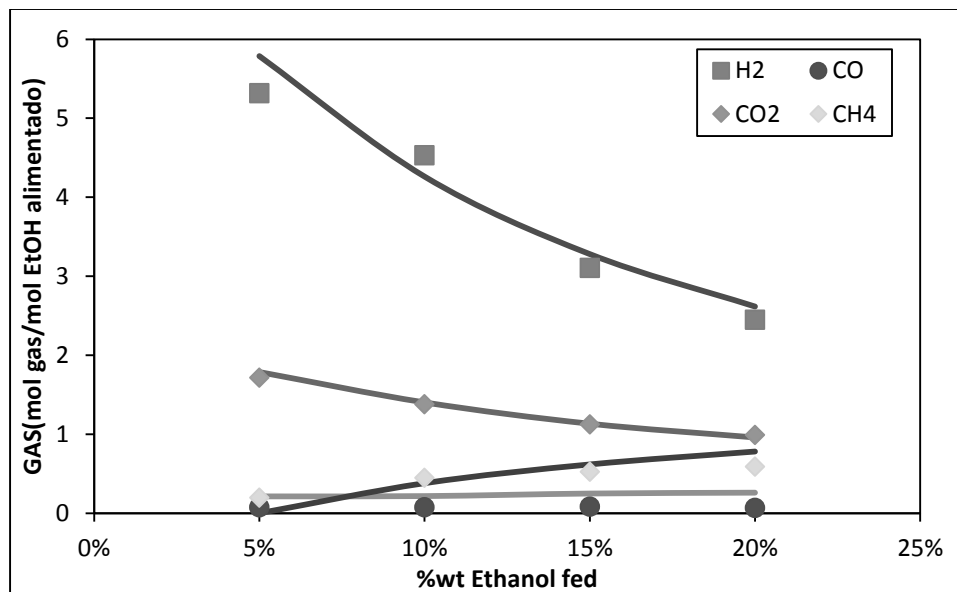


**Figure 23 - Results for the supercritical water gasification of ethanol at 1073.15 K and 22.1 MPa. Solid Line: this work; Symbols: Byrd et al. (2007).**

This same simulation was previously run and presented by Voll et al (2009). It can also be observed that the results presented in this work using non-stoichiometric approach are in accordance with those presented by Voll et al (2009) and the experimental data from Byrd et al. (2007), as it can be seen in Figure 23.

Antal et al. (2000) also developed a series of experiments regarding to supercritical gasification of biomass. These authors gasified corn- and potato-starch gels, wood sawdust and potato wastes. The samples were quickly heated at temperatures above 650 °C and pressures above the critical pressure of water (22 MPa).

Using the non-stoichiometric approach developed in this work, it was possible to simulate and compare the experiments performed by Antal et al. (2000). It was adopted the following premises:

Biomass: Corn-starch

Feed: Water and biomass

Feed Biomass concentration: 10.4% wt.

Pressure: 28 MPa

Temperature: 650 °C

Possible products: H<sub>2</sub>, CO, CO<sub>2</sub>, CH<sub>4</sub>, H<sub>2</sub>O, O<sub>2</sub>, C<sub>2</sub>H<sub>6</sub>, C<sub>3</sub>H<sub>8</sub>, C<sub>6</sub>H<sub>6</sub>, C<sub>solid</sub>, N<sub>2</sub>.  
 Ultimate analysis (Dry basis): As presented in Table 13.

**Table 13 - Ultimate analysis from Corn-starch by Antal et al. (2000).**

<b>Element</b>	<b>%wt</b>
C	42.7%
H	6.2%
O	50.9%
N	0.1%
S	0.1%
Ash	0.1%

Using the ultimate analysis presented in Table 13 it is possible to determine the empirical formula for the biomass, which becomes:

$$CH_{1.742}O_{0.894} \quad (80)$$

Throughout the minimization of the Gibbs energy (equation 69) it was possible to obtain the results presented in Table 14.

**Table 14 - Results from the developed model. Gas composition in dry basis.**

<b>Component</b>	<b>% GAS dry</b>
H <sub>2</sub>	46.52%
CO	1.45%
CO <sub>2</sub>	37.59%
CH <sub>4</sub>	14.44%
O <sub>2</sub>	0.00%
C <sub>2</sub> H <sub>6</sub>	0.00%
C <sub>3</sub> H <sub>8</sub>	0.00%
C <sub>6</sub> H <sub>6</sub>	0.00%
C	0.00%
N <sub>2</sub>	0.00%

Figure 24 presents a comparison between the simulated results in this work with the experimental results reported by Antal et al. (2000). For the simulation of gasification of biomass hereby considered, it can be seen that the results are in good agreement with the experimental data presented in the literature. Therefore, also the non-stoichiometric approach used in the present work is reliable and suitable for simulations of biomass gasification.

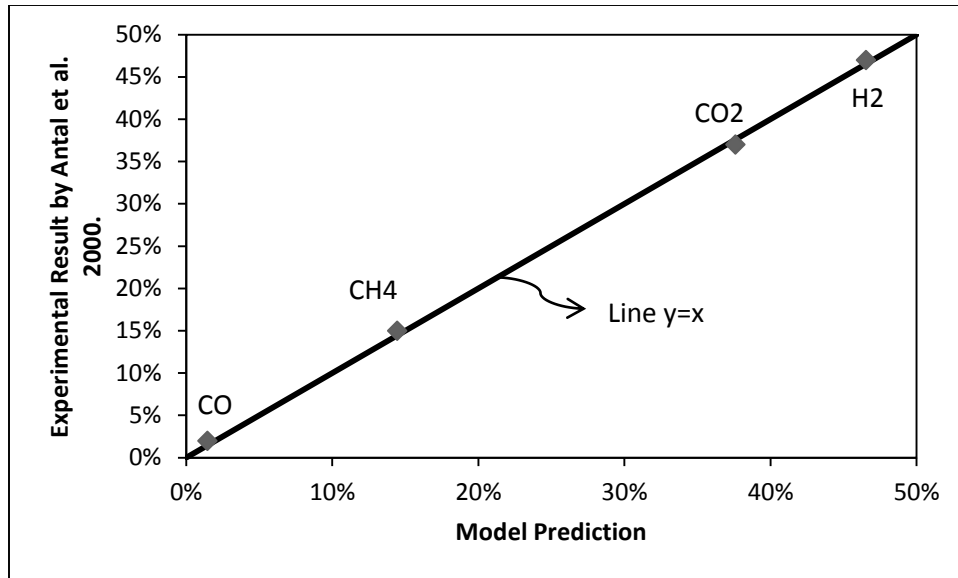
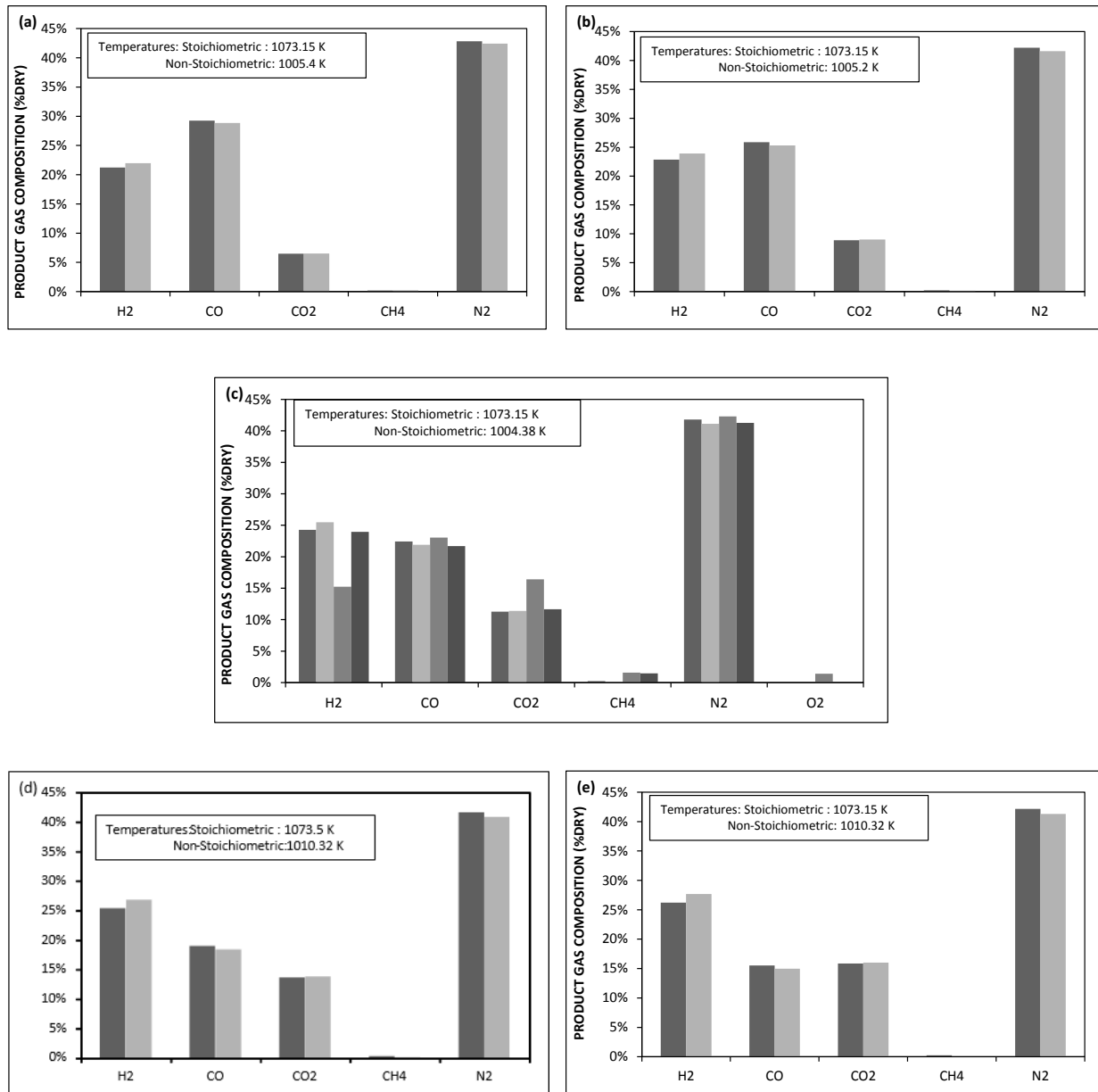


Figure 24 - Comparison between the experimental data from Antal et al. (2000) and the model prediction.

#### 4.4. NON-STOICHIOMETRIC VERSUS STOICHIOMETRIC APPROACHES

In order to compare the stoichiometric and non-stoichiometric approaches, a simulation using the premises of Zainal et al. (2001), section 3.2, was carried out using the non-stoichiometric approach. The results, from scenario 6, presented in Figure 25, are a comparison between the non-stoichiometric and stoichiometric models for the gasification of wood.

Additionally, some simulations comparing both approaches (stoichiometric and non-stoichiometric) were also run considering the Curitiba's municipal solid waste. The results are compared and presented in Figure 26.



**Figure 25 –Scenario 6. Results for stoichiometric model developed based on Zainal et al. (2001) versus results for non-stoichiometric model developed in this work. Bars represent: ■ Stoichiometric, ■ Non-stoichiometric, ■ Alauddin (1996), Experimental, ■ Zainal et al. (2001). Moisture (a) 0%, (b) 10%, (c) 20%, (d) 30% and (e) 40%.**

The results presented in Figure 25 and Figure 26 showed similar results, with good approximation between both methods. It can be noticed also that the temperature between the two approaches may vary. While in the stoichiometric approach the temperature is a premise and in the non-stoichiometric approach the temperature is an

unknown variable. The chemical formula of Curitiba's MSW was adapted to compare the same substances, by taking the sulfur out, as it is in small amount.

Both methods can have similar results, but when simulating a more complex system the non-stoichiometric approach is more advantageous, because in it is not required to specify the reactions that can occur, thus making the simulation more reliable, since none mechanism was guessed. Thus for the optimization of Curitiba's MSW gasification the non-stoichiometric method will be adopted.

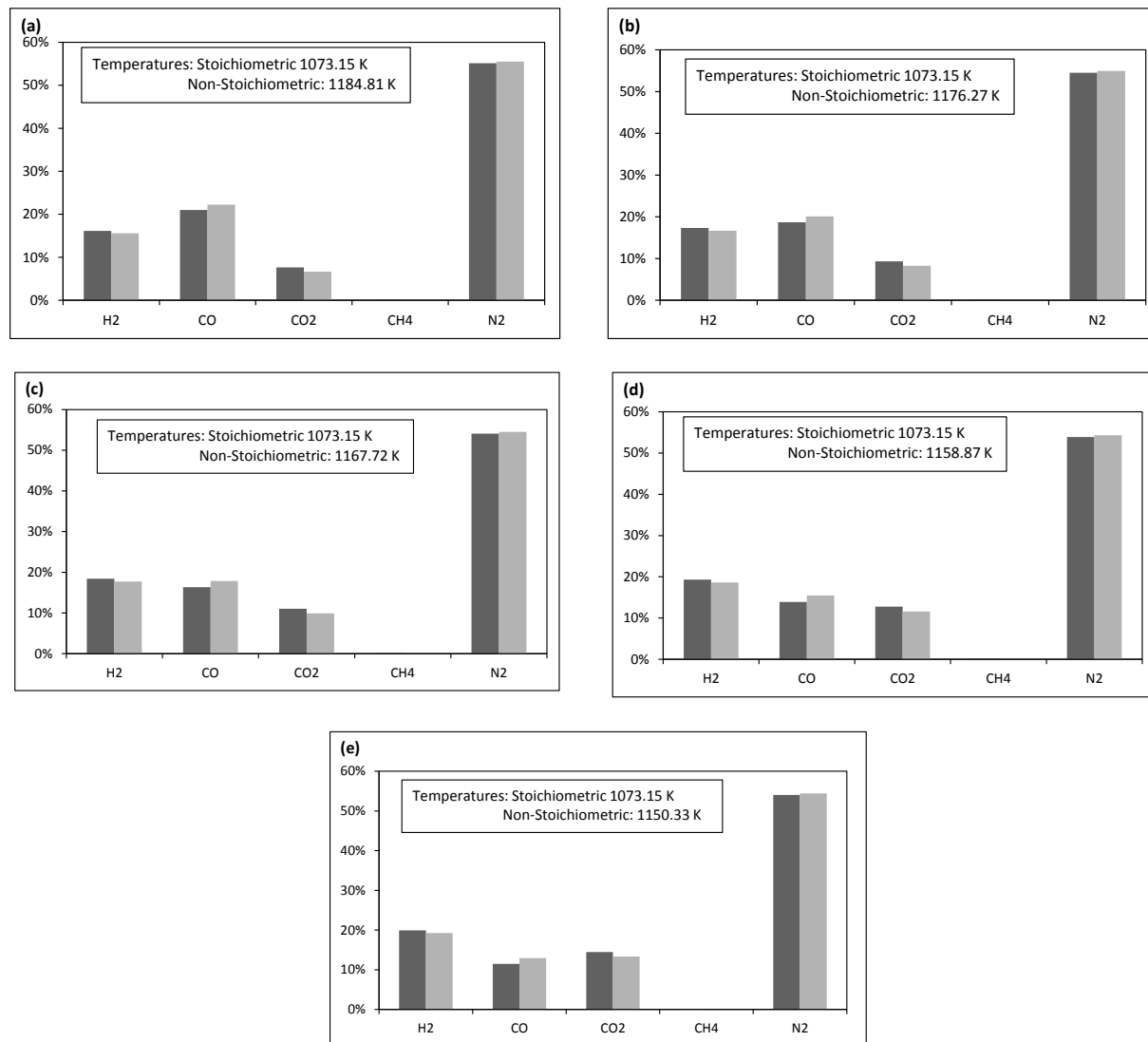


**Figure 26 – Comparison for the gasification of Curitiba's municipal solid waste. Results for stoichiometric model adapted from Zainal et al. (2001) versus results for non-stoichiometric model (Scenario 1) developed in this work. Bars represent: ■ Stoichiometric, ■ Non-stoichiometric. Moisture (a) 0%, (b) 10%, (c) 20%, (d) 30% and (e) 40%.**

#### 4.5. OPTIMIZATION OF CURITIBA'S MSW GASIFICATION

The optimizations are regarding to the best energy output, in the process point of view, looking for the maximum low heating value (LHV) of the product gas.

Simulations of scenario 2 were run and compiled and plotted according to presented in Figure 27 and Figure 28.

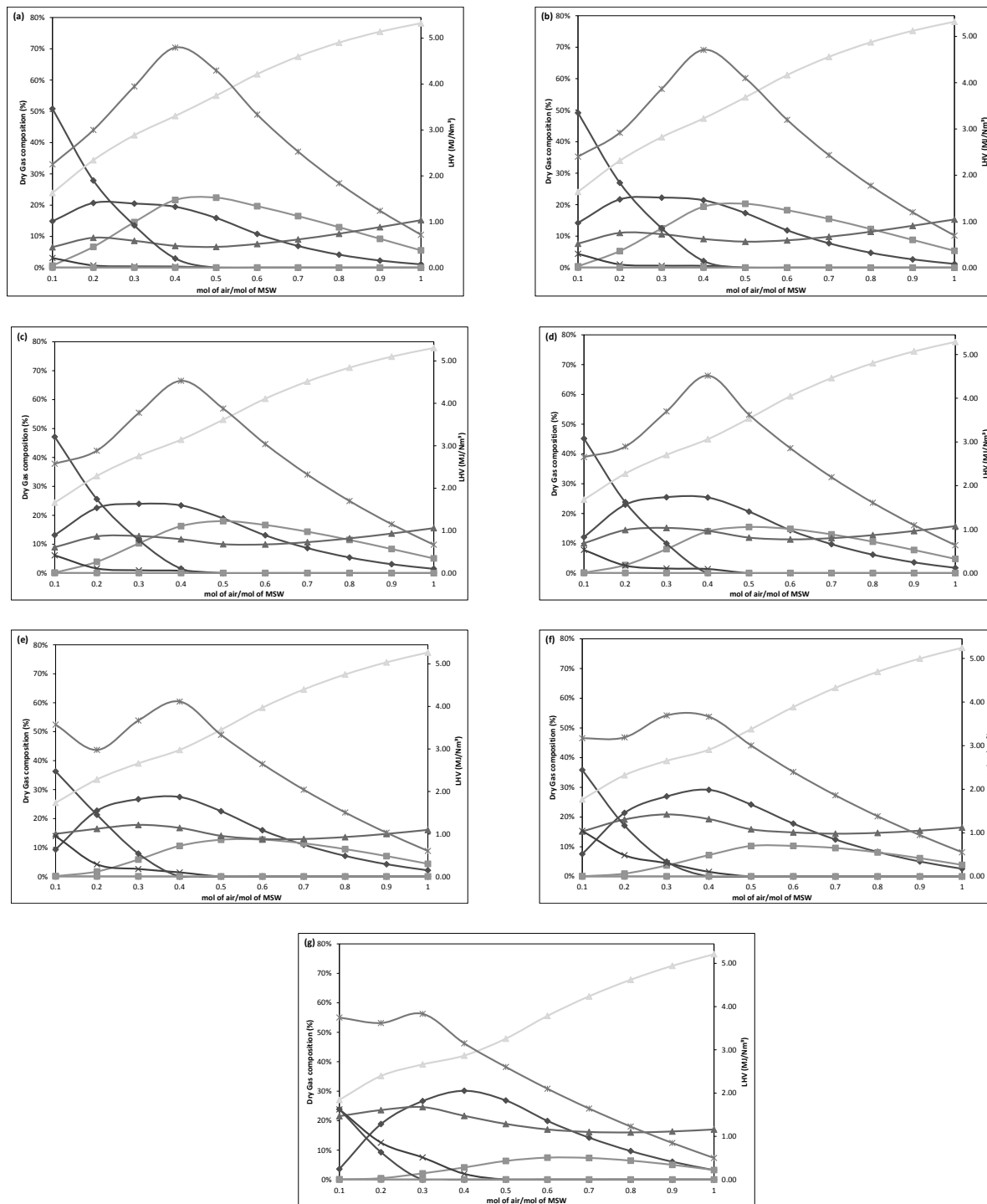


**Figure 27 – Scenario 2. Product gas of Curitiba's MSW gasification. Amount of air varying from 0.1 to 1 mol of air per mol of MSW that enters the gasifier. MSW's moisture varying from 0% to 60%. Legend: —◆— H<sub>2</sub>, —■— CO, —▲— CO<sub>2</sub>, —×— CH<sub>4</sub>, —●— O<sub>2</sub>, —★— C, —■— H<sub>2</sub>S, —★— N<sub>2</sub>, —★— LHV. Moisture (a) 0%, (b) 10%, (c) 20%, (d) 30%, (e) 40%, (f) 50% and (g) 60%.**



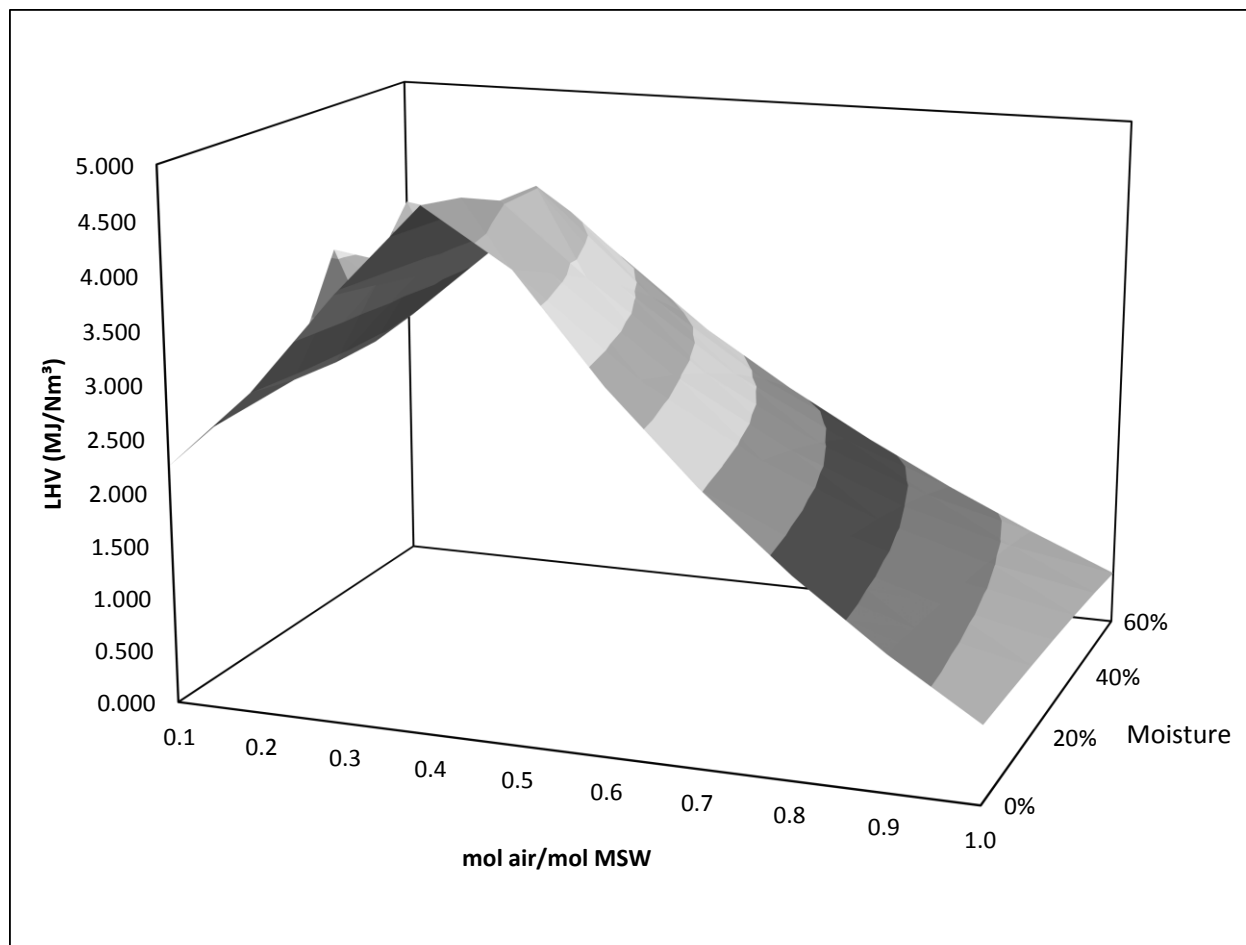


Figure 28 - Scenario 2. Low Heating values of the product gas of Curitiba's MSW gasification.

From the data showed in Table 15 (and Figure 28) it is possible to observe that, for a given moisture, there is an increase of the LHV with the increase of the amount of air per mol of biomass injected in the system, the LHV then, reaches its maximum and then decreases with the increase of air injected in the system.

**Table 15 - Low heating value variation with air inlet amount and moisture.**

		<b>Low Heating Values (MJ/Nm<sup>3</sup>)</b>									
Air input (mol/ mol MSW)		0.1	0.2	0.3	0.4	0.5	0.6	0.7	0.8	0.9	1.0
<b>Moisture</b>	0%	2.250	3.000	3.949	4.796	4.295	3.336	2.529	1.839	1.240	0.717
	10%	2.402	2.919	3.864	4.710	4.098	3.198	2.433	1.774	1.200	0.695
	20%	2.575	2.886	3.776	4.530	3.876	3.040	2.322	1.699	1.152	0.669
	30%	2.654	2.894	3.698	4.516	3.623	2.859	2.193	1.611	1.096	0.638
	40%	3.572	2.978	3.670	4.116	3.333	2.647	2.042	1.507	1.030	0.602
	50%	3.169	3.190	3.694	3.665	3.005	2.398	1.861	1.381	0.948	0.557
	60%	3.747	3.621	3.832	3.150	2.604	2.100	1.642	1.226	0.847	0.500

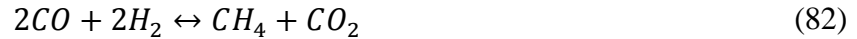
Similar behavior was founded by Ramzam et al. (2011), using municipal solid waste, food waste and poultry waste. As the air amount injected in the system increases, the amount of oxygen supplied to the gasifier increases causing conversion of carbon present in the fuel to rise. However, excess amount of oxygen oxidizes the fuel completely and the LHV of the product gas yield declines.

For a given amount of air, there are two behaviors that can be observed. The first one happens for amounts of air between 0.1 and 0.2 mol of air injected per mol of MSW fed to the system, where, in general, the LHV increases with the increasing moisture levels. The second one is that above 0.2 there is a decrease of LHV with the increase amount of moisture.

The first behavior can be explained due increase of the CH<sub>4</sub> concentration in the product gas, and at the same time the decrease of the concentration of H<sub>2</sub>, CO and C. With the increasing moisture in the system, the level of H<sub>2</sub>O increases and consumes solid carbon, according to reaction in equation 81:



Then the methanation reaction takes place to form CH<sub>4</sub>:



The levels of CO<sub>2</sub> are also increasing with moisture, for any given amount of air, which supports the statement above.

For the second behavior, the amounts of solid carbon above 0.2 mol of air are lower reaching 0 at 0.4 mol of air/mol of MSW fed to the system. Moreover, although the levels of hydrogen (for air>0.4) are increasing, in general the amount of H<sub>2</sub>O injected to the system is even higher, and as LHV of H<sub>2</sub>O is zero thus decreasing LHV with increasing moisture.

The method to evaluate the enthalpy of formation of MSW must be chosen carefully. Another simulation was carried out (Scenario 3) using equation 50. Others premises remain the same stated for Scenario 2.

The results for scenario 3 are shown in Figure 29, Figure 30 and Table 16. These reveal that the final composition of the gas predicted by the model can vary greatly depending on the method adopted to evaluate the MSW enthalpy of formation. In addition, the low heating value can change as well its optimal operation point for the maximum LHV syngas value.

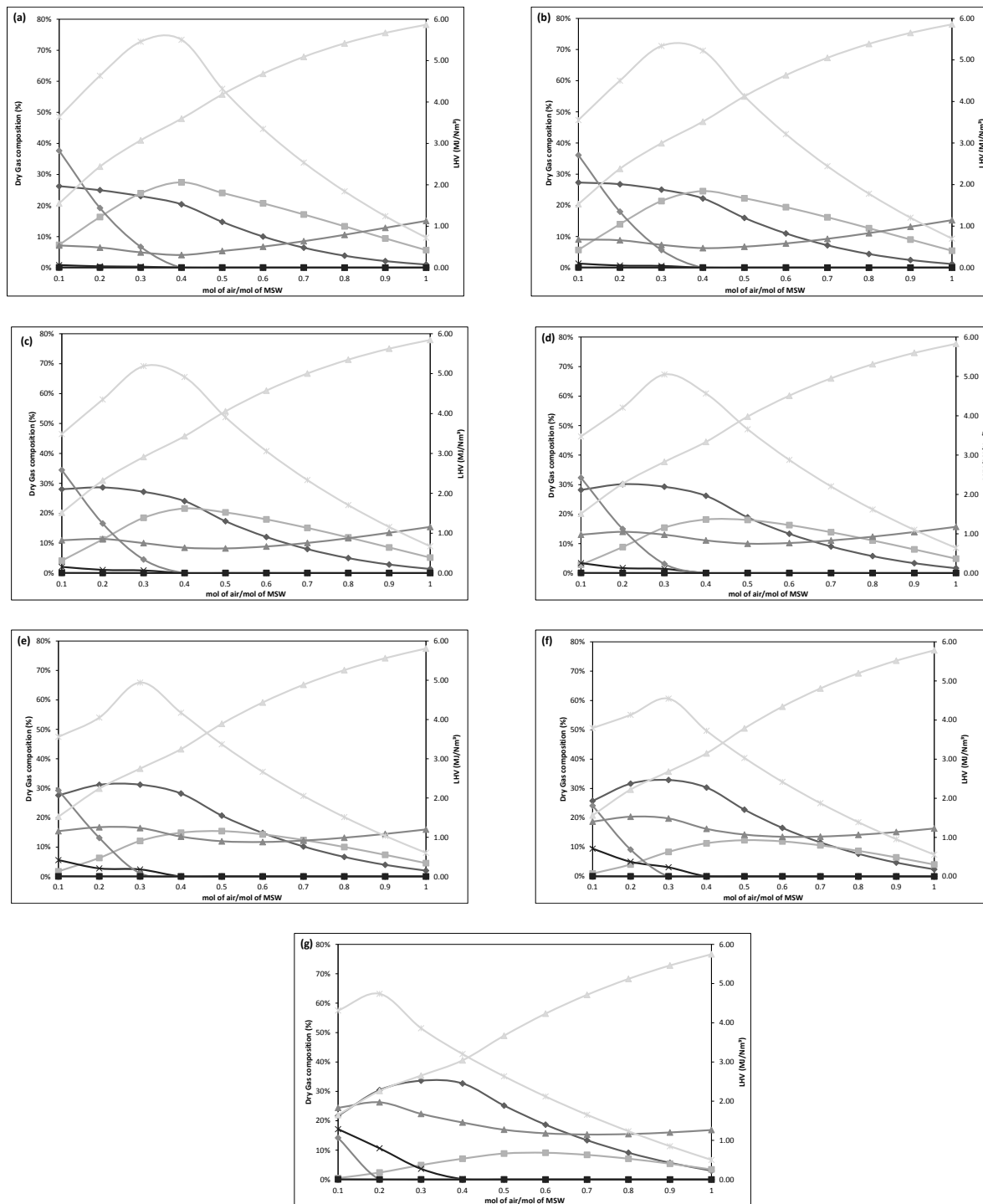


**Figure 29 – Scenario 3. Product gas of Curitiba's MSW gasification. Amount of air varying from 0.1 to 1 mol of air per mol of MSW that enters the gasifier. MSW's moisture varying from 0% to 60%. Simulation carried out using the method proposed from Basu to evaluate the enthalpy of formation.**

**Legend:** ◆ H<sub>2</sub>, ■ CO, ▲ CO<sub>2</sub>, ✕ CH<sub>4</sub>, ● O<sub>2</sub>, ▼ C, ◼ H<sub>2</sub>S, \* N<sub>2</sub>, \* LHV.  
**Moisture (a) 0%, (b) 10%, (c) 20%, (d) 30%, (e) 40%, (f) 50% and (g) 60%.**

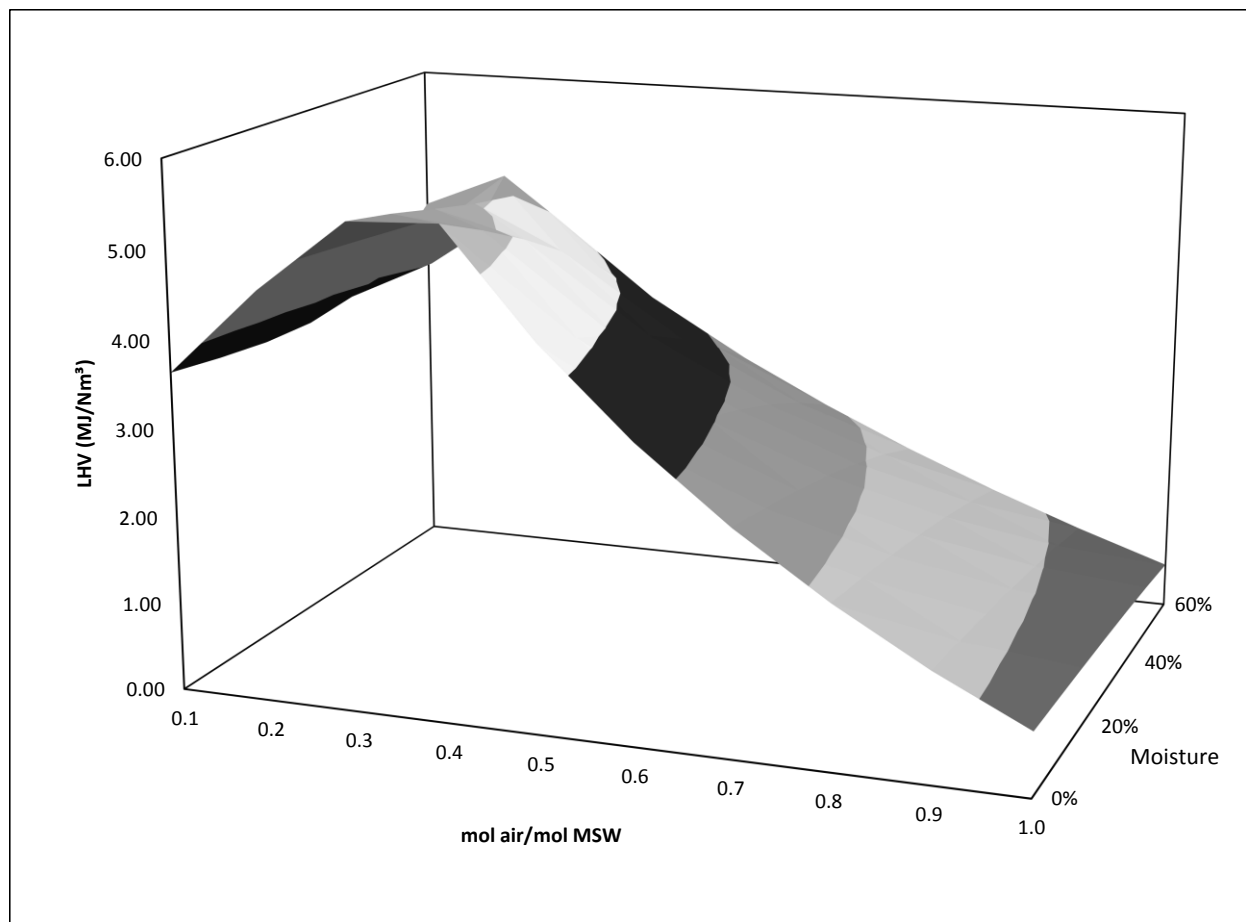


Figure 30 - - Scenario 3. Low Heating values of the product gas of Curitiba's MSW gasification. Simulation carried out using the method proposed from Basu to evaluate the enthalpy of formation.

Table 16 - Scenario 3. Low heating value variation with air inlet amount and moisture. Simulation carried out using the method proposed from Basu to evaluate the enthalpy of formation.

		Low Heating Values (MJ/Nm <sup>3</sup> )									
Air input (mol/ mol MSW)		0.1	0.2	0.3	0.4	0.5	0.6	0.7	0.8	0.9	1.0
Moisture	0%	3.642	4.635	5.457	5.504	4.319	3.350	2.538	1.844	1.243	0.725
	10%	3.554	4.501	5.336	5.226	4.126	3.214	2.442	1.780	1.203	0.700
	20%	3.486	4.351	5.188	4.917	3.908	3.058	2.333	1.705	1.156	0.672
	30%	3.473	4.208	5.048	4.566	3.658	2.878	2.205	1.618	1.100	0.641
	40%	3.558	4.049	4.943	4.174	3.369	2.667	2.054	1.514	1.034	0.604
	50%	3.797	4.133	4.548	3.725	3.032	2.418	1.874	1.388	0.952	0.559
	60%	4.312	4.739	3.862	3.203	2.634	2.119	1.654	1.234	0.851	0.502

For other scenarios (1, 2, 4, 5 and 6), equation 49 was used for the calculation of energy of formation of MSW, due to the consistency of the simulations with results presented in the literature and experimental data.

Another possibility in optimizing the gasification process is to change the pressure in which the gasification occurs. Some results presented in the literature (BASU, 2010; ANTAL ET AL. ,2000; VOLL ET AL. 2009) are about the gasification at supercritical conditions as medium of improving the gasification efficiency. A simulation at high pressure was carried out to verify such behavior (scenario 4). Voll et al. (2009) showed that the approach considering ideal gas behavior is equivalent to the approach considering the non-ideal process. Besides that, the capability of the model developed in this work to fit simulation and experimental data reported by Voll et al. (2009) and Antal et al. (2000) are confirming that assuming ideal gas approach for the gasification processes leads to correct and real results. In order to compare the results simulated, the pressure of 28 MPa was chosen, which is the same pressure for biomass in Antal's work. Aside from the pressure, the other premises are the same as used in scenario 2.

For scenario 4, the results showed in Figure 31, Figure 32, and Table 17 reveal that at 28 MPa the optimum low heating value of the gasification product gas increases in comparison with the optimum value at scenario 2. Showing that supercritical gasification can be an interesting choice for the gasification of MSW.

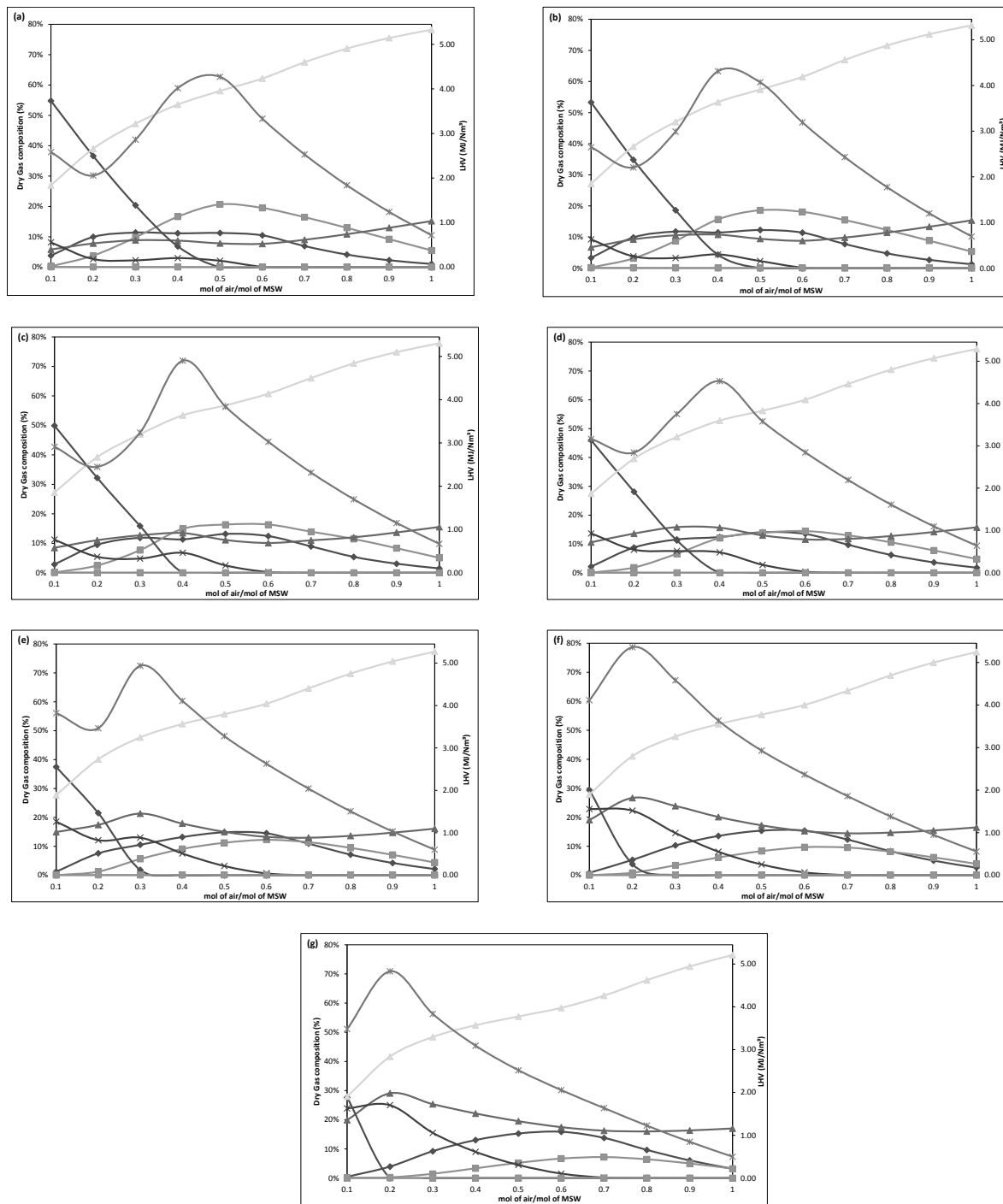


**Figure 31 –Scenario 4. Product gas of Curitiba's MSW gasification. Amount of air varying from 0.1 to 1 mol of air per mol of MSW that enters the gasifier. MSW's moisture varying from 0% to 60%. Pressure of 28 MPa (280 bar). Legend:  $\blacklozenge$  H<sub>2</sub>,  $\blacksquare$  CO,  $\blacktriangle$  CO<sub>2</sub>,  $\times$  CH<sub>4</sub>,  $\bullet$  O<sub>2</sub>,  $\blacktriangledown$  C,  $\blacksquare$  H<sub>2</sub>S,  $\ast$  N<sub>2</sub>,  $\ast$  LHV. Moisture (a) 0%, (b) 10%, (c) 20%, (d) 30%, (e) 40%, (f) 50% and (g) 60%.**

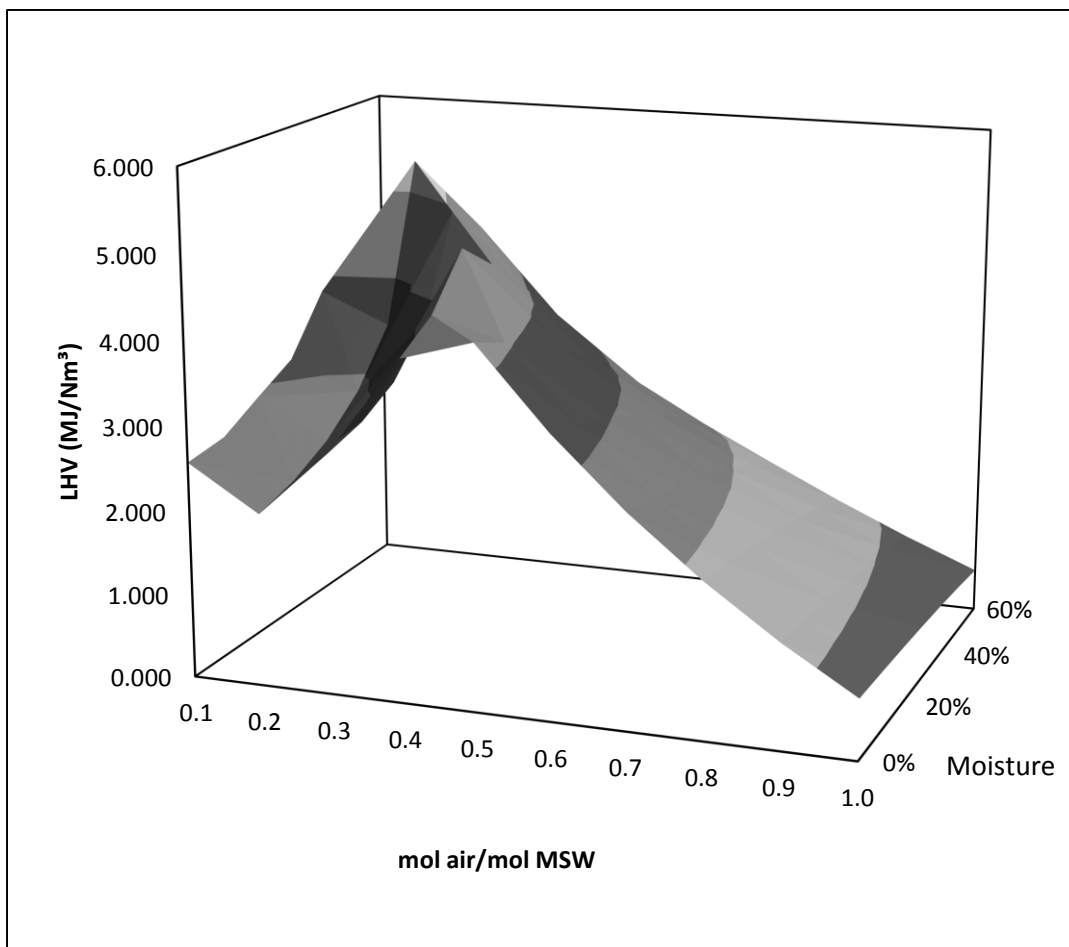


Figure 32 - Scenario 4. Low Heating values of the product gas of Curitiba's MSW gasification. Pressure of 28 MPa (280 bar).

Table 17 - Scenario 4. Low heating value variation with air inlet amount and moisture. Pressure of 28 MPa (280 bar).

		Low Heating Values (MJ/Nm <sup>3</sup> )									
Air input (mol/mol MSW)		0.1	0.2	0.3	0.4	0.5	0.6	0.7	0.8	0.9	1.0
Moisture	0%	2.580	2.057	2.862	4.017	4.271	3.331	2.529	1.839	1.240	0.716
	10%	2.648	2.206	2.990	4.312	4.069	3.192	2.432	1.774	1.200	0.694
	20%	2.912	2.449	3.242	4.903	3.840	3.031	2.317	1.699	1.152	0.669
	30%	3.162	2.841	3.752	4.530	3.579	2.845	2.193	1.611	1.096	0.638
	40%	3.821	3.465	4.937	4.110	3.279	2.627	2.041	1.507	1.030	0.602
	50%	4.112	5.359	4.581	3.634	2.929	2.368	1.859	1.381	0.948	0.557
	60%	3.482	4.830	3.835	3.093	2.520	2.055	1.635	1.226	0.847	0.500



In order to further explore Curitiba's MSW gasification, a simulation for supercritical water gasification was carried out (scenario 5), considering a temperature range of 823 K to 1273.15 K, at 28 MPa. In this simulation, only Curitiba's MSW and water are fed into the gasifier and then the feed concentration of MSW was varied from 100% to 10%. In addition, the process was no longer considered adiabatic. Other conditions are similar to those presented in scenario 4.

From the results showed in Figure 33, Figure 34 and Table 18, it is possible to notice that there is a considerable improvement in the product gas low heating value (LHV). Also the hydrogen concentration in the gas was improved, mainly for higher temperatures. Thus, it is possible to verify that for supercritical conditions it is possible to obtain for the Curitiba's MSW a higher LHV. However, it is important to notice that the process is no longer adiabatic and it is necessary to add energy to the system, which must be taken into account for further process design.

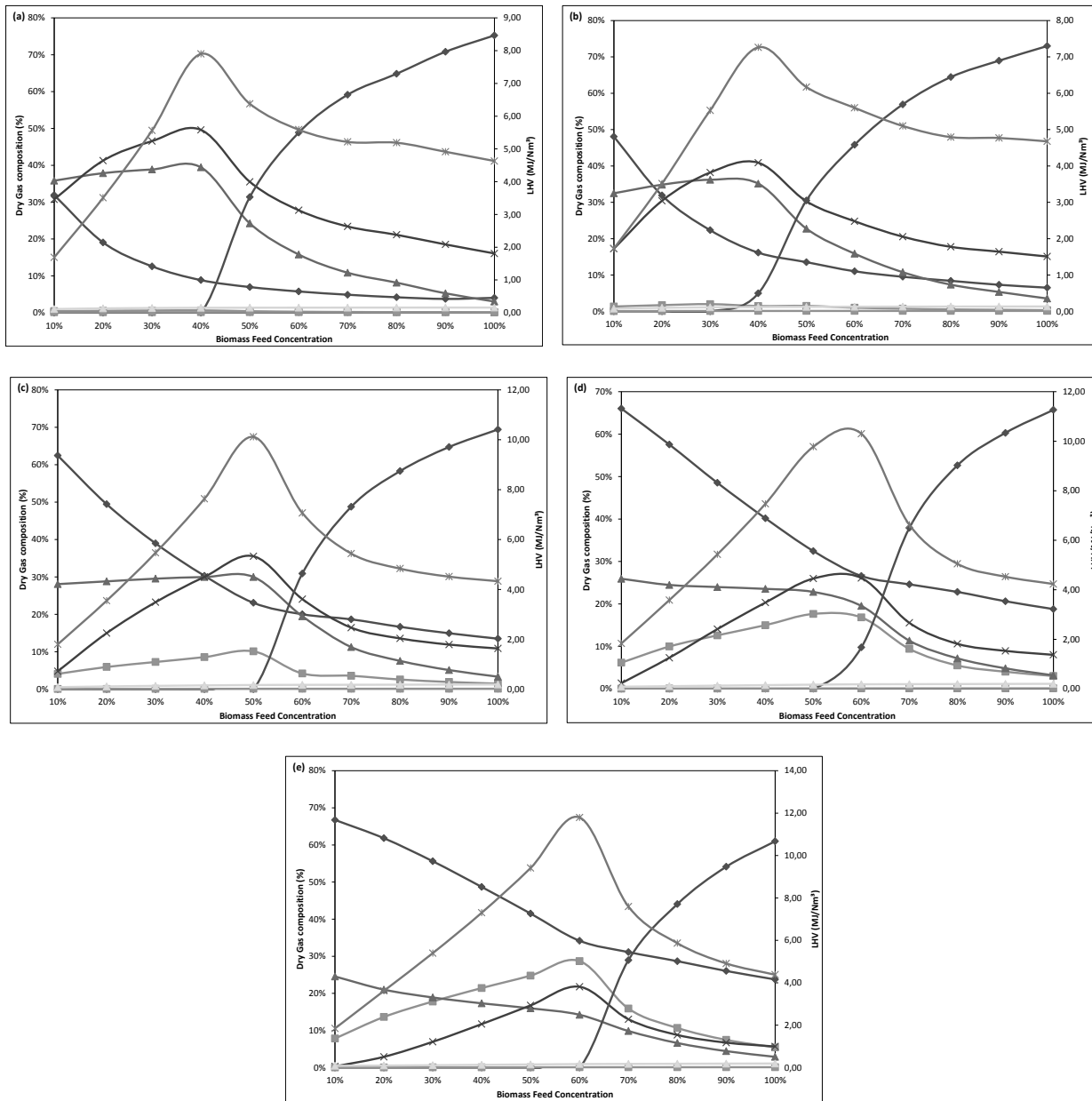
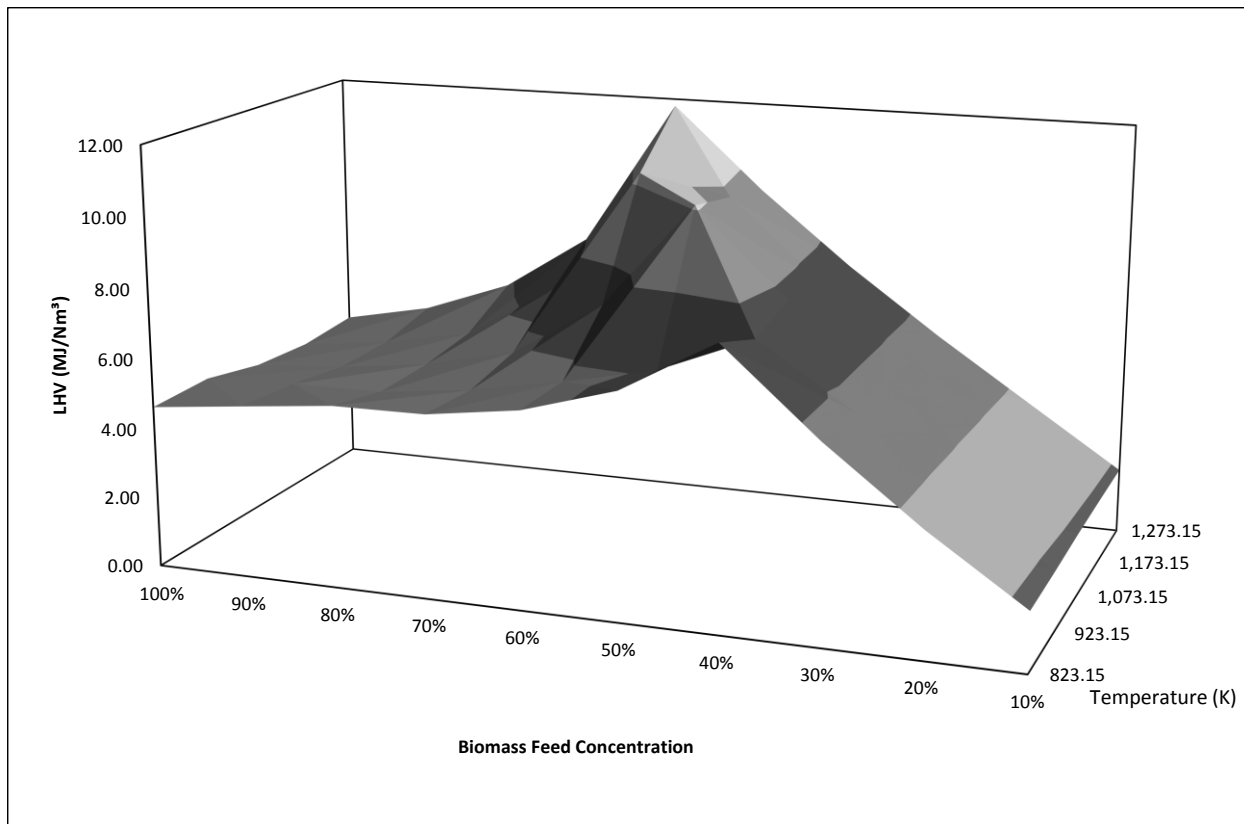


Figure 33 - Scenario 5. Product gas of Curitiba's MSW SCWG gasification. Temperatures of (a) 823.15K, (b) 923.15K, (c) 1073.15K, (d) 1173.15K and (e) 1273.15K. Pressure of 28 MPa (280 bar). Legend:  $\blacklozenge$  H<sub>2</sub>,  $\blacksquare$  CO,  $\blacktriangle$  CO<sub>2</sub>,  $\times$  CH<sub>4</sub>,  $\bullet$  O<sub>2</sub>,  $\star$  C,  $\blacksquare$  H<sub>2</sub>S,  $\ast$  N<sub>2</sub>,  $\ast$  LHV



**Figure 34 - Scenario 5. Low heating value variation with MSW feed inlet variation. Temperatures of 823.15K, 923.15K, 1073.15K, 1173.15K and 1273.15K. Pressure of 28 MPa (280 bar).**

**Table 18 - Scenario 5. Low heating value variation with MSW feed inlet variation. Temperatures of 823.15K, 923.15K, 1073.15K, 1173.15K and 1273.15K. Pressure of 28 MPa (280 bar).**

		Low Heating Values (MJ/Nm <sup>3</sup> )									
Biomass Feed Concentration		100%	90%	80%	70%	60%	50%	40%	30%	20%	10%
Temperature (K)	823.15	4.632	4.913	5.189	5.214	5.587	6.377	7.900	5.562	3.509	1.690
	923.15	4.677	4.771	4.795	5.101	5.600	6.169	7.264	5.530	3.517	1.728
	1,073.15	4.329	4.512	4.833	5.437	7.064	10.115	7.635	5.467	3.549	1.798
	1,173.15	4.234	4.529	5.049	6.623	10.303	9.779	7.471	5.429	3.584	1.832
	1,273.15	4.380	4.913	5.869	7.595	11.799	9.414	7.303	5.399	3.618	1.847

Table 19 presents a compilation from the optimum results for scenarios 2, 3, 4 and 5. It is possible to observe that when only differing in the method for evaluating the enthalpy of formation scenarios 2 and 3 can have different values for the LHV. Furthermore it is possible to see a significant improvement in the LHV from scenario 4 to 5, but it is necessary to point out that scenario 5 is not an adiabatic process, which would have to be taken into account when design the process. The optimum temperature, air amount and moisture also may vary according to the premises adopted.

**Table 19 – Optimum results for scenarios 2, 3 4 and 5.**

Scenario	Optimum LHV (MJ/Nm <sup>3</sup> )	Optimum Temperature (K)	Optimum air amount/mol of MSW	Optimum Moisture	Inlet Feed Concentration
2	4.796	969.85	0.4	0%	N/A
3	5.504	1106.08	0.4	0%	N/A
4	5.359	859.62	0.3	50%	N/A
5	11.799	1273.15	N/A	N/A	60%

## 5. CHAPTER V: CONCLUSIONS

This work reported a theoretical study of municipal solid waste gasification and optimization, regarding the process point of view, of the low caloric value of the gasification product gas.

A methodology to evaluate the ultimate analysis of Curitiba's municipal solid waste was developed, in which data available from literature can be compiled and used for an approximation in lack of direct measurement. A model to evaluate the product gas of the gasification process was developed based on the direct minimization of the Gibbs energy, validated with literature data and used to optimize the gasification processes.

It has been showed that depending on the method for evaluation the enthalpy of formation of the MSW results may vary, been ideal to measure it before going for design phase of the processes. It was also revealed that both stoichiometric and non-stoichiometric approaches can be equivalent, in accordance with already mentioned by Voll et al. (2009). However, with the non-stoichiometric approach it is not necessary to propose specific reactions that represent the global phenomena. In addition, it is possible to adapt more easily the number and type of substances in the product gas, which can vary according to the local MSW composition and type of reactor.

When simulated at supercritical condition, with air as gasification agent and considering adiabatic, the process had its performance, in terms of low heating value of the product gas, improved showing that high pressure gasification can be an interesting process. When simulated at supercritical condition, without air, using water as the gasification agent and considering non-adiabatic, the performance has significantly improved, generating higher values of LHV. However, care must be taken when designing the process, because it is necessary to add heat to the system, been recommended a careful heat balance to correct evaluate possible gains in energy content. The model could not predict the presence of tar, which was represented by the benzene, as it is an equilibrium model and when in real operation equilibrium is not really reached. However, it can be used for the design phase of a gasification plant, and it is able to predict the product gas.

In a general way, from the results obtained in this work it can be seen that the gasification of the municipal solid waste can be technically feasible and used for the generation of electricity by improving the calorific value of the product gas.

As future works that can be developed we recommend: an economic feasibility study for the electric generation from municipal solid waste gasification; ultimate analysis of Curitiba's MSW; experimental runs with the MSW gasification; improvement of the current model adopting experimental results to better predict the tar content.

## 6. REFERENCES

ABRELPE. (2013). *Panorama dos resíduos sólidos no Brasil 2013*. Associação Brasileira de Empresas de Limpeza Pública e Resíduos Especiais - ABRELPE.

ALAUDDIN, Z. (1996). *Performance and characteristics of a biomass gasifier system*. PhD Thesis. University of Wales, College of Cardiff, UK.

ALTERNRG. (n.d.). Retrieved February 03, 2016, from ALTERNRG: [http://www.alternrg.com/waste\\_to\\_energy/](http://www.alternrg.com/waste_to_energy/)

ANTAL, J. M., ALLEN, S. G., SCHULMAN, D., & XU, X. (2000). Biomass Gasification in Supercritical Water. *Ind. Eng. Chem. Res.*, pp. 4040-4053.

BABU, B. V., & SHETH, P. N. (n.d.). MODELING & SIMULATION OF BIOMASS GASIFIER: EFFECT OF OXYGEN ENRICHMENT AND STEAM TO AIR RATIO.

BALCAZAR, J. G. (2011). *MODELAGEM DE CICLOS COMBINADOS INTEGRADOS À INCINERAÇÃO DE RESÍDUOS SÓLIDOS MUNICIPAIS*. Guaratinguetá: UNESP.

BARBA, D., PRISCIANDARO, M., SALLADINI, A., & MAZZIOTTI DI CELSO, G. (2011, January 1). The Gibbs Free Energy Gradient Method for RDF gasification modelling. *Fuel*, pp. 1402-1407.

BARUAH, D., & BARUAH, D. (7 de August de 2014). Modeling of biomass gasification: A review. *Renewable and Sustainable Energy Reviews*, pp. 806-815.

BASU, P. (2010). *Biomass Gasification and Pyrolysis Practical Design and Theory*. Burlington: ELSELVIER.

BEGUM, S., RASUL, M. G., AKBAR, D., & RAMZAN, N. (2013). Performance Analysis of an Integrated Fixed Bed Gasifier Model for Different Biomass Feedstocks. *energies*, pp. 6508-6524.

BRASIL, Ministério de Minas e Energia. (2014). *PLANO DECENAL DE EXPANSÃO DE ENERGIA 2023*. Empresa de Pesquisa Energética, Brasília.

BRASIL, N. P. (2003). *IMPACTOS DO SETOR-ELÉTRICO E DA INDÚSTRIA DE GÁS NATURAL NA CO-GERAÇÃO NO BRASIL*. Rio de Janeiro.

BYRD, A. J., PANT, K. K., & GUPTA, R. B. (2007). Hydrogen Production from Glucose Using Ru/Al<sub>2</sub>O<sub>3</sub> Catalyst in Supercritical Water. *Ind. Eng. Chem. Res.*, 3574-3579.

CARVALHAES, V. (2013). *ANÁLISE DO POTENCIAL ENERGÉTICO DE RESÍDUO SÓLIDO URBANO PARA CONVERSÃO EM PROCESSOS TERMOQUÍMICOS DE GASEIFICAÇÃO*. Brasília: Universidade de Brasília.

CENBIO - Centro Nacional de Referência em Biomassa. (2002). *Estado da Arte da Gaseificação*. CENBIO, São Paulo.

COHCE, M., DINCER, I., & ROSEN, M. (2009, October 07). Thermodynamic analysis of hydrogen production from biomass gasification. *International Journal of Hydrogen Energy*, pp. 4970-4980.

GASIFICATION COUNCIL. (2015). Retrieved May 13, 2015, from GASIFICATION COUNCIL: <http://www.gasification.org/gasificationapplications/>

GHASSEMI, H., & SHAHSAVAN-MARKADEH, R. (2013, December 29). Effects of various operational parameters on biomass gasification process; a modified equilibrium model. *Energy Conversion and Management*, pp. 18-24.

HANNULA, I., & KURKELA, E. (2011, May 12). A parametric modelling study for pressurised steam/O<sub>2</sub> -blown fluidised-bed gasification of wood with catalytic reforming. *BIOMASS & BIOENERGY*, pp. 58-57.

HOORWEG, D., & BHADA-TATA, P. (2012). *WHAT A WASTE A Global Review of Solid Waste Management*. Banco Mundial, Washington.

INSTITUTO BRASILEIRO DE GEOGRAFIA ESTATÍSTICA. (2010). *IBGE*. Retrieved 01 04, 2016, from <http://www.cidades.ibge.gov.br/xtras/perfil.php?codmun=410690&search=parana%7Ccuritiba&lang=>



INTERNATIONAL ENERGY AGENCY. (2015). *WORLD ENERGY OUTLOOK 2015 FACTSHEET Global energy trends to 2040*. Paris.

JARUNGTAMMACHOTE, S., & DUTTA, A. (2008, March 04). Equilibrium modeling of gasification: Gibbs free energy minimization approach and its application to spouted bed and spout-fluid bed gasifiers. *ENERGY CONVERSION & MANAGEMENT*, pp. 1345-1356.

KANGAS, P., HANNULA, I., KOUKKARI, P., & HUPA, M. (2014, Abril 3). Modelling super-equilibrium in biomass gasification with the constrained Gibbs energy method. *Fuel*, pp. 86-94.

Lamers, F., Fleck, E., Pelloni, L., & Kamuk, B. (2013). *Alternative Waste Conversion Technologies*. ISWA - International Solid Waste Association.

LI, C., & SUZUKI, K. (2009). Tar property, analysis, reforming mechanism and model for biomass gasification-An overview. *Renewable and Sustainable Energy Reviews* 13, pp. 594-604.

LIU, Y., & GUO, Q. (2013). Investigation into Syngas Generation from Solid Fuel Using CaSO<sub>4</sub>-based Chemical Looping Gasification Process. *Chinese Journal of Chemical Engineering*, pp. 127-134.

LOPES, E. J. (2014). *Tese de Doutorado:Desenvolvimento de sistema de gaseificação via análise de emissões atmosféricas*. Curitiba.

MACHADO, C. F. (2015). *INCINERAÇÃO: UMA ANÁLISE DO TRATAMENTO TÉRMICO D OS RESÍDUOS SÓLIDOS URBANOS DE BAURU/SP*. Rio de Janeiro: UFRJ.

MOUNTOURIS, A., VOUTSAS, E., & TASSIOS, D. (2006). Solid waste plasma gasification: Equilibrium model development and exergy analysis. *Energy Conversion and Management* 47, pp. 1723-1737.

PATRA, T. K., & SHETH, P. N. (29 de May de 2015). Biomass gasification models for downdraft gasifier: A state-of-the-art review. *Renewable and Sustainable Energy Reviews*, pp. 583-593.

PELLEGRINI, L. F., & JR., S. D. (2007). Exergy analysis of sugarcane bagasse gasification. *ENERGY*, pp. 314-327.

PUIG-ARNAVAT, M., BRUNO, J. C., & CORONAS, A. (2010, Maio 13). Review and analysis of biomass gasification models. *Renewable and Sustainable Energy Reviews*, pp. 2841-2851.

RAMZAN, N., ASHRAF, A., NAVEED, S., & MALIK, A. (2011). Simulation of hybrid biomass gasification using Aspen plus: A comparative performance analysis for food, municipal solid and poultry waste. *BIOMASS&BIOENERGY*, 3962-3969.

TANG, H., & KITAGAWA, K. (2004, December 07). Supercritical water gasification of biomass: thermodynamic analysis with direct Gibbs free energy minimization. *Chemical Engineering Journal*, pp. 261-267.

TAVARES, R. C. (2007). *COMPOSIÇÃO GRAVIMÉTRICA: UMA FERRAMENTA DE PLANEJAMENTO E GERENCIAMENTO DO RESÍDUO URBANO DE CURITIBA E REGIÃO METROPOLITANA*. Curitiba: LACTEC.

VOLL, F., ROSSI, C., SILVA, C., GUIRARDELLO, R., SOUZA, R., CABRAL, V., & CARDOZO-FILHO, L. (2009, October 29). Thermodynamic analysis of supercritical water gasification of methanol, ethanol, glycerol, glucose and cellulose. *International Journal of Hydrogen Energy*, pp. 9737-9744.

WILSON, B., WILLIAMS, N., LISS, B., & WILSON, B. (2013). *A Comparative Assessment of Commercial Technologies for Conversion of Solid Waste to Energy*. EnviroPower Renewable, Inc.

WORLD BANK. (2012). *WHAT A WASTE A Global Review of Solid Waste Management*. Washington.

YOUNG, G. C. (2010). *Municipal solid waste to energy conversion processes : economic, technical and renewable comparisons*. John Wiley & Sons, Inc.

ZAINAL, Z., ALI, R., LEAN, C., & SEETHARAMU, K. (2001). Prediction of performance of a downdraft gasifier using equilibrium modeling for different biomass materials. *Energy Conversion and Management* 42, pp. 149-1515.

ZAMBON, K. L., CARNEIRO, A. A., SILVA, A. N., & NEGRI, J. C. (2005, May). Análise de decisão multicritério na localização de usinas termoelétricas utilizando SIG. *Pesquisa Operacional*, pp. 183-199.

## 7. GLOSSARY

MSW – Municipal Solid Waste

RSU – Resíduo Sólido Urbano

PNRS – National plan for Solid Waste (“*Política Nacional de Resíduos Sólidos*”)

IAP – Environmental Paraná Institute (“*Instituto Ambiental do Paraná*”)

ABRELPE – “Associação Brasileira de Empresas de Limpeza Pública e Resíduos Especiais”

RDF – Residue Derived Fuel

WTE – Waste to Energy

HTW – High temperature Winkler gasifier

CFB – Circulating Fluidized Bed

CFD - Computational fluid dynamics

Symbols in equation 1:

m – kmol of hydrogen content in the formula

p - kmol of oxygen content in the formula

q - kmol of nitrogen content in the formula

a, b, c, d, e and f – reaction’s coefficients

Symbols in equation 4:

m – kmol of hydrogen content in the formula

p - kmol of oxygen content in the formula

$q$  - kmol of nitrogen content in the formula

$r$  - kmol of sulfur content in the formula

Symbols in equation 5:

$\delta$  - kmol of CO being decomposed

Symbols in equation 6:

$\gamma$  – kmol of water in reaction as reagent

Symbols in equation 8:

$m$  – kmol of hydrogen content in the formula

$p$  - kmol of oxygen content in the formula

$q$  - kmol of nitrogen content in the formula

$r$  - kmol of sulfur content in the formula

$\gamma$  – kmol of water in reaction as reagent

$x$  – kmol of air in reactions as reagent

$\delta$  - kmol of CO being decomposed according to equation 55

$\alpha$  – water shift reaction

$\beta$  – Steam reform reaction

$n_i^0$  – Initial number of moles in the system of the component  $i$

$G(\alpha, \beta)|_{T,P}$  – Gibbs free energy of water shift reaction and Steam reform reaction

at constant temperature and pressure

$n_i(\alpha, \beta)$  – Number of moles in the system of the component  $i$  for the water shift reaction and Steam reform reaction

$\mu_i(\alpha, \beta, T)$  – Chemical potential of the component  $i$  for the water shift reaction and Steam reform reaction

$\mu_i$  – Chemical potential of the component  $i$

$\mu_i^0$  – Initial chemical potential of the component  $i$

$R$  – Universal gas constant

$T$  – Temperature

$P_i$  - Pressure of the component  $i$ .

$T_0$  – Reference temperature

$h_i(T)$  – Enthalpy in function of temperature

$C_{P,i}$  – Calorific capacity of component  $i$

LHV – Low Heating Value

HHV – High Heating Value

$H_i^0$  – Initial enthalpy of the component  $i$

L – Lagrangian

$\pi$  – Lagrange multiplier vector

$\psi$  – mass balance of the different components of each constituent written in terms of the amounts of matter (mol)

Symbols in equation (30):

w- water reaction coefficient

m –oxygen reaction coefficient

$x_1, x_2, x_3, x_4$  and  $x_5$  – coefficients of hydrogen, carbon monoxide, carbon dioxide, water steam and methane in the reaction

MM – molecular mass

M – moisture